Research into Material Recovery Techniques and the Utilisation of Solid Fuels in an Industrial Context

A thesis submitted to Cardiff University for the degree of

Doctor of Philosophy
(by published works)

Julian Mark Steer

Institute of Energy, Environment & Sustainability
School of Engineering, Cardiff University

November 2015

Declaration

This work has not previously been accepted in substance for any degree and is not concurrently submitted in candidature for any degree.

Signed …… (J.M. Steer) Date ……

Statement 1
This thesis is being submitted in fulfilment of the requirements for the award of the degree of PhD by published works.

Signed …… (J.M. Steer) Date ……

Statement 2
This thesis is the result of my own independent work/investigation, except where otherwise stated. Other sources are acknowledged by explicit references.

Signed …… (J.M. Steer) Date ……

Statement 3
I hereby give consent for my thesis, if accepted, to be available for photocopying and for inter-library loan, and for the title and summary to be made available to outside organisations.

Signed …… (J.M. Steer) Date ……

Acknowledgments

I would particularly like to thank Dr Richard Marsh for his encouragement and help acting as my supervisor for this PhD and to the many research colleagues who contributed as co-authors to these published works.

I would also like to extend my thanks to Gina Goddard-Bell for her patience proof-reading and to the technical support staff at Cardiff School of Engineering, in particular Malcolm Seaborne, without whom much of this work would not have been possible.

Finally, a massive thank you to my wife Joanne and all my family, for their love and support, it is what makes everything possible and worthwhile in life.

Abstract

This thesis covers two main areas of investigation, the production and recovery of process dusts formed in the steelmaking industry, and secondly the study of the utilisation of coals for injection in a blast furnace and during co-firing with biomass in a utility boiler. These are linked by an overall aim to research the environmental and economic sustainability of industrial processes through increased process efficiency, decreased environmental impacts, and increased recovery of waste. It comprises a summary of the research contribution from six first-author peer reviewed journal publications and nine supplementary contributions for the submission of a PhD by published works.

Process dust research was carried out on a 300t vessel requiring the development of a novel industrial scale isokinetic sampling methodology, capable of sampling frequently enough to measure and analyse mass flow profiles and zinc mass contamination profiles at a higher level of detail than in prior research. A new understanding of the impact of in-process iron ore additions and waste oxide additions were correlated with additional dust and zinc mass peaks. This methodology was also used to prove that a new process change involving a galvanised scrap holding stage could be applied to successfully reduce the zinc contamination. Research into a modified hydrometallurgical leaching method for blast furnace dust gave high zinc extraction, but with low iron extraction, by the novel utilisation of the substituent group effect of carboxylic acid leaching. Further research also identified that improvements in the zinc extraction selectivity could be achieved using a non-aqueous solvent to utilise the Lewis acid effect.

In terms of solid fuel utilisation, factors such as the physical properties, cost, and availability result in end users blending coals to meet their needs. The use of higher volatile matter coals was found to benefit blends with low volatile coal in the context of the blast furnace, but research conducted on a 500MW utility boiler showed that carbon monoxide and dust levels increase. Although grinding coals to a pulverised specification has been proved to benefit utilisation, new findings show that the additional grinding alters the surface chemistry and reactivity of many coals and was related to reduced burnouts compared to some larger particle size specifications.

Research on industrial processes is challenging, but these papers aim to address sustainability issues in terms of the efficient use and recovery of materials.

Table of Contents

1. Introduction to the Thesis

This thesis represents work carried out researching industrial processes in terms of both the economic and environmental sustainability necessary for the future of ironmaking, steelmaking and for coal fired power generation. This involved the investigation into increased process efficiency; the minimisation and recovery of process emissions such as dusts; and reductions in emissions of carbon dioxide through the incorporation of renewable materials.

As required, under the senate regulations for the award of the degree of PhD by published works, the submission comprises the following required parts: A list of the published works to be examined, a critical commentary giving an evaluation of the field of research work indicating the original contribution to learning in that field, and finally, additional conference and co-authored papers contributing to original research.

This thesis represents a body of research work carried out by the author over an extended period of time. It is the culmination of work bringing together a series of published journal papers which describe specific aspects of original research work that address issues of sustainability in industrial processes:

- The first critical commentary section, material recovery research in the steelmaking industry, looks closely at resource efficiency in the Steelmaking industry where co-products in the form of dusts represent significant losses to efficiency in the ironmaking and steelmaking processes. Material recovery is essential to the sustainability of these economically, because the loss of raw materials such as iron

ore and fluxes directly impacts the product yield, whilst indirectly increasing the cost of dealing with these arisings. Secondly, these dusts represent a significant environmental burden, either through fugitive emissions into the surrounding and wider environment or through a requirement to landfill.

In addition to material losses, contamination of these arisings with materials such as zinc makes recovery more problematic. Consequently, the journal papers submitted in section one investigate three separate aspects. The first is the statistical correlation of process variables with dust mass and contamination to understand the most relevant ways to make process changes to reduce dust mass and contamination, the second paper researches alternative processes to reduce zinc contamination in the dusts so that the quantity that can be recovered through the process can be maximised, and the final publication details a novel leaching process to selectively remove zinc contamination from blast furnace dust, without extracting iron, to produce a dust that can recovered through the sinter plant.

- The second critical commentary section, utilisation of solid fuels in power generation and ironmaking, investigates the efficient utilisation of coal in industry. Despite an international effort to move away from coal utilisation because of the impact of its emissions on climate change, it is still a significant global energy resource in a world with increasing energy requirements. In the power industry, its efficient utilisation will still be essential to minimise its legacy on the climate during the transition period to a lower carbon future, and the first paper submitted in section 2 researches the impact of co-firing of coal with renewable biomass feedstock on the burnout and emissions in a down fired utility boiler.

In comparison, coal for metallurgical applications is set to continue to be a primary raw material in the production of iron for the steel industry. Increasing quantities of blast furnace coal injection reduces the coke input and improves the efficiency of ironmaking by directly improving the yield of product. The remaining two papers cover research into improving the utilisation of coal by blending and by investigating fundamental aspects of surface chemistry caused by grinding, which has been shown to affect burnout in an adverse manner.

In addition to the papers discussed, supplementary conference papers and co-authored papers have been included which relate to these areas and represent the authors original contribution to research in this field.

1.1. Aims and objectives

The aim of the first section of the thesis was to maximise the recovery of valuable iron units in the steel industry by conducting rigorous research into the reduction, reuse and recycling of co-product dusts formed during the processes. The main objectives of this work covered the following areas:

- Development of a novel in-line isokinetic sampling methodology capable of extracting representative samples for accurate analytical characterisation of the variation in Basic Oxygen Steelmaking (BOS) dust slurry composition from a pipe carrying slurry at very high flow rates (15000 L/min).
- Quantify and characterise the dust slurry to allow the plotting of accurate dust mass and zinc mass profiles during each trial heat.

- Correlate BOS dust and zinc mass contamination loadings during steel manufacture to raw material inputs, galvanised scrap, waste oxide briquettes (WOBs) and process variables.
- Investigate the effect of a new modified manufacturing process aimed to reduce zinc contamination in BOS dust and therefore increase the quantity of dust that can be re-used.
- Research the suitability of carboxylic acids to leach zinc from blast furnace dust and propose a mechanism of extraction of zinc and iron.
- Use a novel non-aqueous solvent selective leaching method to maximise zinc extraction and minimise iron extraction.

The aim of the second section was to conduct rigorous research into the efficient utilisation of coal by maximising the degree of conversion; firstly in the power industry, where co-firing with biomass affects burnout, emissions and boiler operation, and secondly during ironmaking, where very rapid burnout is required in the hot air blast of the blast furnace raceway region. The main objectives of this work covered the following topics:

- Installation and commissioning of a drop tube furnace.
- Determination of biomass burnout for different particle sizes and at different temperatures compared to coal in a drop tube furnace.
- To measure the effect of biomass co-firing with coal in a 500 MW utility boiler, looking specifically at the effect of particle size and secondary air flow on super-heater temperature distribution, unburnt carbon, ash particle size, and flue gas emissions.

- Research into the effect of blending with low volatile coals on the combustion burnout in air, devolatilisation and kinetics in a drop tube furnace and thermogravimetric analyser (TGA).
- Investigate the effect of the particle size and the process of grinding on the coal burnout and physical properties after combustion in a drop tube furnace.
- Determine the effect of the grinding process on the surface chemistry and structure of coal.

1.2. Thesis structure

The discussion presented in this thesis is divided into two sections for critical commentary as required under the senate regulations for the award of PhD by publication. Each of the sections is subdivided to introduce the context of the research covered in the paper, discuss the findings of the papers submitted, and finally to indicate the original contribution made by the research. The published journal papers for examination are documented in Appendix 1, followed by supplementary published works and conference papers included as supporting work in Appendix 2.

1.3.List of published journal papers for examination

Section 1. Material Recovery Research in the Steelmaking Industry

1. **Steer, J**., Griffiths, A., Heinrich, T., Thomas, A., Barnes, C. Correlation of BOS process variables with dust mass formation and zinc content. Ironmaking and Steelmaking (2014) 41 (7), pp. 554-560. (CORRESPONDING AUTHOR)

2. **Steer, J**., Grainger, C., Griffiths, A., Heinrich, T., Hopkins, A. Characterisation of BOS steelmaking dust and techniques for reducing zinc contamination. Ironmaking and Steelmaking (2014) 41 (1), pp. 61-66 (CORRESPONDING AUTHOR)

3. **Steer, J.M**., Griffiths, A.J. Investigation of carboxylic acids and non-aqueous solvents for the selective leaching of zinc from blast furnace dust slurry. Hydrometallurgy (2013) 140, pp. 34-41 (CORRESPONDING AUTHOR)

Section 2. Utilisation of Solid Fuels in Power generation and Ironmaking

4. **Steer, J**., Marsh, R., Griffiths, A., Malmgren, A., Riley, G. Biomass co-firing trials on a down fired utility boiler. Energy Conversion and Management 66 (2013) pp 285-294. (CORRESPONDING AUTHOR)

5. **Steer, J.M**., Marsh, R., Greenslade, M., Robinson, A. Opportunities to improve the utilisation of granulated coals for blast furnace injection. Fuel 151 (2015) pp 40-49. (CORRESPONDING AUTHOR)

6. **Steer, J.M**., Marsh, R., Morgan, D., Greenslade, M. The effects of particle grinding on the burnout and surface chemistry of coals in a drop tube furnace. Fuel 160 (2015) pp.413-423. (CORRESPONDING AUTHOR)

1.4. List of supplementary published works and conference papers

1. **Steer, J**., Marsh, R., Griffiths, T., Williams, K. Biogas potential and digestion rates of food wastes in anaerobic digestion systems. 23rd International Conference on Solid Waste Technology and Management, Philadelphia, PA USA, March 30- April 2, 2008. (PRESENTING AUTHOR)

2. **Steer, J**., Greenslade, M., Griffiths, T., The effect of blending coals on their suitability for blast furnace coal injection. 5th International Conference of Applied Energy, Pretoria, South Africa, July 1st-4th 2013. (PRESENTING AUTHOR)

3. Raghuyal, S., **Steer, J**., Griffiths, A., Hopkins, A. Characterisation of Chromium-Copper- Arsenic (CCA) treated wood waste from a steel-making environment. WIT Transactions on Ecology and the Environment (2012) 163, pp. 271-282 (CO-AUTHOR)

4. Jaafar, I., Griffiths, A.J., Hopkins, A.C., **Steer, J.M**., Griffiths, M.H., Sapsford, D.J. An evaluation of chlorination for the removal of zinc from steelmaking dusts. Minerals Engineering (2011) 24 (9), pp. 1028-1030 (CO-AUTHOR)

5. Heinrich, T., Griffiths, A.J., **Steer J**., Hopkins, A.C., Griffiths, M.H. In-line sampling of basic oxygen steelmaking dust. 5th World conference on sampling and blending, October 25th-28th 2011, Santiago, Chile. (CO-AUTHOR)

6. Marsh, R., **Steer, J**., Fesenko, E., Griffiths, T., Williams, K. Biomass and waste co-firing in large-scale combustion systems. Proceedings of Institution of Civil Engineers: Energy (161 (3), pp. 115-126 (CO-AUTHOR)

7. Marsh, R., **Steer, J**., Griffiths, T., Williams, K. Quantification of products from thermal decomposition of solid wastes. 23rd International Conference on Solid Waste Technology and Management, Philadelphia, USA, March 30th- April 2nd, 2008. (CO-AUTHOR)

8. Pugh, D., Crayford, A.P., Bowen, P.J., Marsh, R., **Steer, J**. Laminar flame speed and Markstein length characterisation of steelworks gas blends. Applied Energy (2014) 136, pp. 1026-1034 (CO-AUTHOR)

9. Marsh R, **Steer J.M.**, Griffiths A.J., Williams K.P., Biomass co-firing: opportunities and considerations, IEA Clean Coal Conference Workshop on Perspectives on Co-combustion, (2008) (CO-AUTHOR)

Section 1.

Material Recovery Research in the Steelmaking Industry

2. Correlation of BOS Process Variables with Dust Mass Formation and Zinc Content

2.1. Introduction and background

During the Basic Oxygen Steelmaking process, oxygen is injected into a vessel of molten pig iron at supersonic velocities during what is termed as the 'blow' to oxidise the residual carbon and convert it into steel. However, this process creates large quantities of dusts (15-20 kg/t hot metal). These are captured by the off gas system, and represent a loss of valuable iron units as well as being a potential environmental liability either as airborne emissions or, due to captured dust, requiring disposal in landfill [1-3]. The preferred ways for steel manufacturers to deal with these dusts are to minimise how much is produced and maximise how much is reused through the steelmaking process [4, 5].

This paper describes a body of research work carried out to investigate the quantitative effect of BOS process variables on dust and zinc mass, sampled and measured, during twelve full scale 300 t steelmaking 'heats'. Comparisons were then made using statistical linear Pearson correlations and multi-regression analysis.

Firstly, it involved obtaining a detailed understanding of the process to establish the most suitable location and methodology for sampling. Because many thousands of kilogrammes of process dust are produced per heat and the dust is carried in an off gas system with a large area, the BOS dust slurry pipe exiting the manufacturing building was chosen, where the slurry flow from the primary wet scrubber passes through a smaller sampling area compared to other parts of the system. A sampling set-up capable of accurately quantifying the dust was designed and fabricated, so that samples could also be captured for detailed

analysis and characterisation in the laboratory. Finally, detailed process information was obtained from the control system to determine addition times and quantities to compare against the results obtained after analysis and interpretation.

The complexity and scale of the process means that many variables contribute to the amount of dust produced, and also to the levels of zinc contamination which limit the reuse of those dusts. An increase in galvanised metal scrap recycling over recent years has resulted in larger quantities of zinc in the process and therefore carrying through into the process dusts [5-7]. Consequently, there is a requirement to research and understand the impact and interaction of the different process variables on the dust mass and zinc mass to help optimise the process so that the dust production can be minimised and dust reuse can be maximised.

The dusts are reused through the BOS process in the form of waste oxide briquettes (WOBs) which are made by combining the dusts with a suitable binder and compressing them to form a solid briquette. However, in addition to the process variables little research is available on the effect of these briquettes, or the incorporation of in-process additions on the dust mass or zinc mass. This paper used a robust sampling methodology to carry out research on a large scale to further the understanding of these manufacturing processes.

2.2. Research methodology

The main research challenge to measure the effect of the process variables was the sampling of the BOS dust slurry and the reliable measurement of volumetric flow rate so that the mass flow rate could be calculated. To achieve this, a sampling device shown in Figure 1 was designed, manufactured and fitted into the main slurry pipe. A detailed

description of the sampling system was presented in the conference paper “In-line sampling of basic oxygen steelmaking dust” located in Appendix 2 [8].

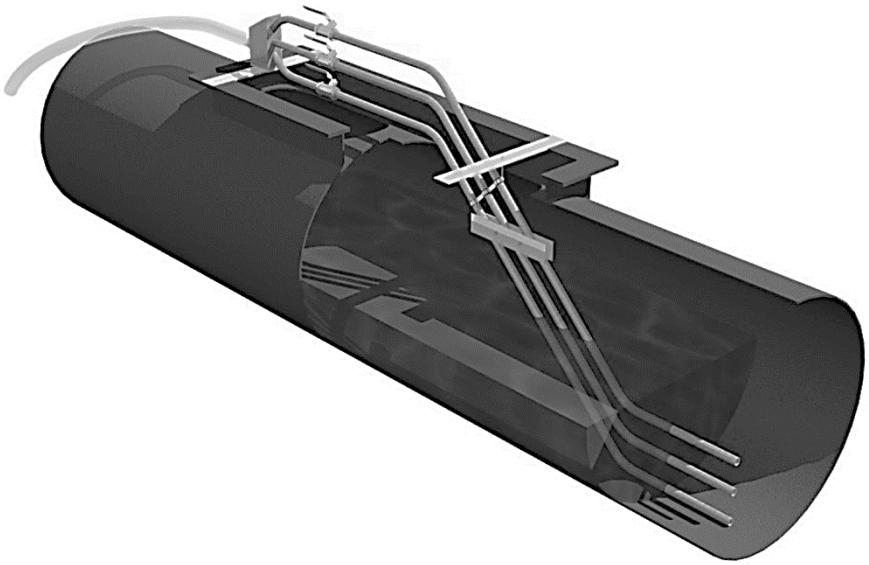

Figure 1. Device for sampling from the BOS dust slurry pipe

The determination of the mass flow of the dust involved measuring the depth and velocity of the BOS dust slurry in a pipe with an internal diameter of 600mm carrying the slurry at a velocity up to 2.8 m/s with peak volume flow rates up to 15000 L/min, see Figure 2. In addition, 10 L slurry samples were taken every minute at peak times during the blow which were bottled, dried and the solid residue analysed. The samples collected were characterised using an inductively coupled plasma spectrophotometer to determine the concentration of zinc in the dust. The concentration of zinc was then applied to the mass flow rates to determine the zinc mass flow rate. These mass flow profiles were subsequently compared to the manufacturing information to compare with process additions.

Figure 2. Picture of BOS slurry pipe and sampling point

2.3.Original research contribution

There is currently limited published work of this type in the literature, partly because of the commercial nature of the research and reasons of confidentiality, but also because these systems are very large-scale industrial processes making measurement difficult to organise, manage and implement.

Gritzan et al [9] carried out valuable work in a similar experiment on a 200 t BOS vessel at TKS Dortmund, but there are some important differences between the studies. In comparison, this study involved sampling the dust in the form of the slurry; the BOS process included the addition of galvanised scrap, measurement of zinc mass flow, and in-process WOB additions. It also included the complete 'heat' rather than specifically on the blow period only. Another important study was carried out by Inaba et al at Kobe Steel's

Kakogawa works which looked in detail at the zinc content in the slurry [10]. In their work, the authors compared the concentration of the zinc in the slurry, but this study involved the more detailed measurement of the volumetric flow rate which allowed the comparison of absolute zinc mass flows. Because of the variation in slurry flow rates during each heat, the zinc concentration profiles were found to vary out of sync with the mass profiles.

Most of the relevant research for BOS dust, or similar dusts such as electric arc furnace dust (EAF), focuses on the downstream treatment or recovery solutions [2, 4, 11, 12]. The following list highlights key original research contributions of this work:

- Developed and applied a novel industrial scale isokinetic methodology to determine accurate mass flows of dust from the steelmaking process. These findings were published, in combination with the analysis of the dust composition, to produce new and more detailed mass flow profiles of the individual components plotted against time and compared with the measured manufacturing process variables.
- Contributed to a new understanding of the impact of different in-process material additions in the BOS process, such as the correlation of iron ore with additional dust in comparison with WOB additions which did not correlate with additional measured dust mass.
- Published research into the incorporation of WOBs as in-process additions which were found to be a stronger predictor variable than the galvanised scrap charge for zinc dust mass. This suggests that multiple WOB additions should be avoided in-process to minimise zinc contamination, and that the relationship between scrap additions and zinc contamination is more dependent on process conditions than the WOB additions.

3. Characterisation of BOS Steelmaking Dust and Techniques for Reducing Zinc Contamination

3.1. Introduction and background

The presence of zinc in process dusts containing iron poses a serious issue to reusing it through the BOS steelmaking process due to its volatilisation, reaction and deposition as zinc compounds which form accretions which can cause damage to the BOS vessel hood and off-gas system [13-16]. Scrap recycling is an integral part of BOS steelmaking, but the increased use of galvanised steel in the marketplace results in its inclusion in the scrap charge, and the zinc then finds its way into the process dusts. Few BOS manufacturing process modification options are available as a solution to deal with this.

This paper describes research carried out on a full scale BOS steel vessel trial. The basis for this work was the hypothesis that zinc could be volatilised from the surface of the metal scrap because of its comparatively low boiling point by utilising the residual heat of the converter between heats and in an inert atmosphere provided by the bath agitation system (BAP). By modifying the manufacturing process in this way, the aim was to collect the zinc dust prior to the liberation of the main bulk of the process dusts during the blow and thereby offering a potential process solution for separation of the dust depending on its zinc concentration.

Zinc present as vapour in the off-gas system can react at high temperatures to form zinc ferrite, which is a very stable and problematic zinc compound to remove from process dusts [17]. However, by liberating the zinc prior to the blow it was also hoped that the formation of zinc ferrite might be minimised, leaving other oxides which are more amenable to

leaching by hydrometallurgy [12, 18]. The paper also investigates the impact of charging regimes on the absolute mass and relative concentration of zinc in BOS dust.

3.2. Research methodology

In comparison to other research in this field, studies have been predominately focussed on downstream solutions involving the post treatment of BOS dusts using hydrometallurgical and pyrometallurgical techniques [4]. These techniques have had varying degrees of success and many are already used industrially for this purpose, but they do not address the source of zinc contamination in BOS dusts.

A limiting reason for upstream process solutions to zinc contamination is the disruption it can have on manufacturing procedures and timings. Consequently this full scale 248 m^3 trial was designed to cause minimum disruption to the operation of the BOS plant. To achieve the research objectives the following set of production conditions were used:

- A fixed amount of galvanised scrap charge per hold heat (20t).
- 2 trials for comparison of the zinc volatilisation with a minimum of 5 heats per trial.
- The converter purged with at least 2 vessel volume changes of nitrogen.
- Maximum purge gas flows (bath agitation process system).
- Converter tilted to increase the possibility of volatilised zinc capture.
- Secondary dust ID fans at maximum load output.
- Secondary dust silo to be emptied prior to the start of the trial.
- Secondary dust silo emptied after the trial and total dust mass recorded.
- Avoid the use of in-process additions during hold trial heats.
- Single converter operation.

- A robust and repeatable sampling method.

3.3.Original research contribution

The originality of this work is the modified galvanised scrap holding process stage carried out in a series of full scale BOS process trials, designed and implemented to test the hypothesis that zinc can be volatilised in-situ prior to a blow.

Work carried out by others in this field has identified that zinc can be volatilised from zinc galvanised metal and that zinc is predominately associated with fine particles [19, 20], but the author is not aware of published work on trials of this scale to demonstrate and measure the effect of holding galvanised scrap.

With a mixture of theory and supporting data, Ma, N.Y showed that spontaneous separation of zinc from iron bearing dusts occurs in the ironmaking and steelmaking off-gas cleaning systems, and that dry off-gas cleaning systems provide the most favourable conditions for zinc to separate from the dust [7]. However, the paper went no further than suggesting that dry dust separators could be arranged in the off-gas cleaning system so zinc could be concentrated, and the majority of solid dusts recycled through the blast furnace. The following list highlights key original research contributions of this work:

- In a BOS charge containing a high zinc input, it was demonstrated that by holding galvanised scrap and utilising the residual heat of the vessel between 'heats', the in-process method reduced the zinc contamination of the BOS dusts by up to 52% of the initial charge.

- Detailed in-process measurements and analysis resulted in the publishing of detailed mass flow profiles and zinc flow profiles during the entire ‘heat’. This data identified peaks and troughs in dust and zinc mass flow which could be targeted to separate off-gas streams and increase the dust recycling opportunities.
- The in-process sampling method identified differences in the zinc oxides formed before and after the blow which might be separated based on their suitability for different treatment techniques.

4. Investigation of Carboxylic Acids and Non-aqueous Solvents for the Selective Leaching of Zinc from Blast Furnace Dust Slurry

4.1. Introduction and background

Processes to extract metal contaminants from steelmaking waste arisings as a means to remediate and reuse them are divided into either thermal pyrometallurgical methods, or hydrometallurgical solution extraction processes.

Hydrometallurgy is a well-established technique to extract metal cations into an aqueous solution and is widely used to extract metals from ores. It has also been used as a technique to treat steelmaking dusts so that the lost iron units can be reused through the manufacturing process [1, 2, 4]. A complete hydrometallurgy process consists of three stages: firstly leaching the metal into solution; secondly to separate and purify it; and finally the recovery of the metal from solution by electrowinning. However, levels of zinc contamination in steelmaking dusts are often too low for the electrowinning of zinc to be an economically attractive option, and too high to recycle back through the process without causing process issues such as accretions on the vessel walls. Factors which determine the most suitable recovery process include the following:

- Value of the recovered metal/s.
- Process selectivity for the required metals.
- The presence of interfering compounds in the sample.
- The chemical forms of the target metals.
- The number of stages, energy and materials required to extract, recover and purify the metals.

- Amount of waste products produced by the process.

To dissolve and recover the metals from the dusts often requires the use of strong chemical reagents, but these are often not selective to zinc alone and can also leach significant quantities of iron [21, 22]. Because the zinc is usually present in different chemical forms, a range of reagents are often required to dissolve specific species of compound. The choice and cost of the process is very dependent on the physical and chemical composition of the sample, which affects the number of stages for the recovery process, the amount of energy used, and the amount of co-products formed.

Many processes have been successfully demonstrated, and acids are often used to leach metals. Hydrochloric, nitric and sulphuric acid are common acidic lixiviants used to recover zinc from steel making dusts, and have demonstrated zinc recovery rates between 75-98% depending on the dust used and on the process conditions. However, significantly high levels of iron are often also co-extracted (up to 50%) which reduces their suitability [23-25].

This paper describes a leaching process to extract zinc contamination from blast furnace dust without removing iron and allowing it to be potentially recovered through the sinter plant/blast furnace. These dusts often contain lower levels of zinc (ca. 2.5%) when compared to BOS dust (ca. 10%) or EAF dust (ca. 20%), but these are no less problematic for recovery as only low zinc levels are permitted through a blast furnace (ca. 150g/t hot-metal) [3].

This research work used organic carboxylic acids with different substituent groups to extract zinc and test the hypothesis that differences in zinc and iron extraction can be explained in

terms of the Lewis and Bronsted-Lowry acid/base theories. This work was extended to use non-aqueous solvents to alter the influence of the substituent groups on the extraction and improve the selectivity for zinc. As a result, the selectivity was explained as a balance between proton dissociation associated with the Bronsted Lowry theory and zinc extraction in terms of the Lewis acid theory.

In addition to this paper, the author carried out other work with colleagues researching potential extraction techniques for steelmaking wastes, resulting in the publication 'Characterisation of Chromium-Copper- Arsenic (CCA) treated wood waste from a steel-making environment' published in WIT Transactions on Ecology and the Environment (2012), and a technical review paper 'An evaluation of chlorination for the removal of zinc from steelmaking dusts, published in Minerals Engineering (2011) [26, 27].

The first paper details the characterisation of treated wood from a coke quenching tower and a series of leaching experiments which formed the precursor to a more detailed hydrometallurgical proposal for extracting copper, chrome and arsenic. The second paper details a pyrometallurgical process using chlorine gas at temperatures up to 750°C, to extract zinc from stockpiled steelmaking dusts by forming the labile $ZnCl_2$.

4.2. Research methodology

A composite representative sample of blast furnace dust was obtained from the settling lagoons by sampling from five separate locations to test the efficacy of the leaching tests using different reagents, concentrations, extraction times and solvents. The experiments were carried out in stoppered 250 ml conical flasks on magnetic stirrer hotplates to ensure constant agitation using 10g of sample and 100g of lixiviant. Where higher temperatures

were used, a water cooled Liebig condenser was incorporated to ensure minimal losses. After leaching, the samples were filtered and dried for further analysis.

The main aim of the research was to achieve high zinc extraction with low iron extraction from a blast furnace dust leaching method, so that the iron units in the treated dust could be potentially recovered through the blast furnace via the sinter plant.

4.3. Original research contribution

This research paper followed standard methodology carried out by other researchers to investigate extraction of zinc from process dusts by leaching in acidic media. However, the novelty of the work lies not in the methodology, but in the selection of carboxylic acids and the identification of the mechanism by which they achieve leaching selectivity for zinc.

These acids were benchmarked against sulphuric, nitric and hydrochloric acid which have been demonstrated by many authors to achieve good zinc extraction. These mineral acids measured high zinc extraction >74%, but also extracted high levels of iron (20-46%). In comparison, the carboxylic acids performed better and the following list highlights the key original research contributions of this work:

- A successful leaching process using the organic carboxylic acid, prop-2-enoic acid, capable of extracting up to 83.1% zinc with 8.5% iron extraction from an oven dried sample of blast furnace dust which had an initial zinc content of 2.3% and iron content of 28.9%.
- Use of a non-aqueous solvent to increase the selectivity of the leaching process by reducing the extraction of iron from 8.5% to 0.1%.

- Identified a method of improving the extraction selectivity using a non-aqueous methylbenzene solvent to alter the acid proton dissociation associated with Bronsted Lowry behaviour.
- Proposed a novel mechanism of zinc extraction thought to be due to the substituent group effect where the group is withdrawing electrons from the organic acid group so it acts as a stronger Lewis acid electron pair receiver.

Section 2.

Utilisation of Solid Fuels for Power generation and Ironmaking

5. Biomass co-firing trials on a down fired utility boiler

5.1. Introduction and background

This paper describes research that investigates the co-firing of biomass with coal, characterising and comparing the fuels and the ash composition; looking at the devolatilisation profiles; flame stability; and most importantly measuring the effects and impact of co-firing on a 500MW boiler at a utility power station.

The co-firing of biomass from renewable sources has been adopted by RWE at Aberthaw power station to meet renewable energy targets set out in the Renewables Obligation [28]. In addition to the differences between coal and biomass characteristics, the boiler is a 'down fired' type specifically designed to give the longer particle residence times needed to burn out the low volatile semi anthracitic coal supplied locally. This has important implications on the stable operation of the boiler, as biomass has much higher volatile matter contents compared to coal; which can affect the flame temperatures, heat profiles, availability of oxygen for combustion, and emissions of NO_x and CO.

The research covered in this paper extends from the laboratory to full industrial scale, comparing the devolatilisation of biomass and coal in a drop tube furnace; investigating flame stability and fouling effects on a 1.5MW combustion test facility at Didcot power station; and finally carrying out co-firing trials on a 500MW industrial utility boiler.

In addition to this work, the author also contributed to a number of other published research papers related to this field, investigating potential energy recovery from waste, which are included in Appendix 2. Particularly relevant for comparison to this co-firing

research is the paper published in the Proceedings of the Institution of Civil Engineers: Energy 'Biomass and waste co-firing in large scale combustion systems' which discussed detailed research into different types of biomass and biomass varieties. This paper looked specifically at the ash properties such as melting and fusion, and their potential impact and suitability in different thermal applications. Although biomass tends to have lower ash contents compared to coal, the composition of the ash discussed in the paper includes more problematic alkali and alkaline earth elements such as potassium and calcium which contribute to fouling and slagging [29].

5.2. Research methodology

The first aspect covered by the paper was the devolatilisation of Miscanthus grass, as a potential source of biomass for co-firing on the full scale trials, measured using a drop tube furnace. This vertical tube furnace was used to replicate the fast particle heating rates typically experienced in pulverised fuel injection and was used to look at the devolatilisation in a dilute particle phase, laminar gas flow, and at temperatures up to 1400°C. Two particle size classifications were obtained by sieving (0.18 - 0.85 mm and 1.18 -2.00 mm) and tested on an oven-dried basis for comparison. The aim of this aspect of the work was to compare the impact of different particle sizes on the extent of devolatilisation, because of its known effect on co-firing described by other authors [30-33].

A 1.5MW combustion test facility located at Didcot power station was used to compare the effect of biomass co-firing at different levels on the slagging tendency. Ceramic sleeve coupons were inserted through sampling ports in the combustor walls to measure the build-up of slag on the coupons for visual comparison of the effects of biomass blends. Many

papers discuss the effect of lower ash fusion temperatures associated with Miscanthus, but few of these have demonstrated it at the scale discussed in this paper [34-37].

The main focus of the paper was the testing carried out on the 500 MW down fired boiler at Aberthaw power station where the biomass was added through four nozzles perpendicular to the boiler walls compared to the down fired configuration for the 36 coal burners. Biomass in the form of woodchips was hammer milled to two different classifications for testing using a 10 mm and a 14 mm screen, and carried by unheated primary air through a central tube in each nozzle at 5 t/h surrounded by an adjustable supply of annular secondary air.

Under normal circumstances the boiler is controlled in 'load sensitive' mode by a logic control system to deliver a constant steam pressure in the steam drum according to load demand. However the co-firing trials were run under 'frequency insensitive' mode so that the unit output remained constant to allow more direct comparisons of the changes without other variables such as the input of coal.

Anecdotal process experience showed that the primary air carrying the biomass had negligible impact on the boiler performance, but the basis for this research paper was the hypothesis that the secondary air could be used to improve biomass co-firing combustion performance by improving mixing. The aim of the trial was to measure the effect of this additional mixing by changing the secondary air damper settings and to measure the impact of the biomass particle size in relation to these changes.

5.3. Original research contribution

This paper represents a rare opportunity to carry out published research on a large scale industrial boiler. Because of the practicalities associated with industrial scale investigations a limited amount of published work is available, and so this research represents a valuable addition to this field, particularly as it describes co-firing high volatile matter content biomass in a boiler designed for combusting low volatile matter coals [38-41]; this paper continues to be well cited by other authors in the field. Because of the wide difference in the properties and proximate analysis of the biomass and coal, the paper gives a valuable insight into the performance and impact of co-firing in some of the most challenging circumstances. The following list highlights the key original research contributions of this work:

- Secondary air around the biomass nozzle is critical to achieving good biomass/air mixing, and therefore reduces any unburnt material due to incomplete combustion. However, it was found that too much secondary air increased the variation of temperature across the super-heaters.
- The rapid devolatilisation of high volatile content biomass leads to a comparatively faster reaction rate compared to the oxidation of non-volatile carbon, reducing the available oxygen in the boiler. This results in increased carbon monoxide and dust levels due to incomplete burnout and potentially limits the overall level of co-firing.
- The addition of the biomass above the primary coal combustion zone was found to produce a variable effect on the formation of NO_x where factors such as the re- burn effect, caused by the addition of higher volatile fuel above the main combustion zone, alter the balance localised equivalence ratio conditions in the furnace.

- Particle size has the largest effect on the unburnt carbon in the fly ash and higher secondary air is limited in its mitigation of this. Milling biomass through finer screens is essential to combustion performance but impacts throughput.

6. Opportunities to Improve the Utilisation of Granulated Coals for Blast Furnace Injection

6.1. Introduction and background

This paper is based on research into the selection of metallurgical coal for injection into the blast furnace, where coals are incorporated as a substitute for the coke charge. Most blast furnace coal injection research is based on a pulverised size specification [42-46], however this paper investigates the blending of coals milled to a larger granulated size coal specification, where there are fewer publications [47-50].

Operators require flexibility in the choice of coals depending on the chemical and physical properties, cost, and availability; this paper looks at the blending of low volatile matter content coals which are less widely used for blast furnace injection because of concerns regarding lower burnout [51, 52]. These represent an economic choice for contributing to a reduction in the cost of ironmaking, but they are also more technically challenging for blast furnace injection where the raceway residence times are very low allowing little time for burnout of lower reactivity chars in comparison to volatiles [53, 54].

The efficient utilisation of coal injected in the blast furnace is dominated by how much coal combusts or gasifies, and this paper investigates and compares this using two methods of thermal analysis, thermogravimetric analysis (TGA) and a drop tube furnace (DTF). These two techniques have been used extensively by researchers to measure different aspects of coal combustion [55-57]. The TGA technique is a static technique which measures the mass change of a small sample (ca. 10-15 mg) placed in an oven with temperature and time. The precision of the balance and resolution of the mass change profiles make it very useful for

measuring the kinetics of the devolatilisation and burnout so that the reactivities can be compared in terms of parameters such as the combustibility index [55, 56, 58-62]. In comparison, the DTF is a dynamic technique based on the continuous addition of a dilute stream of coal into an entrained laminar air flow through a vertical tube furnace. The DTF is used to replicate, as closely as possible, the coal injection conditions in the raceway region of a blast furnace which is a high heating rate environment (>10^4 K/s) [44, 57, 63].

The hypothesis of this work was that blending coals could be used as a technique to improve the burnout and devolatilisation of low volatile content granulated coals, which are more technically challenging coals [45, 63, 64]. The aim of this paper was to quantify the effects of blending in the terms described for TGA and DTF to investigate potential synergistic or inhibitory effects due to devolatilisation or mineral catalysis.

6.2. Research methodology

The TGA was used to apply a non-isothermal iso-conversional kinetic method to calculate and compare the activation energies and combustibility indices of the coals and their blends. The Ozawa, Flynn and Wall model free kinetic method was used to calculate the activation energy as it does not require finding a suitable model to fit the data should the rate limiting mechanism change because of blending [58, 59]. By plotting the logarithm of the heating rate against the reciprocal of the absolute temperature for different degrees of conversion, the straight line fits were used to obtain activation energies for comparison at the different stages of combustion.

In comparison, the DTF was used to determine the burnout under isothermal conditions as a typical hot air blast in the blast furnace of 1100°C. The dilute particle concentration and

high furnace temperatures during the tests results in particle heating rates closer to the high heating rate conditions encountered in the blast furnace raceway. Burnouts were carried out in air and calculated using the ash tracer method [65, 66].

6.3. Original research contribution

The majority of research on blast furnace injection is on coals milled to a pulverised specification [43, 45, 46, 52-54, 67-74]; however, this paper represents an opportunity to look at coal burnout and devolatilisation in terms of granulated coals where the surface area: volume ratio differs, playing a role in the kinetics and on which there is much less published work [47, 48, 50, 75]. In addition, although much work has been carried out into the effects of particle size, shape and mineral catalysis, far less has been carried out in terms of coal blending [64, 76, 77] particularly with respect the use of challenging low volatile matter coals in blends. The following list highlights the key original research contributions of this work.

- Low volatile semi anthracitic coal could be blended with other selected coals to improve the burnout more than the calculated theoretical blend figures.
- Blending high and low volatile coals resulted in volatile yields higher than theoretical figures due to increased particle temperatures caused by volatile matter content combustion and particle swelling.
- Combustibility and activation energy of the low volatile coal could be improved by blending with higher volatile matter content coals.
- Research suggests that higher potassium/aluminium ratios in the mineral ash content has a quantifiable effect on burnout characteristics in granulated coals.

7. The Effects of Particle Grinding on the Burnout and Surface Chemistry of Coals in a Drop Tube Furnace

7.1. Introduction and background

This paper was written in the context of blast furnace coal injection and is based on research into how the process of grinding coals affects their combustion properties by altering the surface chemistry. This work follows on from the previous paper investigating the effect of blending low volatile coals to maximise the flexibility and cost effective selection of coals. In this paper the effect of grinding coals to a larger granulated coal specification was the focus where energy, economic, and environmental savings can be achieved by reduced milling providing the reactivity of the coals are not compromised.

It is generally understood that grinding coals to a smaller particle size classification improves their combustion properties [52, 78, 79], but the basis of this paper is research into how the surface chemistry and combustion reactivity are affected. Many researchers have focussed their work on the beneficial effect on combustibility with smaller particle size due to increased surface area, pore volume, heat transfer and devolatilisation, but it has also been observed by others that grinding can lead to segregation effects which negatively impact reactivity [80-83]. Research on the influence of the coal chemistry tends to focus on the analysis of the bulk [63, 73, 81, 84-90] rather than the surface, so this paper gives a valuable insight into this aspect, particularly how the surface chemistry relates to the reactivity.

For the same reasons as the previous paper, the coal burnout was measured using a drop tube furnace (DTF) to mimic, as closely as possible, the coal injection conditions experienced in the raceway region of a blast furnace. The coal samples and the char residues produced

post burnout were analysed using X-ray diffraction, Laser diffraction and X-ray photoelectron spectroscopy (XPS) to compare the effects of grinding and the impact on burnout. XPS was chosen in particular because of its suitability to describe the surface chemistry in detail, demonstrated in the work of others in this field, giving bonding and structural information [87, 91-93].

This research paper is based on the hypothesis that the process of grinding can affect the type and variety of surface functionality and bonding which could lead to some larger particle sized coals displaying better burnouts. The aim of the research was to apply advanced XPS analytical techniques, usually used for determining catalytic mechanisms, to obtain a novel understanding of the surface chemistry of coals related to the burnouts. In this way explaining why, for some coals, larger particle sizes have improved burnout compared to smaller ones.

7.2. Research methodology

The foundation of the methodology for this work was the grinding and classification of the coal samples into the following three particle size classifications:

1. 100% < 106 µm
2. 100% < 500 µm
3. 100% < 1000 µm, 50% <250 µm

The majority of research studies investigate the effect of particle size based on specific size fractions [80, 83, 94] obtained by sieve classification rather than the effect of grinding used to obtain a specific particle size classification. It has been shown that it can lead to segregation effects because of the heterogeneous nature of coal and its distribution of

macerals and minerals. For that reason, each sample was prepared by classifying, grinding and reclassifying to meet the specification. This has the advantage of using the whole portion of a specific coal sample rather than a selected portion which might represent a heterogeneous fraction of the whole which could be of a different hardness. However, it has the disadvantage of a wider, less specific distribution, potentially leading to a corresponding variation in results.

The DTF was used to determine the burnouts in air under isothermal conditions at the same temperature as a typical hot air blast in the blast furnace of 1100°C.

7.3.Original research contribution

The particle size ranges tested and obtained using the grinding/classification/regrinding method in this paper, give a valuable insight into burnout properties of the complete sample rather than a size selected portion. Because harder particles are more difficult to grind they tend to be larger compared to those that are softer and easier to grind, leading to segregation which can occur based on their properties and composition. However, this method attempts to avoid these effects based on composition differences providing research applicable to real systems.

In comparison to the prior art in this field, this research investigates far wider particle sizes than other work, ranging from a pulverised specification to a granulated coal specification. The following list highlights the key original research contributions of this work:

- The most important finding is that the process of grinding alters the surface chemistry in a detrimental way, so that smaller size classifications that underwent

more grinding had a reduced burnout compared to the larger size classifications which underwent less grinding.

- The process of grinding influences the char formed in the drop tube furnace. The chars formed from larger coal particles tend to fragment while those from smaller particles exhibit swelling.
- There are far fewer carbon-oxygen bonding species on the surface of samples that have undergone more grinding. However, grinding reduces the percentage of sp^2 hybrid bonding which is associated with lower reactivity graphitic chars.
- Adapted the XPS curve fitting technique and identified its limitations with the quantification of each bonding species to describe the surface chemistry of coals and the relationship with combustion burnout.

8. Conclusions

The main conclusions taken from the submitted published journal papers are presented in the following two sections.

Section 1. Material Recovery Research in the Steelmaking Industry

Recovery of materials lost as dust emissions during steelmaking is essential to the economic and environmental sustainability of the industry, however there is limited detailed research on this at an industrial scale. The papers describe three different aspects of this subject, representing new and unusual research findings important to the process yield through the recovery of iron and the minimisation of process emissions requiring disposal.

1. The formation and minimisation of dusts produced during the steelmaking process.
2. A modified steelmaking process to reduce zinc contamination in dusts.
3. A dust leaching method capable of high zinc extraction but with low iron extraction.

Due to the scale and complexity of the industrial processes, carrying out research into the quantification, characterisation, and treatment of these dusts was a significant challenge. This required a rigorous scientific approach to the techniques and methodology necessary to deal with multiple process variables, and the difficulty of obtaining reliable representative samples in a very dynamic large scale system. The following is a list of the main conclusions of this work.

- Process material additions can affect the dust mass and composition in different ways depending on the materials and the timing of these additions. In particular, a significant correlation was measured for the in-process addition of iron ore with additional process dust. This new finding suggests that the form of the iron ore

should be modified, additions should be minimised, or that they should be added with the initial charge to prevent the loss of iron units in the form of dusts. However, in comparison, the addition of the WOBs did not correlate with additional dust, possibly due to the consolidated briquetted form of the waste oxide.

- Zinc contamination is a real issue to the recovery of process dusts because it leads to deposits which can form damaging scabs on the vessel. These build up and then fall off due to their weight damaging the refractory walls. Significantly, the in-process WOB additions were found to be a stronger predictor for zinc than the galvanised scrap charge. This new finding suggests that the chemical form of the zinc is an important factor, and that an alternative addition regime is necessary to minimise dust contamination.
- Through research into the devolatilisation of zinc it was proved that by applying a novel change to the BOS process, zinc could be devolatilised from a high galvanised scrap charge by utilising the residual heat of the BOS vessel. This valuable proof opens the door to further research related to the relationship of the zinc volatilisation with the off-gas composition and temperature variation during the process, to obtain phase shift diagrams for different zinc species to further understand and optimise the conditions necessary to minimise the impact of contamination.
- This research yielded a new level of detail in the profiles of dust and zinc mass variations in real-time during the BOS process which identified the potential for an in-process separation of dust either based on the zinc content, or alternatively by the chemical form of the oxide identified by this work, utilising differences in the extractability of those forms in the final dust.

- Acidic leaching processes have been well researched to extract zinc from process dusts, but this research proposed a new mechanism for the selective leaching of zinc from blast furnace process dust explained in terms of a balance between the Bronsted-Lowry and the Lewis acid theory. The result of this was the proposed explanation that the selection of a suitable acid depends not only on the acidic strength, but also on the substituent group effect. Correspondingly the carboxylic acid prop-2-enoic acid was found to extract up to 83.1% zinc with only 8.5% iron extraction.
- This research theory was tested using a non-aqueous solvent to improve the selectivity of the process, maximising the zinc extraction by facilitating stronger Lewis acid behaviour due to a substituent group effect, and minimising the iron extraction associated with Bronsted Lowry proton dissociation from 8.5% to 0.1%.

Section 2. Utilisation of Solid Fuels for Power Generation and Ironmaking

The three papers in this section form the basis of research into the efficient utilisation of solid fuels, firstly as biomass/coal co-firing in a utility power generation boiler, and secondly as coal injection in ironmaking. In both circumstances the complete devolatilisation and burnout of solid fuels is essential to maximise their utilisation, and the findings from this research identifies some specific relationships between the properties and process. The following list details the main conclusions of this work:

- New findings on a down fired utility boiler operating under co-firing conditions identified that rapid combustion of the high volatile matter content of the biomass consumed the available oxygen rapidly, resulting in increased carbon monoxide and dust levels due to the incomplete burnout. This also has potential implications for

the use of high volatile matter coal blends injected in the blast furnace resulting in a decrease in the permeability of the blast furnace.

- It is widely understood that particle size and milling are very important for the devolatilisation and burnout of solid fuels in all applications. Although milling biomass to smaller particle sizes consumes energy and can result in screen blockages, it also resulted in less unburnt carbon in the fly ash in a down fired utility boiler. In comparison, milling coal to a pulverised fuel specification was found to alter the surface chemistry, reducing reactive carbon-oxygen bonding on the surface leading to correspondingly lower burnouts with smaller particle sizes for some coal types; however, there was a limit to the benefit of this before effects due to increasing particle size such as reduced surface area, porosity and mass diffusion became more dominant.
- Coal blending with higher volatile content coal or biomass was found to improve overall volatile yields and burnout in the high heating rate environment of the drop tube furnace used to replicate the blast furnace raceway or boiler injection. However, oxidant availability and mixing was found to be a dominating factor in the larger scale systems because of the faster reaction rate of volatiles compared to chars.
- The ash mineral composition of coal and biomass pose different challenges and opportunities for their utilisation. The higher concentration of alkali and alkali earth metals in the biomass ash can form low melting point oxides, as measured by the ash flow index, which contribute to slagging and fouling. In comparison, new research into the mineral content of the ash and its distribution through coal ash samples

identified phase changes as mullite and illite showing correlation with burnout, suggesting a potential catalytic role related to burnout.

- Particle swelling and fragmentation effects were measured for coals of different rank and particle size. The swelling effect increases the porosity of the coals reducing any rate limiting mass diffusion effects, but the increasing char particle size has potential implications on blast furnace gas permeability if there is incomplete burnout in the raceway. In contrast, the fragmentation of coal associated with larger coal classifications will have a counterbalancing effect to the lower surface area of the larger particles, and also benefits from less change in the surface chemistry because of reduced milling.

9. Limitations and Future work

Section 1. Material Recovery Research in the Steelmaking Industry

- Obtaining representative in-process samples from the dynamic and variable system of the BOS plant was a challenge, but no less difficult was taking samples from the static system of the blast furnace lagoons where material is stored in very large quantities. In both locations a great deal of attention was paid to this issue, but because of the industrial scale at which this work was carried out, this still remains a potential limitation of the work. In both cases, future work taking more samples over a longer period of time would increase the confidence in the research findings on such a large scale.
- The zinc content of the BOS process dust was proven to be successfully reduced by a modified process, but further research to identify ways to optimise the process by identifying the limiting factors affecting the mechanisms of volatilisation and improving the reduction in zinc would have a positive impact on the process.
- The sampling, preparation and analysis technique used to determine the dust and zinc mass flows was very time consuming. To apply this information to the BOS process would require an in-process separation system which would require the research, development and testing of an in-line analysis technique capable of feedback into the process.
- The selective extraction method for leaching zinc without leaching iron from blast furnace dust was based on a composite blast furnace sample, but this does not measure the ability of the technique to deal with sample compositions which vary

considerably depending on blast furnace conditions. Future work could address this by testing samples of blast furnace dust produced at different times and with different compositions.

- Blast furnace dust is produced under reducing conditions, whereas other steelmaking dusts are produced in oxidising conditions. Further research into the efficacy and selectivity of the hydrometallurgical leaching research using these dusts would advance the understanding of the extraction mechanism.

Section 2. Utilisation of Solid Fuels for Power Generation and Ironmaking

- It was a limitation of the co-firing work that the biomass drop tube furnace devolatilisation tests were carried out on Miscanthus grass, whereas the utility boiler work was based on woodchip alone due to a lack availability of the former for industrial size trials. Even though the biomass had similar volatile matter content, future tests should be carried out on the same feedstock. Also, because of wet biomass 'bridging' in the feeder probe, the drop tube furnace runs were carried out on dry biomass which leaves a potential variable untested; very low biomass sample addition rates of 'wet' biomass might allow future comparison tests at higher moisture possible.
- XPS proved a valuable technique to measure changes in the surface chemistry of samples before and after thermal testing in the drop tube furnace, but was limited to atmospheric pressures. Further in-situ research at higher temperatures or pressure would add further value to this work, potentially identifying the specific

catalytic or combustion bonding and mechanisms associated with differences in the burnout and gasification.

- Having identified the effect of size classification on particle swelling and fragmentation at atmospheric pressure in a high heating environment, it is possible that pressure increases experienced in the blast furnace raceway might be an important variable for future research as the diffusion of products and reactant gases has been shown to vary in some circumstances by other authors.
- The steady state reaction conditions used for the experimental work and the use of mass loss as a measure of conversion gives a valuable relative comparison between samples but assumes complete consumption of the volatiles if the benefits are to be realised. However, there is a diminishing availability of oxidants in the raceway, which could result in unconsumed volatiles capable of re-condensing into problematic species further up the furnace shaft. Future work could involve a non-steady state testing regime more realistic of the raceway environment, where limited oxygen availability might be used to mimic this effect and measure unburnt products.

References

[1] Makkonen HT, Heino J, Laitila L, Hiltunen A, Pöyliö E, Härkki J. Optimisation of steel plant recycling in Finland: Dusts, scales and sludge. Resources, Conservation and Recycling. 2002;35:77-84.

[2] Offenthaler D, Antrekowitsch J, Edlinger A. Zinc containing steel mill dusts - Between recycling and landfilling. REWAS'04 - Global Symposium on Recycling, Waste Treatment and Clean Technology. 2005:2133-41.

[3] EuropeanCommission. Best Available Techniques Reference Document on the Production of Iron and Steel. In: Control IPPa, editor.: JOINT RESEARCH CENTRE: Institute for Prospective Technological Studies; Sustainable Production and Consumption Unit; European IPPC Bureau; 2010.

[4] Nyirenda RL. The processing of steelmaking flue-dust: A review. Minerals Engineering. 1991;4:1003-25.

[5] Delhaes C, Hauck A, Neuschutz D. Mechanisms of dust generation in a stainless steelmaking converter. Steel Research. 1993;64:22-7.

[6] Doronin IE, Svyazhin AG. Properties of steelmaking dust and the mechanism of its formation. Metallurgist. 2012;55:879-86.

[7] Ma NY. On the separation of zinc from dust in ironmaking and steelmaking off-gas cleaning systems. TMS Annual Meeting. 2008:547-52.

[8] Heinrich T, Griffiths, A., Steer, J., Griffiths, M., Hopkins, A.,. In-line sampling of basic oxygen steelmaking dust. 5th world conference on sampling and blending. Santiago, Chile2011. p. 353-60.

[9] Gritzan A, Neuschütz D. Rates and mechanisms of dust generation in oxygen steelmaking. Steel Research. 2001;72:324-30.

[10] Inaba T, Semura K, Horikawa K. Behavior of zinc in BOF with charging zinc coated scrap. Proceedings ICS 2008: The 4th International Congress on the Science and Technology of Steelmaking2008. p. 686-9.

[11] Oda H, Ibaraki T, Abe Y. Dust recycling system by the rotary hearth furnace. Nippon Steel Technical Report. 2006:147-52.

[12] Vereš J, Jakabský S, Lovás M. Zinc recovery from iron and steel making wastes by conventional and microwave assisted leaching. Acta Montanistica Slovaca. 2011;16:185-91.

[13] Besta P, Samolejová A, Janovská K, Lenort R, Haverland J. The effect of harmeful elements in production of iron in relation to input and output material balance. Utjecaj štetnih elemenata pri proizvodnji sirovog željeza u odnosu na ulaznu i izlaznu materijalnu bilancu. 2012;51:325-8.

[14] Koros PJ, Hellickson DA, Dudek FJ. Issues in recycling galvanized scrap. Iron and Steelmaker (I and SM). 1996;23:21-7.

[15] Kryachko GY, Orel GI, Vasyuchenko PA, Safina LA. Maintaining the working profile of blast furnaces during service. Metallurgist. 2005;49:424-31.

[16] Yang X, Chu M, Shen F, Zhang Z. Mechanism of zinc damaging to blast furnace tuyere refractory. Acta Metallurgica Sinica (English Letters). 2009;22:454-60.

[17] Leclerc N, Meux E, Lecuire JM. Hydrometallurgical extraction of zinc from zinc ferrites. Hydrometallurgy. 2003;70:175-83.

[18] Hilber T, Marr R, Siebenhofer M, Zapfel W. Solid/liquid extraction of zinc from EAF-dust. Separation Science and Technology. 2001;36:1323-33.

[19] Pluschkell W, Janke, D. Thermodynamics of zinc reactions in the BOF steelmaking process. Toronto, Canada1992. p. 717-22.

[20] Inaba K, Semura, K., Horikawa, K. Behaviour of zinc in BOF with charging zinc coated scrap. 4th International congress on the science and technology of steelmaking2008.

[21] Van Herck P, Vandecasteele C, Swennen R, Mortier R. Zinc and lead removal from blast furnace sludge with a hydrometallurgical process. Environmental Science and Technology. 2000;34:3802-8.

[22] Soria-Aguilar MJ, Carrillo-Pedroza FR, Preciado-Nuñez S. Treatment of BF and BOF dusts by oxidative leaching. Proceedings of the 2008 Global Symposium on Recycling, Waste Treatment and Clean Technology, REWAS 2008. 2008:589-96.

[23] Havlik T, Kukurugya F, Orac D, Vindt T, Miskufova A, Takacova Z. Leaching of zinc and iron from blast furnace dust in sulphuric acid solutions. Metall. 2012;66:267-70.

[24] Langová Š, Leško J, Matýsek D. Selective leaching of zinc from zinc ferrite with hydrochloric acid. Hydrometallurgy. 2009;95:179-82.

[25] Asadi Zeydabadi B, Mowla D, Shariat MH, Fathi Kalajahi J. Zinc recovery from blast furnace flue dust. Hydrometallurgy. 1997;47:113-25.

[26] Raghuyal S, Steer J, Griffiths A, Hopkins A. Characterisation of Chromium-Copper-Arsenic (CCA) treated wood waste from a steel-making environment. WIT Transactions on Ecology and the Environment. 2012;163:271-82.

[27] Jaafar I, Griffiths AJ, Hopkins AC, Steer JM, Griffiths MH, Sapsford DJ. An evaluation of chlorination for the removal of zinc from steelmaking dusts. Minerals Engineering. 2011;24:1028-30.

[28] Ofgem. Renewables obligation. 2015. https://www.ofgem.gov.uk/environmental-programmes/renewables-obligation-ro. Accessed September 2015.

[29] Marsh R, Steer J, Fesenko E, Cleary V, Rahman A, Griffiths T, et al. Biomass and waste co-fring in large-scale combustion systems. Proceedings of Institution of Civil Engineers: Energy. 2008;161:115-26.

[30] Lu H, Ip E, Scott J, Foster P, Vickers M, Baxter LL. Effects of particle shape and size on devolatilization of biomass particle. Fuel. 2010;89:1156-68.

[31] Peters B, Bruch C. Drying and pyrolysis of wood particles: Experiments and simulation. Journal of Analytical and Applied Pyrolysis. 2003;70:233-50.

[32] Austin PJ, Kauffman CW, Sichel M. Ignition and volatile combustion of cellulosic dust particles. Combustion Science and Technology. 1996;112:187-98.

[33] Guo Q, Chen X, Liu H. Experimental research on shape and size distribution of biomass particle. Fuel. 2012;94:551-5.

[34] Baxter XC, Darvell LI, Jones JM, Barraclough T, Yates NE, Shield I. Miscanthus combustion properties and variations with Miscanthus agronomy. Fuel. 2014;117:851-69.

[35] Michel R, Kaknics J, Bouchetou ML, Gratuze B, Balland M, Hubert J, et al. Physicochemical changes in Miscanthus ash on agglomeration with fluidized bed material. Chemical Engineering Journal. 2012;207-208:497-503.

[36] Monti A, Di Virgilio N, Venturi G. Mineral composition and ash content of six major energy crops. Biomass and Bioenergy. 2008;32:216-23.

[37] Rizvi T, Xing P, Pourkashanian M, Darvell LI, Jones JM, Nimmo W. Prediction of biomass ash fusion behaviour by the use of detailed characterisation methods coupled with thermodynamic analysis. Fuel. 2015;141:275-84.

[38] Raatikka LM. Woody biomass co-firing in pulverized coal fired boilers. American Society of Mechanical Engineers, Power Division (Publication) POWER. 1 ed2011. p. 339-50.

[39] Wang X, Tan H, Niu Y, Pourkashanian M, Ma L, Chen E, et al. Experimental investigation on biomass co-firing in a 300 MW pulverized coal-fired utility furnace in China. Proceedings of the Combustion Institute. 2011;33:2725-33.

[40] Zuwala J, Sciazko M. Full-scale co-firing trial tests of sawdust and bio-waste in pulverized coal-fired 230t/h steam boiler. Biomass and Bioenergy. 2010;34:1165-74.

[41] Zygmanski W, Sciazko M, Zuwala J. Biomass co-firing in pulverized coal-fired utility boiler. 23rd Annual International Pittsburgh Coal Conference, PCC - Coal-Energy, Environment and Sustainable Development2006.

[42] Bortz S, Flament G. Experiments on pulverized-coal combustion under conditions simulating blast-furnace environments. Ironmaking and Steelmaking. 1982;10:222-9.

[43] Carpenter A M. Use of PCI in blast furnaces. IEA Clean Coal Centre; 2006.

[44] Du SW, Chen WH, Lucas JA. Pulverized coal burnout in blast furnace simulated by a drop tube furnace. Energy. 2010;35:576-81.

[45] Raygan S, Abdizadeh H, Rizi AE. Evaluation of Four Coals for Blast Furnace Pulverized Coal Injection. Journal of Iron and Steel Research International. 2010;17:8-12,20.

[46] Suzuki T, Hirose R, Morimoto K, Abe T. pulverized coal combustion in high temperature furnaces for steel making (first report: evaluation method of combustibility for pulverized coaL). Bulletin of the JSME. 1984;27:2803-10.

[47] Maldonado R, Hanniker G, Pettifor M. Granular coal injection into blast furnaces at the scunthorpe works of the british steel corporation. Proceedings - Ironmaking Conference1985. p. 425-35.

[48] Energy USDo. Blast Furnace Granulated Coal Injection System Demonstration Project:. P.O. Box 880, 3610 Collins Ferry Road, Morgantown, WV 26507-0880: National Energy Technology Laboratory; 2000.

[49] Hill DG, Makovsky LE, Sarkus TA, McIlvried HG. Blast furnace granular coal injection at Bethlehem Steel's Burns Harbor Plant. Mineral Processing and Extractive Metallurgy Review. 2004;25:49-65.

[50] Guo H, Su B, Zhang J, Shao J, Zuo H, Ren S. Energy conservation for granular coal injection into a blast furnace. JOM. 2012;64:1002-10.

[51] Kunitomo K, Orimoto T, Nishimura T, Naito M, Yagi JI. Effects of volatile matter of pulverized coal on reducing agents rate of blast furnace and combustion behavior of coal mixture. Tetsu-To-Hagane/Journal of the Iron and Steel Institute of Japan. 2004;90:190-7.

[52] Chen WH, Du SW, Yang TH. Volatile release and particle formation characteristics of injected pulverized coal in blast furnaces. Energy Conversion and Management. 2007;48:2025-33.

[53] Zhang SF, Bai CG, Wen LY, Qiu GB, Lü XW. Gas-particle flow and combustion characteristics of pulverized coal injection in blast furnace raceway. Journal of Iron and Steel Research International. 2010;17:8-12.

[54] Guo B, Zulli P, Rogers H, Mathieson JG, Yu A. Three-dimensional simulation of flow and combustion for pulverised coal injection. ISIJ International. 2005;45:1272-81.

[55] Artos V, Scaroni AW. T.g.a. and drop-tube reactor studies of the combustion of coal blends. Fuel. 1993;72:927-33.

[56] Biswas S, Choudhury N, Sarkar P, Mukherjee A, Sahu SG, Boral P, et al. Studies on the combustion behaviour of blends of Indian coals by TGA and Drop Tube Furnace. Fuel Processing Technology. 2006;87:191-9.

[57] Li H, Elliott L, Rogers H, Austin P, Jin Y, Wall T. Reactivity study of two coal chars produced in a drop-tube furnace and a pulverized coal injection rig. Energy and Fuels. 2012;26:4690-5.

[58] 11358-2:2014 BI. Plastics-Thermogravimetry (TG) of polymers part 2: Determination of activation energy. 2014.

[59] Flynn JHW, L.A. General Treatment of the Thermogravimetry of Polymers. Journal of research of the national bureau of standards-A Physics and Chemistry. 1966;70A.

[60] Morgan PA, Robertson SD, Unsworth JF. Combustion studies by thermogravimetric analysis. 1. Coal oxidation. Fuel. 1986;65:1546-51.

[61] Morgan PA, Robertson SD, Unsworth JF. Combustion studies by thermogravimetric analysis. 2. Char oxidation. Fuel. 1987;66:210-5.

[62] Russell NV, Beeley TJ, Man CK, Gibbins JR, Williamson J. Development of TG measurements of intrinsic char combustion reactivity for industrial and research purposes. Fuel Processing Technology. 1998;57:113-30.

[63] Chan ML, Jones JM, Pourkashanian M, Williams A. Oxidative reactivity of coal chars in relation to their structure. Fuel. 1999;78:1539-52.

[64] Moon C, Sung Y, Ahn S, Kim T, Choi G, Kim D. Thermochemical and combustion behaviors of coals of different ranks and their blends for pulverized-coal combustion. Applied Thermal Engineering. 2013;54:111-9.

[65] Ballantyne TR, Ashman PJ, Mullinger PJ. A new method for determining the conversion of low-ash coals using synthetic ash as a tracer. Fuel. 2005;84:1980-5.

[66] Chen W-H, Du S-W, Tsai C-H, Wang Z-Y. Torrefied biomasses in a drop tube furnace to evaluate their utility in blast furnaces. Bioresource Technology. 2012;111:433-8.

[67] Davis KA, Hurt RH, Yang NYC, Headley TJ. Evolution of char chemistry, crystallinity, and ultrafine structure during pulverized-coal combustion. Combustion and Flame. 1995;100:31-40.

[68] Gupta S, Al-Omari Y, Sahajwalla V, French D. Influence of carbon structure and mineral association of coals on their combustion characteristics for Pulverized Coal Injection (PCI) application. Metallurgical and Materials Transactions B: Process Metallurgy and Materials Processing Science. 2006;37:457-73.

[69] Ishii K. Advanced pulverised coal injection technology and blast furnace operation: Elsevier science ltd; 2000.

[70] Kalkreuth W, Borrego AG, Alvarez D, Menendez R, Osório E, Ribas M, et al. Exploring the possibilities of using Brazilian subbituminous coals for blast furnace pulverized fuel injection. Fuel. 2005;84:763-72.

[71] Li H, Elliott L, Rogers H, Wall T. Comparative study on the combustion performance of coals on a pilot-scale test rig simulating blast furnace pulverized coal injection and a lab-scale drop-tube furnace. Energy and Fuels. 2014;28:363-8.

[72] Lu L, Sahajwalla V, Harris D. Coal char reactivity and structural evolution during combustion-factors influencing blast furnace pulverized coal injection operation. Metallurgical and Materials Transactions B: Process Metallurgy and Materials Processing Science. 2001;32:811-20.

[73] Oka N, Murayama T, Matsuoka H, Yamada S, Yamada T, Shinozaki S, et al. The influence of rank and maceral composition on ignition and char burnout of pulverized coal. Fuel Processing Technology. 1987;15:213-24.

[74] Yi B, Zhang L, Mao Z, Huang F, Zheng C. Effect of the particle size on combustion characteristics of pulverized coal in an O2/CO2 atmosphere. Fuel Processing Technology. 2014;128:17-27.

[75] Steer JM, Marsh R, Greenslade M, Robinson A. Opportunities to improve the utilisation of granulated coals for blast furnace injection. Fuel. 2014.

[76] Su S, Pohl JH, Holcombe D, Hart JA. Slagging propensities of blended coals. Fuel. 2001;80:1351-60.

[77] Wang CA, Liu Y, Zhang X, Che D. A study on coal properties and combustion characteristics of blended coals in northwestern China. Energy and Fuels. 2011;25:3634-45.

[78] Barranco R, Colechin M, Cloke M, Gibb W, Lester E. The effects of pf grind quality on coal burnout in a 1 MW combustion test facility. Fuel. 2006;85:1111-6.

[79] Zhang H, Cen K, Yan J, Ni M. The fragmentation of coal particles during the coal combustion in a fluidized bed. Fuel. 2002;81:1835-40.

[80] Cloke M, Lester E, Belghazi A. Characterisation of the properties of size fractions from ten world coals and their chars produced in a drop-tube furnace. Fuel. 2002;81:699-708.

[81] Huggins FE. Overview of analytical methods for inorganic constituents in coal. International Journal of Coal Geology. 2002;50:169-214.

[82] Suarez I-R, Crelling, J.C. Applied coal petrology: The role of petrology in coal utilisation: Academic Press; 2008.

[83] Ural S, Akiylidz M. Studies of the relationship between mineral matter and grinding properties for low-rank coals. International Journal of Coal Geology. 2004;60:81-4.

[84] Liu J, Jiang X, Shen J, Zhang H. Chemical properties of superfine pulverized coal particles. Part 1. Electron paramagnetic resonance analysis of free radical characteristics. Advanced Powder Technology. 2014;25:916-25.

[85] Menendez R, Alvarez D, Fuertes AB, Hamburg G, Vleeskens J. Effects of clay minerals on char texture and combustion. Energy and Fuels. 1994;8:1007-15.

[86] Pohl JH. Influence of mineral matter on the rate of coal char combustion. ACS Symposium Series1986. p. 430-6.

[87] Shaolong W, Wei-Yin C, Guang S. Roles of mineral matter in the early stages of coal combustion. Energy and Fuels. 2009;23:710-8.

[88] Spears DA. Role of clay minerals in UK coal combustion. Applied Clay Science. 2000;16:87-95.

[89] Wei Z, Michael Moldowan J, Dahl J, Goldstein TP, Jarvie DM. The catalytic effects of minerals on the formation of diamondoids from kerogen macromolecules. Organic Geochemistry. 2006;37:1421-36.

[90] Zhang H, Pu WX, Ha S, Li Y, Sun M. The influence of included minerals on the intrinsic reactivity of chars prepared at 900 °C in a drop tube furnace and a muffle furnace. Fuel. 2009;88:2303-10.

[91] Geng W, Kumabe Y, Nakajima T, Takanashi H, Ohki A. Analysis of hydrothermally-treated and weathered coals by X-ray photoelectron spectroscopy (XPS). Fuel. 2009;88:644-9.

[92] Pietrzak R, Grzybek T, Wachowska H. XPS study of pyrite-free coals subjected to different oxidizing agents. Fuel. 2007;86:2616-24.

[93] Xia W, Yang J, Liang C. Investigation of changes in surface properties of bituminous coal during natural weathering processes by XPS and SEM. Applied Surface Science. 2014;293:293-8.

[94] Li F, Zhang J, Qi C, Pang Q, Rao J, Ma C. Investigation on the dual influence of pansteel pulverized coal combustion process by coal quality and particle size. Materials Science and Technology Conference and Exhibition 2013, MS and T 20132013. p. 566-73.

Appendix 1 Published journal papers for examination

Minor contribution	Moderate contribution	Majority contribution

Contribution to published journal papers for examination					
Paper	Concept	Structure/ design	Experimental	Data Analysis	Paper writing
Section 1. Material Recovery Research in the Steelmaking Industry					
Steer, J., Griffiths, A., Heinrich, T., Thomas, A., Barnes, C. Correlation of BOS process variables with dust mass formation and zinc content. Ironmaking and Steelmaking (2014) 41 (7), pp. 554-560.					
Steer, J., Grainger, C., Griffiths, A., Heinrich, T., Hopkins, A. Characterisation of BOS steelmaking dust and techniques for reducing zinc contamination. Ironmaking and Steelmaking (2014) 41 (1), pp. 61-66					
Steer, J.M., Griffiths, A.J. Investigation of carboxylic acids and non-aqueous solvents for the selective leaching of zinc from blast furnace dust slurry. Hydrometallurgy (2013) 140, pp. 34-41					
Steer, J., Marsh, R., Griffiths, A., Malmgren, A., Riley, G. Biomass co-firing trials on a down fired utility boiler. Energy Conversion and Management 66 (2013) pp 285-294.					

Paper	Concept	Structure/ design	Experimental	Data Analysis	Paper writing
Section 2. Utilisation of Solid Fuels in Power generation and Ironmaking					
Steer, J., Marsh, R., Griffiths, A., Malmgren, A., Riley, G. Biomass co-firing trials on a down fired utility boiler. Energy Conversion and Management 66 (2013) pp 285-294.					
Steer, J.M., Marsh, R., Greenslade, M., Robinson, A. Opportunities to improve the utilisation of granulated coals for blast furnace injection. Fuel 151 (2015) pp 40-49.					
Steer, J.M., Marsh, R., Morgan, D., Greenslade, M. The effects of particle grinding on the burnout and surface chemistry of coals in a drop tube furnace. Fuel 160 (2015) pp.413-423.					

Correlation of BOS process variables with dust mass formation and zinc content

J. Steer*[1], A. Griffiths[1], T. Heinrich[1], A. Thomas[2] and C. Barnes[2]

The basic oxygen steelmaking (BOS) process typically produces a dust rich in valuable iron units and often contaminated with zinc. This paper takes a look at statistical correlation and multiple regressions of process variables with the quantity of dust and the zinc mass contained in the dust. A robust inline sampling system was designed and installed to isokinetically sample the primary BOS dust slurry from a 248 m^3 capacity BOS converter at Tata Steelworks Port Talbot (UK). This system was used to measure the dust mass and composition changes against time for 12 large scale trial heats and to compare with the process information data for a statistical evaluation of the variables. Statistically significant Pearson linear correlations were measured for the total dust mass produced with the iron ore and for the zinc mass contained in the dust with the addition of waste oxide briquettes (WOBs). A multiple regression analysis model showed strong associated correlations between the zinc mass contained in the dust with the galvanised scrap and WOB additions and explained 73% of the zinc mass variance.

Keywords: Basic oxygen steelmaking, Dust, Zinc, Statistical, Regression

Introduction

Many thousands of tonnes of iron bearing dusts are produced per year from steelmaking, and reducing or reusing these plays a major role in the sustainability of steel manufacture both environmentally and economically.[1,2] These dusts represent an environmental disposal liability, as they are usually classified as hazardous waste because of heavy metal constituent compounds and are often stockpiled.[3,4]

The quantity and composition of dusts produced during the basic oxygen steelmaking (BOS) process vary considerably and are generally contaminated with zinc, either from the raw materials used or particularly from the process of recycling zinc galvanised scrap during manufacturing.[5–7] However, the environmental burden of disposal and the high levels of iron contained in the dusts are significant drivers in reducing the quantities produced and the level of zinc contamination.

This paper discusses the results from 12 full scale BOS trial heats, conducted at Tata Steelworks Port Talbot (UK). A bespoke isokinetic sampling method was developed and installed to determine the mass flow of primary BOS dust produced during each heat. Samples were also taken at regular intervals to characterise the composition of the dust and therefore calculate the mass flow of the zinc liberated during each heat.

It is very difficult task to sample and measure BOS dust robustly on such a large scale and in such a dynamic environment. This work represents an important opportunity to look at dust mass and dust composition profiles so accurately. From the results, the variables understood to affect the BOS dust have been examined statistically to quantify their significance on the dust mass and the zinc mass produced.

Methodology

The primary dust, collected by the off gas system of the BOS converter, is liberated at very high rates during the blow part of each heat and is extremely challenging to measure. The dust is collected as slurry from the BOS off gas using venturi water scrubbers and transported to clarifier settling tanks via large pipes where the slurry sampling point was located.

The manufacture of steel in the BOS plant is extremely dynamic, as the manufacturing variables change in response to parameters such as the scrap charge, raw materials, hot metal composition and the final specification of the steel. No two heats are exactly the same, and consequently, the quantity and composition of the dust produced also vary; for this reason, a statistical evaluation of the parameters allows a more quantitative scientific evaluation of the variables.

Trial conditions

This paper evaluates the effect of BOS variables on the dust mass produced and its composition, but it is not an evaluation of the statistical variation of the BOS process itself. The results come from a series of different trials to reduce the zinc content of the primary dust,[8] to investigate the use of waste oxide briquettes (WOBs) and also to measure the dust mass during normal operating conditions. Consequently, the results were

[1]Cardiff School of Engineering, Cardiff University, Queen's Buildings, the Parade, Cardiff, Wales CF24 3AA, UK
[2]Tata steel UK, Port Talbot, UK

*Corresponding author, email SteerJ1@cardiff.ac.uk

Published by Maney on behalf of the Institute
Received 8 July 2013; accepted 18 August 2013
DOI 10.1179/1743281213Y.0000000152

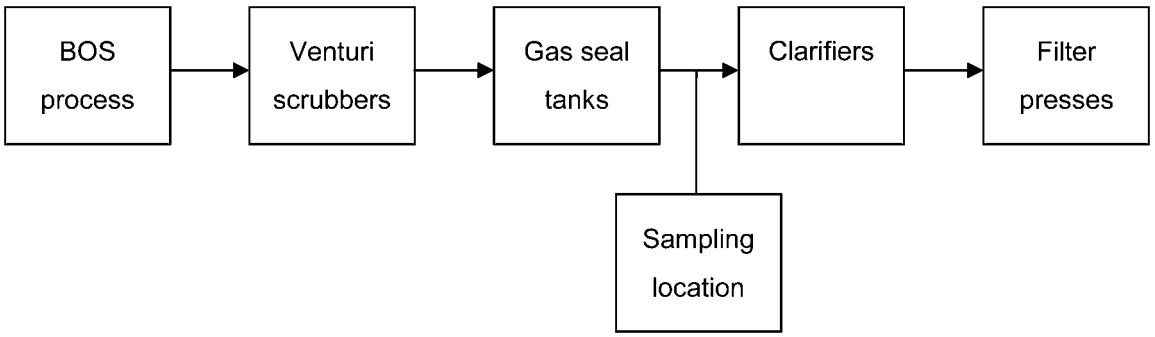

1 Sampling location of primary dust extraction system

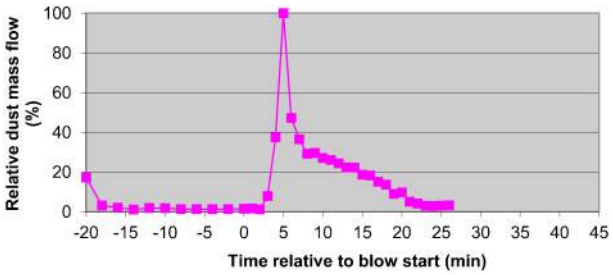

2 Relative dust mass flow profile

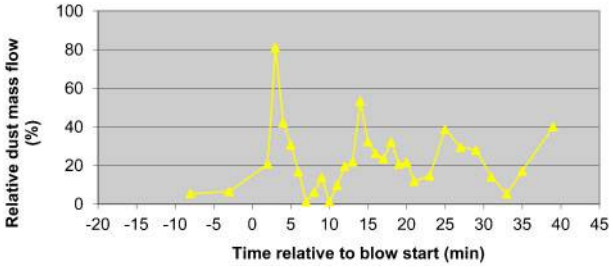

3 Relative dust mass flow profile illustrating dust peaks throughout heat

derived from a wide range of processing conditions, some of which would not occur during normal processing but provide a unique and useful examination of the limits of variation:

(i) standard control heats (×2): incorporating a 20 t charge of galvanised scrap; normal processing conditions
(ii) low galvanised scrap input heats (×2): zero galvanised scrap charge; normal processing conditions
(iii) galvanised scrap hold heats (×2): a 20 t charge of galvanised scrap with up to 15 min scrap hold time
(iv) waste oxide briquette investigation heats (×6): high and low WOB charges.

Sampling and analysis

In order to obtain inline data of the variation in primary dust, a sampling system was installed to sample the slurry isokinetically. Figure 1 shows the location of the pipe carrying the BOS dust slurry, at flowrates up to 15 000 L min^{-1}.[9] Samples (10 L) were taken at regular intervals, every 2 min outside the blow and every minute during the blow, while flow measurements were taken

Table 1 List of independent variables*

Dust mass/t	Total dust mass measured for duration of heat
Relative dust mass/%	Dust mass as a percentage of the maximum rate measured
Duration of heat/min	Tap to tap duration and includes delays
Duration of blow/min	Duration from the start to finish of the oxygen injection
Scrap total/t	Total addition of scrap minus the galvanised scrap charge
Additions total/t	Includes additions of fluxes
Hot metal charge/t	Molten iron charge
WOB charge/t	WOB additions
Iron ore charge/t	Iron ore added to regulate temperature
Total converter mass/t	Total mass in the converter after all additions
Oxygen addition/Nm^3	Total quantity of oxygen added to converter
Lance height/m	Height of lance
Dust during blow/t	Dust produced during the oxygen blow period only
Dust outside blow/t	Dust produced before and after the oxygen blow period
Zinc mass/kg	Zinc mass liberated in the primary dust
Relative zinc mass/%	Zinc mass as a percentage of the maximum rate measured
Galvanised scrap charge/t	Total galvanised scrap charge to converter
Carbon content/t	Carbon mass in hot metal charge
Temperature/°C	Final converter temperature
Silicon/t	Silicon mass in hot metal charge
Manganese/t	Manganese mass in hot metal charge
Phosphorous/t	Phosphorous mass in hot metal charge
Sulphur/t	Sulphur mass in hot metal charge
Titanium/t	Titanium mass in hot metal charge

*The study also included more specific variables not included in this paper such as dolomet, dolaflux, lime, WOB iron content, WOB calcium content and liquid height in converter.

every second using a Marsh-McBirney Flo-Dar open channel flowmeter.

Samples were analysed for solid content to determine the mass flow of the slurry using the flow measurements, and the metal concentration was determined using a Perkin Elmer Optima 2100DV inductively coupled plasma spectrometer. The PASW Statistics 18 package was used for the regression analyses.

Results and discussion

Dust formation

European 'best available technique' figures for the quantity of dust generated from a BOS converter range from 15 to 20 kg t^{-1} of liquid steel.[10] Dust formation in a BOS converter has been studied by various researchers, and the dominant mechanisms are the ejection of fine metal and slag droplets caused by bursting CO bubbles of the film in the melt, vapourisation and spitting of material and entrainment of fines during top charging material additions.[5,11–14]

As expected, it is clear from the literature that there are many variables that affect the quantity of dust produced during a steelmaking heat. The dust mass profiles of heats vary significantly, as shown in the following examples, which are plotted as relative quantities of the maximum dust mass rate recorded for all the trial heats. The heat duration varied depending on factors such as material and equipment availability, product specification and manufacturing constraints or pressures. Consequently, for this study, a heat was defined as the period between tapping the converter from the previous heat and tapping of the trial heat. As a result, the x axis figures were normalised to the oxygen blow start at 0 min to allow direct comparisons of each heat. Note that there was a delay between the blow start and the first sample measured at the sampling point corresponding to the time taken for the dust to arrive at the sampling point; this residence time varied between 3 and 4 min depending on the slurry flowrate, which varies itself, depending on the off gas flowrate.

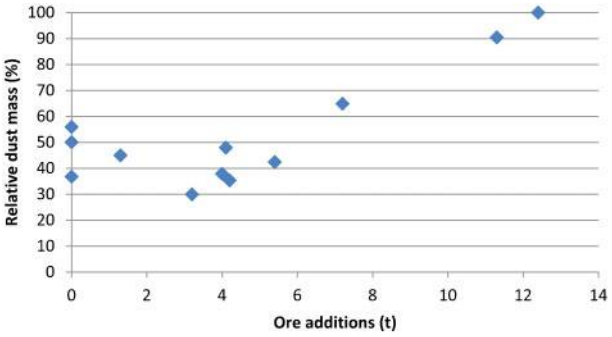

4 Dust mass correlation plots of iron ore additions

Figure 2 shows the relative dust mass flow profile of a more regular heat, where the rate of dust mass generated showed an initial peak when the blow starts followed by a steady decrease in the dust generation rate until the blow ends after ~20 min. Gritzan *et al.* suggested that decreasing carbon content in the melt, and the formation of a filtering slag, means less metal droplets are ejected, and therefore, less dust is produced over blowing time.[11]

During the trials, large dust mass peaks were also measured and observed during and after the blow period as shown in Fig. 3. The magnitude and frequency of these peaks, in particular the relation with the zinc mass, are compared statistically to help understand their relationship with the variables.

Statistical correlations of variables with dust mass and zinc mass

The variables correlated with the dust mass produced during different heat conditions are shown in Table 1. To evaluate the dependence of dust mass on different variables, the Pearson product moment correlation coefficient was used as a measure of the linear dependence between two factors. The correlation R value ranges between $+1$ and -1; the former indicates a perfect linear correlation where the increase in a variable X leads to an increase in variable Y, while the latter indicates a perfect linear correlation where the increase in a variable X leads to a decrease in the variable Y. A value of 0 indicates no correlation between the two variables. The p value is the probability value; if this value is less than the significance level quoted, 0·05 or 0·01, then the null hypothesis can be rejected and the R value is significant and a correlation in the variables is statistically likely.

Dust mass

The dust mass profiles of the BOS heats during the trials all show peak mass flows during the initial oxygen blow

Table 2 List of variables with no significant correlation with dust mass

Variables	*R* value	*p* value
Duration of heat/min	0·455	0·137
Duration of blow/min	0·009	0·977
Additions total/t	0·271	0·394
Hot metal charge/t	0·121	0·707
WOB charge/t	−0·327	0·300
Total converter mass/t	0·221	0·468
Oxygen addition/Nm^3	−0·542	0·069
Lance height/m	0·488	0·108
Scrap additions/t	−0·567	0·054
Galvanised scrap charge/t	−0·233	0·467
Carbon content/t	0·215	0·502
Temperature/°C	−0·112	0·744
Silicon/t	−0·318	0·314
Manganese/t	0·166	0·606
Phosphorous/t	−0·561	0·058
Sulphur/t	−0·298	0·346
Titanium/t	−0·242	0·448

Table 3 Dust mass correlation with iron ore additions

Variables	*R* value	*p* value	Significance level
Iron ore additions	0·789	0·002	0·01

Table 4 Dust mass (outside blow) correlation with iron ore additions

Variables	R value	p value	Significance level
Iron ore additions	0·868	0·000	0·01

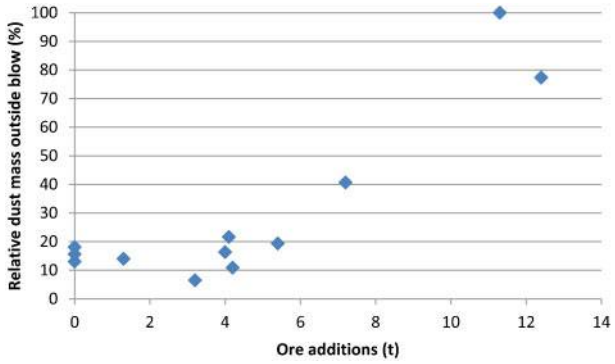

5 Dust mass (outside blow) correlation plots with iron ore additions

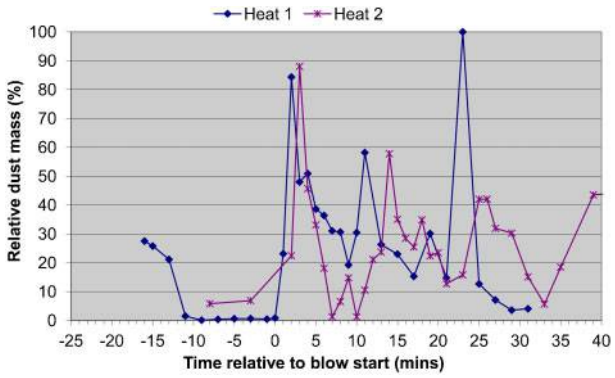

6 Relative dust mass profiles of two heats incorporating multiple ore additions

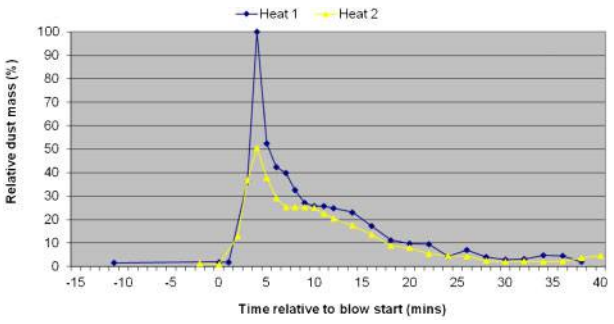

7 Relative dust mass profiles for heats incorporating multiple WOB additions

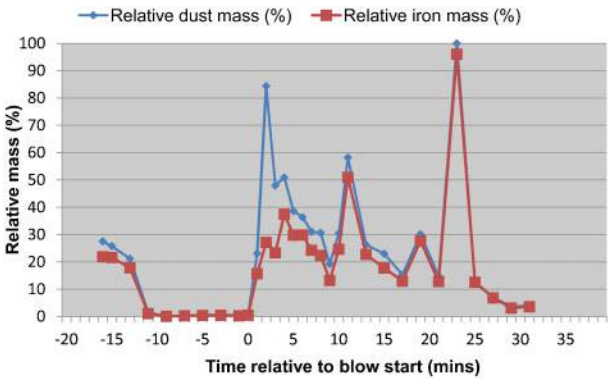

8 Comparison of dust mass and iron mass profiles of heat 1

period, as shown in the selected examples in Figs. 2 and 3 and the blow times were between 17 and 20 min.

Correlations with the dust mass produced during steelmaking were examined with all of the variables listed in Table 1. Each of the independent variables was correlated with the dependent dust mass variable and also plotted as a scatter plot to establish linear or non-linear relationships. The null hypothesis, that there is no linear correlation between the dust mass and the variable, could not be rejected for those which were not significant at the 0·05 or 0·01 levels, as listed in Table 2.

Although the independent variables listed in Table 2 may not be significant enough to reject the null hypothesis, they could still play a role in the dust mass formation. It is possible that there were insufficient heats to obtain a statistically significant sample of the profiles of dust produced. The Pearson correlations identify significant linear relationships, and it must be noted that weaker ones, or additive/synergistic effects between variables, may not be picked up by this term.

However, a significant linear correlation was identified between the dust mass produced and iron ore additions. The ore additions were used to regulate the temperature during steelmaking and showed a strong positive correlation factor of 0·789 at a significance level of 99%, as shown in Table 3 and in the scatter plot of Fig. 4.

The strong correlation for iron ore additions was examined more closely outside of the blow, and the

Table 6 Zinc mass correlation with WOB additions

Variables	*R* value	*p* value	Significance level
WOB additions	0·697	0·012	0·05

Table 5 Timings of iron ore additions relative to blow start

	Blow duration /min	Ore additions/t	Ore addition time relative to blow start/min	Significant peak times relative to blow start/min	Process observations
Heat 1	18	4·5	+2	+2	Build-up on converter skirt and some falling debris
		5·8	+17	+11	
		2·1	+19	+23	
Heat 2	19	4·7	+3	+3	Blow interrupted after 2 min then restarted after 8 min
		4·3	+16	+14	
		2·3	+19	+25	

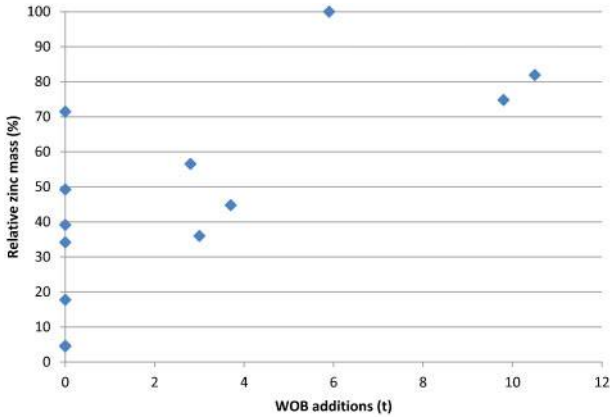

9 Zinc mass correlation plots with WOB additions

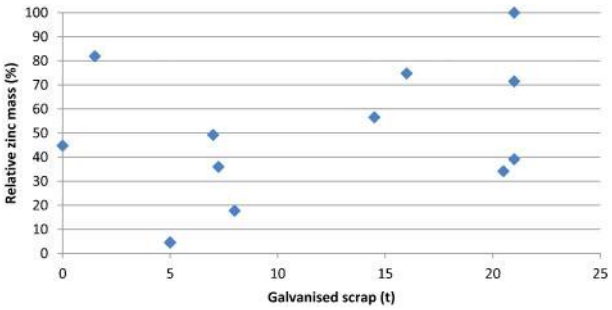

10 Zinc mass correlation plots with galvanised scrap

results, in Table 4 and in Fig. 5, showed an even stronger correlation factor of 0·868 during this period, significant at 99%. The results suggest that there is a correlation between ore additions and dust liberation, particularly strongly with additions outside the blow.

Ore additions are usually added with the slag formers at the initial blow stage, but some had multiple ore additions during the heat. Dust mass profiles of two of these heats are shown in Fig. 6 and show a more erratic variation compared to more 'typical' profiles such as Fig. 2. It should be noted that many of the dust mass peaks were liberated outside the initial blow period when the largest dust mass spikes normally occur.

The relationship between times of the ore additions and the relative dust mass peaks is shown in Table 5. It should be remembered that there is a residence time of $\sim$3 min before the dust was measured at the sampling point. Some of the peaks correspond with the ore addition times, while others are syncopated. It is a possibility that because of significant dust masses, measured during the trials, dust build-up occurred and was periodically dislodged by the pneumatic dust removal system.

It is interesting to compare the dust mass profiles for the heats with ore additions (no WOB additions), shown in Fig. 6, with those for heats with WOB additions (no ore additions), shown in Fig. 7. The profiles including ore additions have dust mass spikes throughout the process, whereas the profiles including WOB additions have the more 'typical' BOS dust mass profile with an initial spike followed by a gradual decline. These results might suggest that the iron ore pellets are more prone to breaking up and contributing to additional dust.

Profiles for the dust mass, and the iron mass contained in the dust, were plotted for comparison in Fig. 8. The iron contained in the dust corresponds very well with the dust mass peaks, suggesting that the effect was due to the ore additions and not any debris from previous heats. The initial dust mass peak composition consists of the initial additions of slag formers top charged to the converter.

Zinc mass

Zinc is very important to the options available for recycling dust through the ironmaking or steelmaking processes. The two main sources of zinc input into the BOS process during the trials were the zinc galvanised scrap charge and the WOBs.

The zinc content of the WOBs was measured between 2·5 and 3 mass-%; however, the zinc content of the galvanised scrap is more difficult to quantify because of the various coating specifications used in the recycled scrap charge. Common hot dip galvanised steel sheets have zinc coatings within the range of 90–1200 g m^{-2}, giving zinc concentrations potentially as high as 4 mass-%.[15] Data from a previous internal scrap sampling study suggest that the zinc content of galvanised steel scrap was expected to be in the region of 2·39 mass-%.[16] Because of this, the strength of the correlations with the galvanised zinc scrap may show variation.

The WOB additions in Table 6 and Fig. 9 showed a strong positive correlation of 0·697 with the zinc mass contained in the dust, which was significant at the 99% level.

However, although the galvanised scrap is a significant source of zinc input, the *R* value correlation of 0·414, shown in Table 7 and Fig. 10, was weaker and <95% significant compared to the WOBs.

Zinc is present in different forms in the galvanised scrap and in the WOBs. In galvanised scrap, it is present as elemental zinc and zinc–iron alloys, and a typical hot dip galvanised coating can consist of five different zinc–iron alloy layers.[17] In WOBs, the zinc is present as particulate oxide compounds, such as zinc oxide and zinc ferrite, bound together as a solid briquette lump.

Temperature and the CO_2/CO concentration ratio of the gas determine the oxidisation behaviour of zinc in the BOS converter,[18] and it is worth noting that galvanised zinc scrap is added to the converter before the hot metal. Its route from volatilisation to capture as dust is very different to the WOBs, which are added during the blow when the physical and chemical

Table 7 Zinc mass correlation with galvanised scrap

Variables	*R* value	*p* value	Significance level
Galvanised scrap addition	0·414	0·181	n/s

Table 8 Zinc mass linear regression model summary

Predictor variables	Dependent variables	*R* value	R^2
WOB additions/t Galvanised scrap/t	Zinc mass/kg	0·853	0·728

environments are aggressively dynamic. It is also possible that zinc losses may have occurred, which were not captured in the measured primary dust, due to the point at which the zinc is liberated from the galvanised scrap in the process.[8]

To investigate the combined effect of galvanised scrap and WOB charge, a multiple linear regression was evaluated. The R value of 0·853 for the zinc mass linear regression model, shown in Table 8, suggests a strong correlation between the predictor variables and the zinc mass contained in the BOS dust. The R^2 value tells us that 73% of the variance of dust mass could be predicted by the combination of the two variables chosen for the model.

The results in Table 9 compare the associated relationship of the predictor variables to the dependent variable, the zinc mass contained in the BOS dust. The significance values for the two predictor values suggest that both were statistically reliable as both were $<0{\cdot}05$ ($>95\%$). The result suggests that for every tonne of galvanised scrap in the initial charge, there was a corresponding increase in zinc mass in the BOS dust of 12·3 kg (1·2 mass-%). In comparison, there was a much higher increase of 35·0 kg (3·5 mass-%) zinc for each tonne of WOB added.

A closer investigation of the effect of WOBs on the dust mass profile and the zinc mass profile was carried out to establish if they were linked. The relative correlations of the dust mass peaks and the zinc mass peaks are compared in Figs. 7 and 11 respectively. The relative dust mass of the two heats both show regular profiles associated with normal BOS processing, with a single sharp initial peak followed by a gradual decline.

In contrast, the profiles of the zinc mass contained in the dust were much more irregular with multiple peaks. This suggests that the additional zinc mass, which correlated with the WOB additions, was not caused by the additional dust mass.

Closer examination of correlations with the WOB additions, shown in Table 10, details the WOB quantity, process addition times and peak times. Unlike the iron ore additions, which correlated with the dust mass produced, the WOB additions show no such correlation. However, the significant correlation with zinc mass contained in the dust, as discussed previously, also shows a relationship between the addition times and the peak times (when accounting for the residence time at the sampling point of ~3 min.

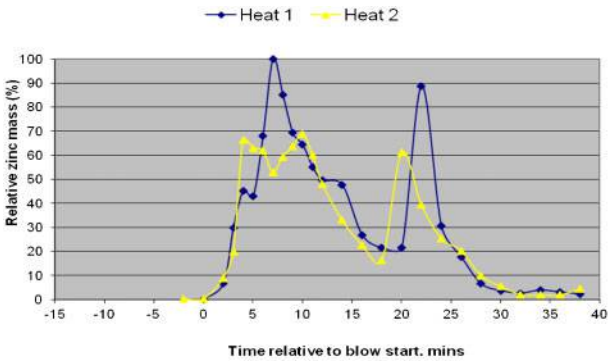

11 Relative zinc mass profiles for heats incorporating multiple WOB additions

Conclusions

The experimental work carried out and presented in this paper compares the effect of variables over a range of different BOS conditions. It involved robust isokinetic sampling and detailed measurement of the dust mass produced and the dust composition over the entire heats of 12 large scale manufacturing trials. The following conclusions have been drawn from the findings.

In terms of the total dust mass produced during heats, and with the dust mass produced outside the blow period, the most significant positive linear correlation was measured for additions of iron ore. In comparison, similar quantities of WOB additions added in a similar way through the blow did not show the same dust mass correlation or peak mass flows. It is not clear from this study why the iron ore differs so significantly from the WOBs. It is possible that the ore alters the slag composition and increases foaming and dust release or that the smaller ore pellets were retained more easily in the slag phase compared to larger WOB briquettes, or alternatively, that the ore picked up moisture contamination during stock handling leading to steam explosion during the rapid heating associated with material charging.

Although no correlation was measured for the WOB additions with the dust mass, a strong linear correlation

Table 9 Zinc mass linear regression coefficients and significance results

Predictor variables	Dependent variables	Regression coefficients	Significance
WOB additions/t	Zinc mass/kg	35·0	0·002
Galvanised scrap/t		12·3	0·020

Table 10 Timings of WOB additions relative to blow start

	Blow duration/min	WOB addition/t	Addition time relative to blow start/min	Significant peak times relative to blow start/min
Heat 119	3·0	+2	+4	
	2·2	+4	+7	
	5·3	+19	+22	
Heat 218	6·0	+2	+4 to 10	
	3·9	+17	+20	

was measured with the zinc mass contained in the dust. This correlation also agreed with peaks observed in the zinc mass profile that corresponded well with the addition times. No linear correlation was found with the galvanised scrap charge, but regression analysis showed a strong associated correlation between the zinc mass and the galvanised scrap and WOB additions, and 73% of the zinc mass variance could be predicted by the combination of those two variables chosen for the model.

Acknowledgements

The authors express their gratitude to Tata Steel UK for their support of this study and the practical assistance by C. Grainger and F. Abbott of Tata Steel UK.

References

1. H. T. Makkonen, J. Heino, L. Laitila, A. Hiltunen, E. Pöyliö and J. Härkki: 'Optimisation of steel plant recycling in Finland: dusts, scales and sludge', *Resour. Conserv. Recycl.*, 2002, **35**, (1–2), 77–84.
2. D. Offenthaler, J. Antrekowitsch and A. Edlinger: 'Zinc containing steel mill dusts – between recycling and landfilling', Proc. REWAS'04 – Global Symp. on 'Recycling, waste treatment and clean technology', Madrid, Spain, September 2005, TMS, 2133–2141.
3. Environment Agency: 'Hazardous waste, interpretation of the definition and classification of hazardous waste – technical guidance WM2', Environment Agency, Bristol, UK, 2011.
4. R. L. Nyirenda: 'The processing of steelmaking flue-dust: a review', *Miner. Eng.*, 1991, **4**, (7–11), 1003–1025.
5. C. Delhaes, A. Hauck and D. Neuschutz: 'Mechanisms of dust generation in a stainless steelmaking converter', *Steel Res.*, 1993, **64**, (1), 22–27.
6. I. E. Doronin and A. G. Svyazhin: 'Properties of steelmaking dust and the mechanism of its formation', *Metallurgist*, 2012, **55**, (11–12), 879–886.
7. N. Y. Ma: 'On the separation of zinc from dust in ironmaking and steelmaking off-gas cleaning systems', Proc. TMS Annual Meet., March 2008, TMS, 547–552.
8. J. Steer, C. Grainger, A. Griffiths, M. Griffiths, T. Heinrich, A. Hopkins: 'Characterisation of BOS steelmaking dust and techniques for reducing zinc contamination', *Ironmaking Steelmaking*, 2014, **41**, (1), 61–66.
9. T. Heinrich, A. Griffiths, J. Steer, M. Griffiths and A. Hopkins: 'In-line sampling of basic oxygen steelmaking dust', Proc. 5th World Conf. on 'Sampling and blending', Santiago, Chile, October 2011.
10. European Commission: in 'Best available techniques reference document on the production of iron and steel', (ed. I. P. P. a. Control); 2010, Joint Research Centre, Institute for Prospective Technological Studies, Sustainable Production and Consumption Unit, European IPPC Bureau.
11. A. Gritzan and D. Neuschütz: 'Rates and mechanisms of dust generation in oxygen steelmaking', *Steel Res.*, 2001, **72**, (9), 324–330.
12. L. Nedar: 'Dust formation in a BOF converter', *Steel Res.*, 1996, **67**, (8), 320–327.
13. L. M. Simonyan and N. M. Govorova: 'Features of dust formation in the oxygen-blowing of melts and possible uses of captured dust', *Metallurgist*, 2011, **55**, (5–6), 450–458.
14. R. Tsujino, M. Hirai, T. Ohno, N. Ishiwata and T. Inoshita: 'Mechanism of dust generation in a converter with minimum slag', *ISIJ Int.*, 1989, **29**, (4), 291–299.
15. B. Ozturk and R. J. Fruehan: 'Vaporization of zinc from steel scrap', *ISIJ Int.*, 1996, **36**, S239–S242.
16. P. J. Koros, D. A. Hellickson and F. J. Dudek: 'Issues in recycling galvanized scrap', *Ironmaking Steelmaking*, 1996, **23**, (1), 21–27.
17. A. R. Marder: 'Metallurgy of zinc-coated steel', *Prog. Mater. Sci.*, 2000, **45**, (3), 191–271.
18. W. Pluschkell and D. Janke: 'Thermodynamics of zinc reactions in the BOF steelmaking process', Proc. 75th Steelmaking Conf., Toronto, Ont., Canada, April 1992, ISS, 717.

Characterisation of BOS steelmaking dust and techniques for reducing zinc contamination

J. Steer*[1], C. Grainger[2], A. Griffiths[1], M. Griffiths[1], T. Heinrich[1] and A. Hopkins[1]

The basic oxygen steelmaking (BOS) process generates a significant amount of iron bearing dusts, and the recovery of these affects the economics and sustainability of the process. However, zinc contamination of the dust restricts how much can be recovered through the process. An inline sampling system was used to isokinetically sample primary BOS dust from the slurry pipe of a 248 m^3 capacity BOS converter at Tata Steelworks Port Talbot (UK). The process was benchmarked with low galvanised scrap trials and control trials before investigating a new in-process zinc separation technique. This trial involved holding galvanised scrap in a hot converter purged with nitrogen, to volatilise the zinc from the primary dust system for capture in the secondary dust system, before the blow. Using this technique, the zinc contamination of the primary BOS dust was reduced by up to 52% of the initial zinc mass contained in the galvanised scrap charge.

Keywords: Basic oxygen steelmaking, Dust, Zinc, Scrap, Volatilisation

Introduction

Many thousands of tonnes of iron bearing dusts are produced each year from steelmaking plants, and reusing these is a valuable way of recovering 'lost' iron and improving yield; this plays a major role in the sustainability of steel manufacture both environmentally and economically.[1,2] These dusts represent an environmental liability if they are not recycled, as they are usually classified as hazardous waste because of heavy metal constituent compounds.[3,4]

Dusts produced during the basic oxygen steelmaking (BOS) process are generally contaminated with zinc, either from the raw materials used or particularly from the process of recycling zinc galvanised scrap during manufacturing.[5–7] Zinc is not easily removed from BOS dust, and typically, the levels are too low for economical recovery by external processors such as smelters. However, high levels of iron and the environmental burden of disposal are a worthwhile reason for dust recovery through the iron or steelmaking processes.

Basic oxygen steelmaking dust can be recycled through the steelmaking process by the manufacture and incorporation of waste oxide briquettes (WOBs) made from the waste dusts. Alternatively, they can also be recycled through the blast furnace route via the sinter plant. However, zinc contamination in the blast furnace can lead to operational issues such as accretions and wear of the refractory lining, so it is limited to 0·3 kg Zn $tonne^{-1}$ of hot metal.[8–11] Unfortunately, large quantities of the dust are often stockpiled. Iron can be recovered, and zinc contamination can be removed, in BOS dusts using pyrometallurgical and hydrometallurgical techniques; however, there is an energy, material and process cost associated with these methods.[4]

This work involved full scale manufacturing testing in a 248 m^3 capacity BOS converter, with the aim of investigating if zinc contamination in the BOS dust could be reduced by holding galvanised scrap in a hot BOS converter before the blow.

This paper assesses the impact of charging different amounts of galvanised scrap, characterises the zinc contamination of BOS dust and analyses the impact of the different scrap charges by measuring the mass and concentration of the zinc in the BOS dust extraction systems.

Methodology

Zinc metal has a boiling point of 907°C, and laboratory studies showed that it can be completely volatilised from a galvanised metal surface when heated in an inert atmosphere at 900°C for 15 min.[12,13]

To investigate this at an industrial scale, galvanised scrap was held in the hot converter for up to 15 min before the addition of the molten iron. The temperature in the converter was not measured on a continuous basis, but typical spot measurements post-tapping are in the region of 1600°C, and temperatures above 1000°C are recorded for up to 2 h post-tapping.[14]

To potentially increase the rate of vaporisation, the bath agitation system (BAP), which is used to purge nitrogen through the bottom of the converter to facilitate mixing, was increased to enhance the diffusion of zinc from the liquid and to prevent oxidation of the zinc in the converter.[15] For the low zinc and control

[1]Cardiff School of Engineering, Cardiff University, Queen's Buildings, The Parade, Cardiff CF24 3AA, UK
[2]Tata Steel UK, Port Talbot, UK

*Corresponding author, email SteerJ1@cardiff.ac.uk

Published by Maney on behalf of the Institute
Received 31 July 2012; accepted 25 January 2013
DOI 10.1179/1743281213Y.0000000106

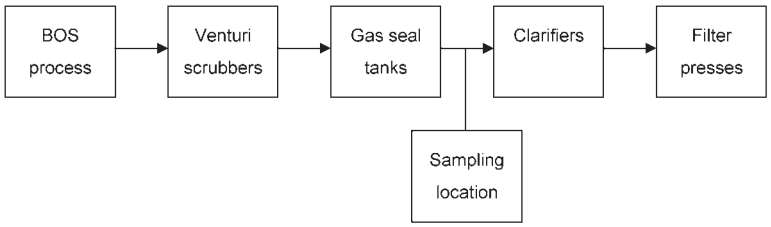

1 Sampling location of primary dust extraction system

trials, a total flow of 515 $Nm^3\ h^{-1}$ was used, whereas for the hold trials, where the maximum volatilisation was required, the BAP was increased to 1600 $Nm^3\ h^{-1}$ during the hold period.

At Tata Steelworks Port Talbot (UK), there are two main dust extraction systems on the BOS converters: a primary wet system that collects the dust from the offgas using venturi water scrubbers, and a secondary dry system using filter bags, which collects dust from the area around the converters and the roof space in the BOS building.

By tilting the converter during the scrap holding stage, towards the secondary dust extraction system, the aim was to divert volatilised zinc away from the primary dust system for collection in the secondary system. This project was initiated during a period of reduced production when there was sufficient time in the production schedule to accommodate a scrap holding period.

Trial conditions

The following specific production trial heats were arranged to investigate typical baseline steelmaking conditions and low galvanised scrap conditions and to maximise the effect of a galvanised scrap hold:

(i) control heats (×2) (20 t charge of galvanised scrap; no scrap hold; BAP purge levels ~515 $Nm^3\ h^{-1}$; secondary dust fans at ~50% of maximum)
(ii) low zinc heats (×3) (no galvanised scrap charge; no scrap hold; BAP purge levels ~515 $Nm^3\ h^{-1}$; secondary dust fans at ~50% of maximum)
(iii) galvanised scrap hold heats (×2) (20 t charge of galvanised scrap; up to 15 min scrap hold time; BAP purge levels ~1600 $Nm^3\ h^{-1}$; converter tilting and rocking; secondary dust fans ~90% maximum; primary dust fans reduced during hold).

Sampling and analysis

The primary dust extraction from the BOS offgas system uses a wet scrubber system that collects the dust as a slurry first in seal tanks and then transferred to clarifiers for settlement and dewatering before filter pressing.

In order to obtain inline data of the variation in primary dust, a sampling system was installed to sample the slurry isokinetically. Figure 1 shows the location of the pipe carrying the BOS dust slurry at flowrates up to 15 000 L min^{-1}.[16] Samples (10 L) were taken at regular intervals, every 2 min outside the blow and every minute during the blow, while flow measurements were taken every second using a Marsh McBurney Flo-dar open channel flowmeter. The secondary dust samples were dip sampled from a holding silo.

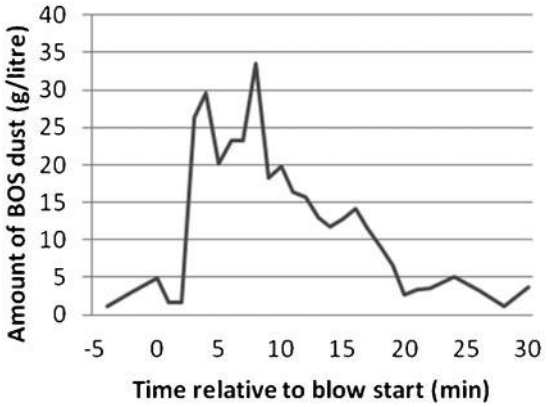

2 Basic oxygen steelmaking dust generation during control heat 1

Samples were analysed for solids content, particle size and sieve classification to determine the particle size and zinc mass distribution. The metal concentration and chemical composition were determined using a Perkin Elmer Optima 2100DV inductively coupled plasma spectrometer and a Philips 3830 PW X-ray diffractometer (XRD) respectively, and selected samples were analysed using a scanning electron microscope (SEM).

Results and discussion

Dust formation

European 'best available technique' figures for the quantity of dust generated from a BOS converter range from 15 to 20 kg t^{-1} of liquid steel.[17] Dust formation in a BOS converter has been studied by various researchers, and the dominant mechanisms are the ejection of fine metal and slag droplets caused by bursting CO bubbles in the melt, vaporisation and spitting of material, and entrainment of fines during top charging material additions.[5,15,18–20]

Figure 2 shows a 'typical' rate of dust extracted by the primary extraction system (g L^{-1}) against time. These figures were normalised to the oxygen blow start at 0 min. The BAP nitrogen flowrate during the scrap addition was 515 $Nm^3\ h^{-1}$, which is around one-third of its maximum. A time lag was measured between blow start and the rapid increase in dust levels, which corresponds to the residence time for the dust to reach the sampling point, between 3 and 4 min, depending on the dust slurry flowrate. An initial high dust mass peak occurred at the start of the blow followed by a steady decrease in the dust generation rate until the blow end after ~20 min. Occasional dust peaks were measured after the blow due to top charging of slag formers and

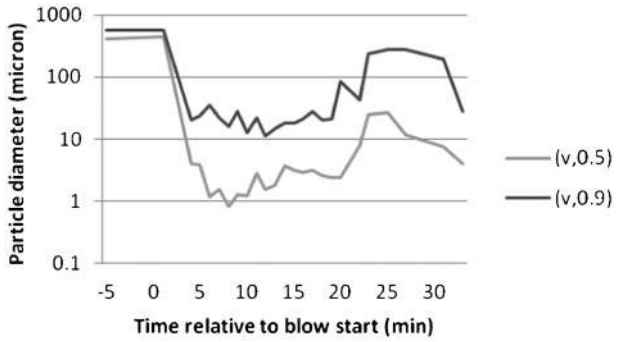

3 Particle size distribution during control heat 1

coolants. Decreasing carbon content in the melt, and the formation of a filtering slag, means that less metal droplets are ejected and therefore less dust is produced over blowing time.[18]

Zinc compounds found in BOS dusts

Because of the high vapour pressure of zinc at steelmaking temperatures, typically ~1600°C, the suitable thermodynamics for dissolution, and the high production rate of process gas, zinc effectively vapourises out of the melt.[21] The majority of zinc contained in the scrap is liberated out of the molten metal, leaving final zinc levels in steel and slag <50 ppm.

After zinc volatilises from the converter, the zinc vapour gets transported away in the offgas system. Temperature and the CO_2/CO concentration ratio of the gas determine the oxidisation behaviour of zinc.[21] The average measured BOS gas was 14%CO_2 and 65%CO. Owing to the closed hood offgas system, the ratio changed only marginally during a blow, shifting from 25%CO_2 and 55%CO at the beginning of the blow to 12%CO_2 and 75%CO at the end. The slightly higher oxidisation potential of the gas at the later stages of the blow has only a marginal impact on the oxidisation behaviour. At the gas ratios in this order of magnitude, zinc vapour is oxidised readily in the temperature range of 400–600°C; however, oxidisation is suppressed at higher temperatures, which affects what type of zinc compounds are formed.[21]

During the blow, the temperature of the offgas in the turnover section, before the wet scrubber, typically ranges from 800 to 1100°C. Therefore, at the gas CO_2/CO ratios experienced, oxidisation is expected to be suppressed, causing zinc to stay in its vapour phase longer; consequently, the zinc will have increased opportunity to react with iron to form zinc ferrite ($ZnFe_2O_4$) instead of zinc oxide (ZnO).

Zinc can be extracted from ZnO using hydrometallurgical extraction under relatively mild acid or alkaline conditions. However, $ZnFe_2O_4$ is very stable and insoluble in most acidic, alkaline and chelating media under mild conditions, and so, it is difficult to recover by hydrometallurgical processes. The more aggressive conditions required to extract zinc from the ferrite often increases the extraction of iron as well and reduces the benefits of the recovery process.[22]

Figure 3 shows the variation in mean particle size diameters against the blow time for the primary dust of control heat 1. The two lines show that $D_{(v,0\cdot5)}$ and $D_{(v,0\cdot9)}$ correspond to 50 and 90% of sample volume, which is below the quoted mean particle size diameter.

For the periods before and after the blow, the samples had a much higher mean particle size diameter, up to 567 and 279 μm respectively. However, during the blow period, when particle collisions are increased by the high velocity injection 'blowing' of oxygen, 90% of the dust particles had a measured mean particle size diameter of <36 μm.

Further investigation using an SEM is shown in Fig. 4 for the periods before, during and after the blow. The sample was also classified into different particle sizes by wet sieving, and the average zinc contents for each range are shown in Table 1.

Figure 4*a* shows the fine particles formed during the blow period, which are often submicrometre and form agglomerates, typically below 63 μm; they make up to 72·5 mass-% and are mainly iron. The particles are produced over the complete blowing period, but production rate decreases with time. When analysed more closely using energy dispersive X-ray spectroscopy (EDAX), the SEM images of this range indicate a broadly uniform distribution of zinc through the sample; this makes it more difficult to separate the zinc from the dust mixture.

The results shown in Table 1 indicate that during a 'typical' heat, the highest average zinc content of 6·7% was associated with these fine particles. Similar findings were observed after sieving other trial heats. Zinc levels up to 15% were measured for some 'spot' samples in the first half of the blow, before the zinc levels decrease during the second half. The higher temperatures, and the CO_2/CO offgas ratio during the blow, may facilitate the formation of zinc ferrites in these dusts, thus making these compounds more difficult to treat.

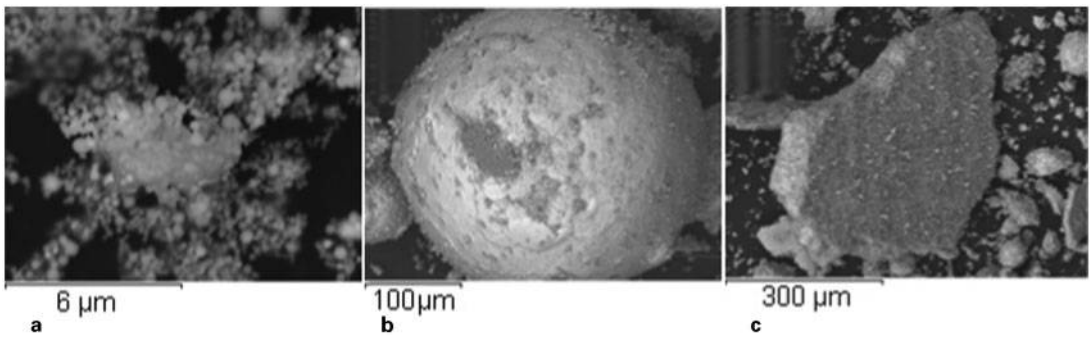

a Fine particles formed during blow period; *b* Spherical particles formed outside blow period; *c* Angular particles formed during initial blow period

4 Images (SEM) of most distinctive dust particles

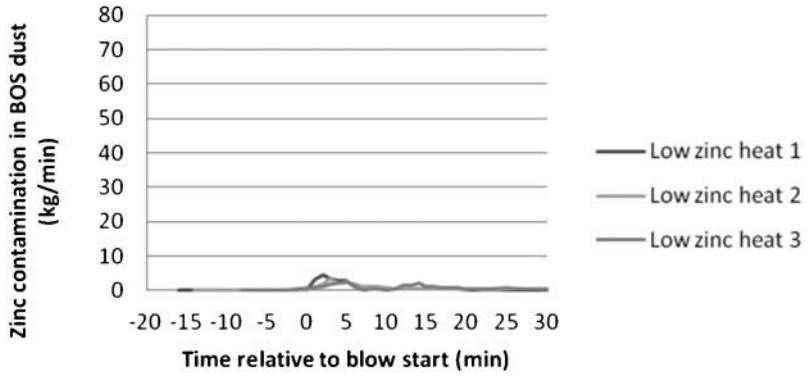

5 Zinc contamination in primary dust low zinc heats 1–3

The image in Fig. 4*b* shows spherical particles produced after hot metal charging, and outside of the blow period as 'carry over' material, EDAX analyses of these show that they are predominately composed of iron. They are typically in the region of 63–106 μm and account for 6·5% of the dust mass. It should be easier to separate the zinc compounds attached to these iron spheres compared to those shown in Fig. 4*a*, because they are more discreet particles.

Figure 4*c* shows the angular shaped particles predominantly found at the beginning of the blow. They account for a 21% share of the dust mass between 107 and 850 μm and typically consist of top charged material like dolomite and lime (Ca) or remains of the desulphurisation slag (S, Na and K). The EDAX results indicate that zinc rich compounds are attached to the surface. As with Fig. 4*b*, the discreet zinc compounds should be more amenable to separation techniques such as hydrocyclone and hydrometallurgy.

The two most commonly identified zinc phases in steel and iron making dusts are zincite (ZnO) and zinc ferrite ($ZnFe_2O_4$), plus the possibility of complex ferrites such as $(ZnMnFe)_2O_4$.[23–25] However, in the composite sample from control heat 1, only zincite (ZnO) was identified by the XRD, but the limit of detectability of some crystalline phases can be up to 5% depending on the strength of their response. It is well understood that minor amounts of certain crystalline phases can disappear in the background.[26]

Zinc mass variation during different steelmaking process conditions

The concentration of zinc contained in galvanised scrap varies for different coating methods and specifications, depending on the industrial application for the product. Zinc in galvanised scrap is present as pure zinc and zinc–iron alloys. A typical hot dip galvanised coating consists of five different zinc–iron alloy layers.[27] Common hot dip galvanised steel sheets have zinc coatings within the range of 90–1200 g m^{-2}, giving zinc concentrations as high as 4 mass-%.[13] Data from a scrap sampling study suggest that the zinc content of galvanised steel scrap can be expected to be in the region of 2·39%.[11] Based on the 20 t galvanised scrap charge used during the control and hold trials, this would equate to 478 kg zinc per heat.

Low zinc galvanised scrap trial

First, three low zinc scrap trials were run to measure any zinc contamination that might 'bleed' through the offgas system and also to measure any zinc contamination that might be present in the 'non-zinc' scrap charge. Previous studies have shown how difficult it can be to segregate zinc contaminated scrap, but the profiles shown in Fig. 5 for the three trials showed very low levels of zinc, <30 kg in total in the primary BOS dust.

Control trial

Figure 6 shows the profile of the zinc mass collected in the primary BOS dust during the two control trials when 'typical' process conditions and scrap materials were used. The total zinc mass collected in the dust during the trials was 426 and 623 kg respectively. The control trial 2 had a higher zinc mass than trial 1; this was expected due to the addition of zinc containing WOBs during the latter stages of control trial 2.

During control trial 1, the primary dust system collected 426 kg and the secondary system collected 20 kg during the trial heat. The total zinc mass output of 446 kg is consistent with the estimated zinc input for 20 t of galvanised scrap of 478 kg and indicates a close correlation with that of the input. The second control trial showed an increased zinc mass due to the addition of 5·9 t of WOBs. Zinc content of the WOBs was 3 mass-%, therefore contributing an additional 177 kg of zinc. The primary dust system collected 603 kg and the secondary system collected 20 kg during the trial heat. The total zinc mass output of 623 kg was also consistent with the estimated zinc input, indicating that the dust collection system captured the expected zinc mass.

Table 1 Zinc content of BOS dust composite control trial sample classified by wet sieving

	Particle size range classification				
	<20 μm	20–45 μm	45–63 μm	63–106 μm	107–850 μm
Mass/%	67·4	3·9	1·2	6·5	21·0
Zinc/%	6·7	2·0	0·6	0·9	0·7

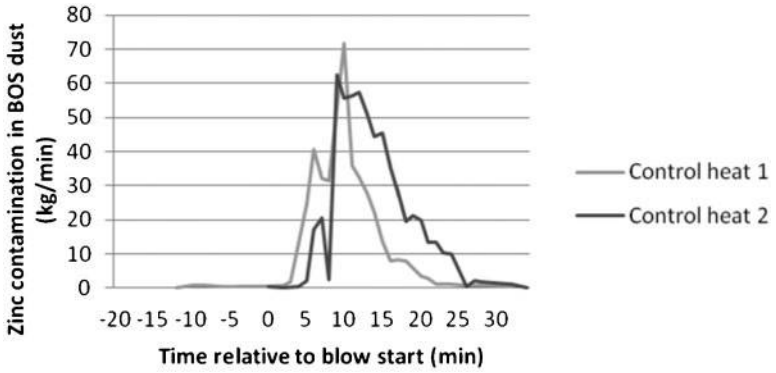

6 Zinc contamination in primary dust control trial heats 1 and 2

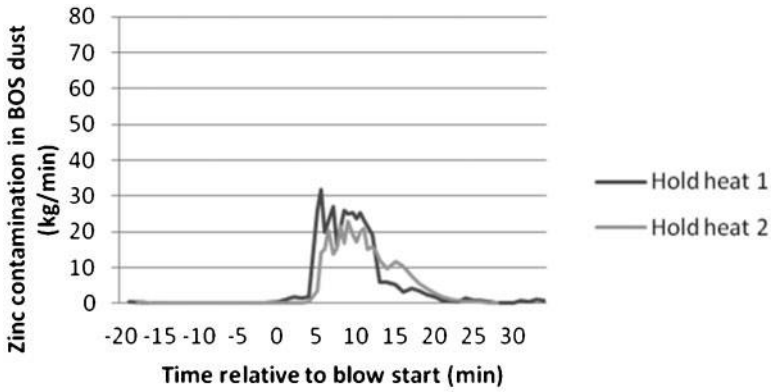

7 Zinc contamination in primary dust hold heats 1 and 2

Galvanised scrap hold trial

In Fig. 7, the profile of zinc mass collected in the primary BOS dust was much lower than the control heats, and the total zinc measured for the two trials was 234 and 206 kg respectively for scrap hold times of 11 and 15 min. Compared to the approximate theoretical mass of zinc calculated for 20 t of galvanised scrap of 478 kg, the hold trials show a very large reduction.

The zinc mass flows shown for hold heats 1 and 2 had the same zinc input as control trial 1; however, the masses of 234 and 206 kg collected were much lower than the 426 kg during control trial 1. Thus, the residual heat of the converter, scrap holding, tilting of the converter, and increasing secondary extraction fans diverted 52% of the zinc contained in the scrap away from the primary BOS dust.

However, zinc capture in the secondary dust silo was not successfully measured, potentially because the hold trials were carried out during double converter operation when the secondary dust from both converters was collected in the same silo. Additionally, the secondary dry dust collection system had a measured residence time of 45 min for the dust to travel through the filter bag system before collection in the silo, making it very difficult to correlate changes in zinc contents with changes in the process. Furthermore, it was not possible to arrange an empty holding silo at the beginning and end of the trials to correlate accurately with the start and finish of the trial.

Conclusions

Seventy-one per cent of the BOS dust mass produced during the control trial was zinc rich fine particles with a size of <45 μm. The remaining 29% of the mass was a coarse dust made up predominately of iron spheres, with zinc contamination of $<1\%$, and potentially more suitable for recycling by the blast furnace via the sinter plant.

Oxides of zinc formed outside of the blow period appear to be present as more discreet particles, which are likely to be more suitable for separation. However, those formed during the blow appear to be more agglomerated, due to the conditions of their formation in the offgas system, and are less likely to be separated easily.

By holding the scrap for >10 min in a nitrogen purged, hot converter, the zinc contamination of the primary BOS dust could be reduced by up to 52% of the initial zinc mass contained in the galvanised scrap charge.

Acknowledgements

The authors express their gratitude to Tata Steel UK for their support of this study and the practical assistance by F. Abbott and K. Linsley of Tata Steel UK.

References

1. H. T. Makkonen, J. Heinoa, L. Laitilab, A. Hiltunenc, E. Pöyliöd and J. Härkkia: 'Optimisation of steel plant recycling in Finland: dusts, scales and sludge', *Resour. Conserv. Recycl.*, 2002, **35**, (1–2), 77–84.
2. D. Offenthaler, J. Antrekowitsch and A. Edlinger: 'Zinc containing steel mill dusts – between recycling and landfilling', Proc. Global Symp. on 'Recycling, waste treatment and clean technology', Fundacion Inasmet, TMS, Madrid, Spain, September 2005, 2133–2141.
3. Environment Agency: 'Hazardous waste: interpretation of the definition and classification of hazardous waste – technical guidance WM2', Environment Agency, Rotherham, UK, 2011.

4. R. L. Nyirenda: 'The processing of steelmaking flue-dust: a review', *Miner. Eng.*, 1991, **4**, (7–11), 1003–1025.
5. C. Delhaes, A. Hauck and D. Neuschutz: 'Mechanisms of dust generation in a stainless steelmaking converter', *Steel Res.*, 1993, **64**, (1), 22–27.
6. I. E. Doronin and A. G. Svyazhin: 'Properties of steelmaking dust and the mechanism of its formation', *Metallurgist*, 2012, **55**, (11–12), 879–886.
7. N. Y. Ma: 'On the separation of zinc from dust in ironmaking and steelmaking off-gas cleaning systems', Proc. TMS Annual Meet., New Orleans, LA, USA, March 2008, TMS, 547–552.
8. P. Besta, A. Samolejová, K. Janovská, R. Lenort and J. Haverland: 'The effect of harmeful elements in production of iron in relation to input and output material balance', *Metalurgija*, 2012, **51**, (3), 325–328.
9. G. Y. Kryachko, G. I. Orel, P. A. Vasyuchenko and L. A. Safina: 'Maintaining the working profile of blast furnaces during service', *Metallurgist*, 2005, **49**, (11–12), 424–431.
10. X. Yang, M. Chu, F. Shen and Z. Zhang: 'Mechanism of zinc damaging to blast furnace tuyere refractory', *Acta Metall. Sin.*, 2009, **22**, (6), 454–460.
11. P. J. Koros, D. A. Hellickson and F. J. Dudek: 'Issues in recycling galvanized scrap', *Iron Steelmaker*, 1996, **23**, (1), 21–27.
12. A. Franzen and W. Pluschkell: 'Removal of zinc layers from coated steel strip by evaporation', *Steel Res.*, 2000, **70**, (12), 508–512.
13. B. Ozturk and R. J. Fruehan: 'Vaporization of zinc from steel scrap', *ISIJ Int.*, 1996, **36**, S239–S242.
14. C. Williams: Personal communication, 2013.
15. L. Nedar: 'Dust formation in a BOF converter', *Steel Res.*, 1996, **67**, (8), 320–327.
16. T. Heinrich, A. Griffiths, J. Steer, M. Griffiths and A. Hopkins: 'In-line sampling of basic oxygen steelmaking dust', Proc. 5th World Conf. on 'Sampling and blending', Gecamin, Santiago, Chile, October 2011, 353.
17. European Commission: 'Best available techniques reference document on the production of iron and steel', Joint Research Centre, Institute for Prospective Technological Studies, Sustainable Production and Consumption Unit, European IPPC Bureau, Seville, Spain, 2010.
18. A. Gritzan and D. Neuschütz: 'Rates and mechanisms of dust generation in oxygen steelmaking', *Steel Res.*, 2001, **72**, (9), 324–330.
19. L. M. Simonyan and N. M. Govorova: 'Features of dust formation in the oxygen-blowing of melts and possible uses of captured dust', *Metallurgist*, 2011, **55**, (5–6), 450–458.
20. R. Tsujino, M. Hirai, T. Ohno, N. Ishiwata and T. Inoshita: 'Mechanism of dust generation in a converter with minimum slag', *ISIJ Int.*, 1989, **29**, (4), 291–299.
21. W. Pluschkell and D. Janke: 'Thermodynamics of zinc reactions in the BOF steelmaking process', Proc. 75th Steelmaking Conf., Toronto, Ont., Iron and Steel society, Canada, April 1992, ISS, 717.
22. N. Leclerc, E. Meux and J. M. Lecuire: 'Hydrometallurgical extraction of zinc from zinc ferrites', *Hydrometallurgy*, 2003, **70**, (1–3), 175–183.
23. H. Krztoń: 'Quantitative phase composition of steelmaking dust from polish steel industry', *Solid State Phenom.*, 2010, 31–37.
24. H. Oda, T. Ibaraki and Y. Abe: 'Dust recycling system by the rotary hearth furnace', *Nippon Steel Tech. Rep.*, 2006, **94**, 147–152.
25. J. Vereš, S. Jakabský and M. Lovás: 'Zinc recovery from iron and steel making wastes by conventional and microwave assisted leaching', *Acta Montan. Slovaca*, 2011, **16**, (3), 185–191.
26. T. Hilber, R. Marr, M. Siebenhofer and W. Zapfel: 'Solid/liquid extraction of zinc from EAF-dust', *Sep. Sci. Technol.*, 2001, **36**, (5–6), 1323–1333.
27. A. R. Marder: 'Metallurgy of zinc-coated steel', *Prog. Mater. Sci.*, 2000, **45**, (3), 191–271.

Hydrometallurgy 140 (2013) 34–41

Contents lists available at ScienceDirect

Hydrometallurgy

journal homepage: www.elsevier.com/locate/hydromet

Investigation of carboxylic acids and non-aqueous solvents for the selective leaching of zinc from blast furnace dust slurry

Julian M. Steer *, Anthony J. Griffiths

Cardiff School of Engineering, Cardiff University, Queen's Buildings, The Parade, Cardiff CF24 3AA, United Kingdom

ARTICLE INFO

Article history:
Received 25 March 2013
Received in revised form 5 August 2013
Accepted 11 August 2013
Available online 5 September 2013

Keywords:
Blast furnace dust
Carboxylic acid
Leaching
Zinc extraction
Hydrometallurgical

ABSTRACT

The recycling of iron bearing dusts produced during iron and steel manufacturing processes is vital to the sustainability of these processes; however, contamination of these dusts with zinc increases the difficulty to do this. Blast furnace dust, collected by a wet scrubber system, was sampled and characterised to investigate the removal of zinc to produce a treated residue with low zinc content suitable for recycling through the blast furnace.

This paper examines a leaching process for the dust using different organic carboxylic acids, to establish if they were capable of extracting high levels of zinc and low levels of iron. Prop-2-enoic acid was found to be particularly effective, extracting high levels of zinc up to 85.7% and low levels of iron, 8.5%. The paper also discusses the mechanisms of extraction more specifically for organic carboxylic acids and found that the iron extraction was well explained by the variation in pH and the Bronsted–Lowry theory; whereas zinc extraction was well explained by substituent group effects and the Lewis acid/base theory.

The novel use of a non-aqueous solvent with prop-2-enoic acid, to minimise the ion solvating ability and proton dissociation, was found to reduce the level of iron extraction from 8.5% to 0.1% without detrimental effect on zinc extraction when leaching. A range of mineral and carboxylic acids were also tested to investigate and compare the effect of pH and chemical structure on the leaching efficacy.

1. Introduction

Reuse and recycling plays a major role in the sustainable manufacture of steel both environmentally and economically (Makkonen et al., 2002; Offenthaler et al., 2005). Many thousands of tonnes of iron bearing dusts are produced per year from blast furnace ironmaking, and reusing these is a valuable way of recovering lost iron and improving yield. In addition to the revenue associated with the dusts, they also represent an environmental liability if they are not recycled, as these dusts are usually classified as a hazardous waste because of their constituent compounds such as heavy metals (Environment-agency, 2011; Nyirenda, 1991).

Dusts produced during iron and steel making are generally contaminated with zinc; either from the raw materials used, or particularly from the process of recycling zinc galvanised steel during manufacturing (Delhaes et al., 1993; Doronin and Svyazhin, 2012; Ma, 2008). Typical levels of contamination are often too low for economic recovery of zinc by external processors such as smelters. However, high levels of iron, and the environmental liability associated with its disposal, are a worthwhile reason for dust recovery through the iron or steelmaking processes.

In the reducing atmosphere of an ironmaking blast furnace, temperatures can reach in excess of 2000 °C; any zinc compounds that are present are chemically reduced to metallic zinc with a relatively low boiling point (907 °C) for a metal. The zinc can be volatilised into the off gas system where it can oxidise and re-condense in the cooler regions of the furnace; it deposits either onto cooler surfaces or onto dust particulates such as iron and carbon.

Zinc contamination in the blast furnace can lead to operational issues such as accretions and wear of the refractory lining, and these limit how much zinc can be present in the furnace (Besta et al., 2012; Kryachko et al., 2005; Yang et al., 2009). Consequently, many techniques have been explored to either eliminate or reduce the zinc contamination so that greater amounts of dusts can be recovered more easily (Callenfels and Je, 2004; Das et al., 2007; Duan et al., 2012; Heard et al., 2002; Kurunov, 2012; Ma, 2008; Oda et al., 2006). A successful method of removing zinc from the blast furnace dust slurry would allow more dust to be recycled through the blast furnace; potentially allowing the recovery of iron units from other zinc contaminated dust sources, such as those generated by basic oxygen steelmaking (BOS).

In the blast furnace area three main types of process dusts are usually collected: A dry dust collected around the tapping area; a dry dust separated from the off gas by a gravity dust catcher; and blast furnace dust slurry collected by a wet scrubber system. This paper explores the hydrometallurgical leaching of zinc and iron from a blast furnace dust slurry collected from an integrated steelworks. The aim of the work was to

* Corresponding author. Tel.: +44 29 20870599; fax: +44 29 20874939.
E-mail address: SteerJ1@cardiff.ac.uk (J.M. Steer).

0304-386X/$ – see front matter © 2013 Elsevier B.V. All rights reserved.
http://dx.doi.org/10.1016/j.hydromet.2013.08.011

investigate the efficacy and selectivity of different carboxylic acids to leach high quantities of zinc and only low quantities of iron, to produce a residue suitable for recycling through the blast furnace.

Best available technique data for the mass of slurry produced from a blast furnace ranges between 2 and 22.5 kg/t of hot metal produced and for an annual ironmaking output of 3.5 Mt this would give between 7000 and 78,750 t/a (Rainer Remus et al., 2013). For a successful leaching process of a slurry with an iron content of 35% by mass, this would represent between 2450 and 27,563 t/a of iron which could be recycled through the blast furnace and add to the iron yield. This would realise a significant economic and sustainability saving associated with the iron; however, such a leaching process would also require the recovery of the extracted zinc and reuse of lixiviate.

2. Acidic leaching of zinc from steelmaking dusts

A well-studied and utilised technique for the removal of zinc from basic oxygen steelmaking dust (BOS) and electric arc furnace dust (EAF) is hydrometallurgical leaching (Havlik et al., 2012a; Langová et al., 2009; Leclerc et al., 2002; Oustadakis et al., 2010; Trung et al., 2011). Leaching is often used as the first step of a process to solubilise metal cations in solution for subsequent separation and purification using techniques such as electrowinning to obtain a high quality product in its own right. However, it can also be used as a technique to remove the zinc from the dust so that the dust can be reused directly in the ironmaking process.

This technique has been applied to blast furnace dust (BF) by Havlik et al., who investigated the use of 1 mol/L sulphuric acid and measured up to 80% extraction of zinc at ambient temperature, with 'relatively low' amounts of leached iron (Havlik et al., 2012b). Veres et al. used microwaves and 1 mol/L sulphuric acid to leach zinc; 5 min at 160 W was used to obtain 86% zinc extraction with only 4% iron extraction (Vereš et al., 2011).

Acidic leaching of BF dust with hydrochloric acid was carried out by Van Herck et al. who obtained 78% zinc extraction with concentrated hydrochloric acid. However, by changing the reduction/oxidation (redox) potential using the salt $FeCl_3$, they obtained up to 98% zinc extraction, although this resulted in 49% extraction of the iron (Van Herck et al., 2000). Soria-Aguilar investigated the effect of oxidants using ozone, with different acid and alkaline solutions, to obtain zinc extractions from 5% to 80% (Soria-Aguilar et al., 2008). Huang et al. found that sulphuric acid gave 74% extraction of the zinc when they investigated different lixiviants such as ferric chloride and amines (Huang et al., 2007). Asadi et al. also used 1 mol/L sulphuric acid at ambient temperature to obtain zinc extraction around 80% with only 7% iron extraction (Asadi Zeydabadi et al., 1997).

3. Experimental

3.1. Materials

The sample used in this paper was a composite blast furnace dust slurry sample taken from settling lagoons at a selection of 5 separate points, in this way the composite sample included dust produced and collected over a period of 1 month (British-standards, 2006a). These samples were combined, mixed, and sub-sampled to give a homogenous sample which was as representative of production over a month as possible (British-standards, 2006b).

A particle size classification was carried out by wet sieving using five sieves of 20 μm; 45 μm; 63 μm; 106 μm; and 850 μm. The results shown in Fig. 1 indicate that the [d50] median value of the particle size distribution was 14.6 μm and the [d80] was 45.2 μm.

The sample was oven dried for further analyses and the chemical composition was determined by atomic emission spectroscopy, using a Perkin Elmer Optima 2100DV inductively coupled plasma spectrometer. Table 1 shows the average chemical composition of the blast furnace dust slurry from monthly composite samples taken from the dust lagoons over a period of 18 months.

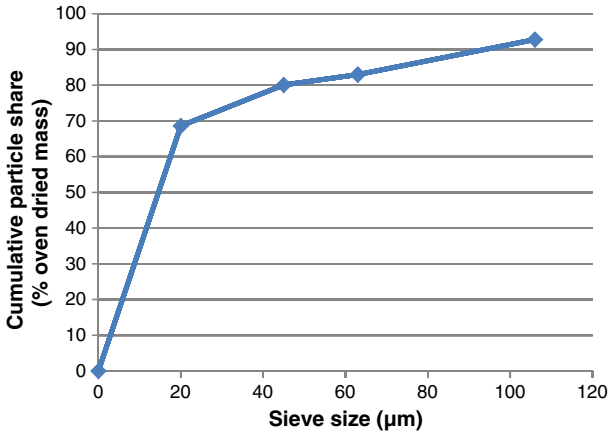

Fig. 1. Particle size classification obtained by sieving.

The sample used in this study was taken during a period of higher than typical zinc levels. It was taken to specifically investigate methods of treatment as recycling this dust through the ironmaking process, without treating it to reduce the level of contamination, would be very problematic. Although the long term average zinc content shown in Table 1 was 0.6%, the study sample was measured at 2.25%.

The main components of the dust are the iron and carbon, both of which are constituents of the raw material of iron ore and coke into the blast furnace. The other components are present as contaminants and the standard deviation shows some large variations in the composition of this material; this is a reflection of variations in the raw material charge and operational conditions in the blast furnace.

Closer examination of the iron and carbon content, plus the zinc contamination, associated with the different particle size fraction collected by wet sieving, is shown in Table 2. In terms of zinc, the highest levels are associated with the fine particles, whereas with carbon the highest levels are associated with the coarse particles. In comparison, high levels of iron are associated with fine and coarse particles with lower levels in the particle size range between 45 μm and 850 μm.

The mineralogical composition of the sample, shown in Fig. 2, was determined using a Phillips 3830 PW X-ray diffractometer (XRD). The three main crystalline mineral phases of iron were identified as hematite, wuestite and magnetite as expected from the iron ore. Carbon, from the coke or coal input into the blast furnace, was also identified along with calcite from the limestone flux charge which is used to remove impurities from the iron in the furnace.

The two most commonly identified zinc phases in steel and ironmaking dusts are zincite (ZnO) and zinc ferrite, plus the possibility of complex ferrites such as $(ZnMnFe)_2O_4$ (Oda et al., 2006; Vereš et al., 2011).

In the blast furnace dust slurry sample used in this study zincite (ZnO) was the only form identified by the XRD; however, it is well understood that minor amounts of certain crystalline phases can disappear in the background (Hilber et al., 2001).

Scanning electron micrographs (SEM) of the blast furnace dust slurry, shown in Fig. 3, were run to investigate the particle distribution, size and composition. Since heavy elements (high atomic number) backscatter electrons more strongly than light elements (low atomic

Table 1
Average chemical composition of blast furnace dust slurry samples (oven dried mass %).

Component	Fe	Ca	Si	Al	Mg	Mn	C	Zn
Mass % (standard deviation)	36.2 (7.7)	5.0 (1.8)	4.6 (0.5)	1.8 (0.4)	1.0 (0.4)	0.3 (0.1)	18.5 (11.3)	0.6 (0.6)

Table 2
Chemical composition of a wet sieved blast furnace dust slurry sample (oven dried mass %).

	Particle size classification range (%)					
	<20 μm	20–45 μm	45–63 μm	63–106 μm	106–850 μm	>850 μm
Mass (%)	68.6	11.5	2.9	9.8	6.9	0.3
Zn (%)	3.2	0.5	0.4	0.4	0.3	0.1
Fe (%)	39.1	30.3	16.9	7.8	2.8	44.7
C (%)	21.8	43.6	67.3	80.8	85.4	n/a

number), they appear brighter in the image. The pictures show some large particles less than 400 μm which were dark; and lighter coloured smaller particles and agglomerated groups of light coloured small particles.

The larger, lower atomic number particles are consistent with the results in Table 2 which showed that particles between 63 μm and 850 μm were predominately carbon, representing 16.7% of the total sample mass. The smaller particles appear to agglomerate during drying for SEM preparation of the samples, but those less than 45 μm were brighter, which corresponds to concentrations of heavy elements such as iron and zinc above 30%.

3.2. Experimental

The leaching experiments were carried out in stoppered 250 mL conical flasks using magnetic stirrer hotplates to stir the samples. 10 g of a sample was added to the flask and 100 g of the lixiviant to give a solid:liquid (S:L) ratio of 1:10. Where the samples were heated, a reflux setup, using a water cooled Liebig condenser, was used to ensure that any losses would be minimised. Leaching experiments were run in duplicate and analysis of each sample was also run in duplicate. The relative mean for the extractions at 95% confidence intervals was 1.4% of the iron extractions and 2.1% of the zinc extractions. Masses and pH measurements were recorded at every stage of the experiments and any evaporative losses were corrected for where required.

After leaching, the solid/liquid mixture was filtered and the solid retentate residue was dried at 60 °C until a constant weight was obtained. The residue was then analysed using a Perkin Elmer Optima 2100DV inductively coupled plasma spectrometer after microwave acid digestion. The aim of the experimental work was to investigate the selective leaching of zinc from the blast furnace dust slurry so that the leached dust could be recycled through the ironmaking process. For this reason the percentage extractions of zinc and iron were calculated using Eq. (1), relative to the initial dust and recovered solid retentate after extraction, using a mass balance method that accounted for extraction mass losses.

$$\frac{\text{Mass of zinc (sample)} - \text{Mass of zinc (solid retentate)}}{\text{Mass of zinc (sample)}} \times 100 \quad (1)$$

Table 3 shows the different parameters used to investigate the leaching of zinc from the blast furnace dust slurry.

4. Results and discussion

It is well proven that zinc can be extracted from blast furnace dust slurry using acidic hydrometallurgical techniques, but it is the selectivity of the chosen acid and extraction conditions that determines if it could be considered for development as an industrial process. In this paper, a variety of carboxylic acids were compared to each other, and to mineral acids, to compare the efficacy and mechanism of the extraction.

Although the main oxidation states of zinc are +1 and +2, it is the +2 which predominates. Typical reactions of ZnO and $ZnFe_2O_4$ with common mineral acids such as H_2SO_4 and HCl are expected to follow the following acid–base reactions (Havlik et al., 2005).

$$ZnO + H_2SO_4 \rightarrow ZnSO_4 + H_2O \quad (2)$$

$$ZnFe_2O_4 + H_2SO_4 \rightarrow ZnSO_4 + Fe_2(SO_4)_3 + H_2O \quad (3)$$

$$ZnO + 2\,HCl \rightarrow ZnCl_2 + H_2O \quad (4)$$

$$ZnFe_2O_4 + 8\,HCl \rightarrow ZnCl_2 + 2\,FeCl_3 + 4\,H_2O \quad (5)$$

It is well documented that different acids and reaction conditions result in variability in how much zinc is extracted, and significant work has been carried out examining the kinetics of these reactions. In their study of the kinetics of dissolution of ZnO in aqueous sulphuric acid solutions, Guśpiel and Riesenkampf highlighted the importance of mass transfer control and found that the ZnO dissolution rate was diffusion-controlled over a wide range of acid concentrations

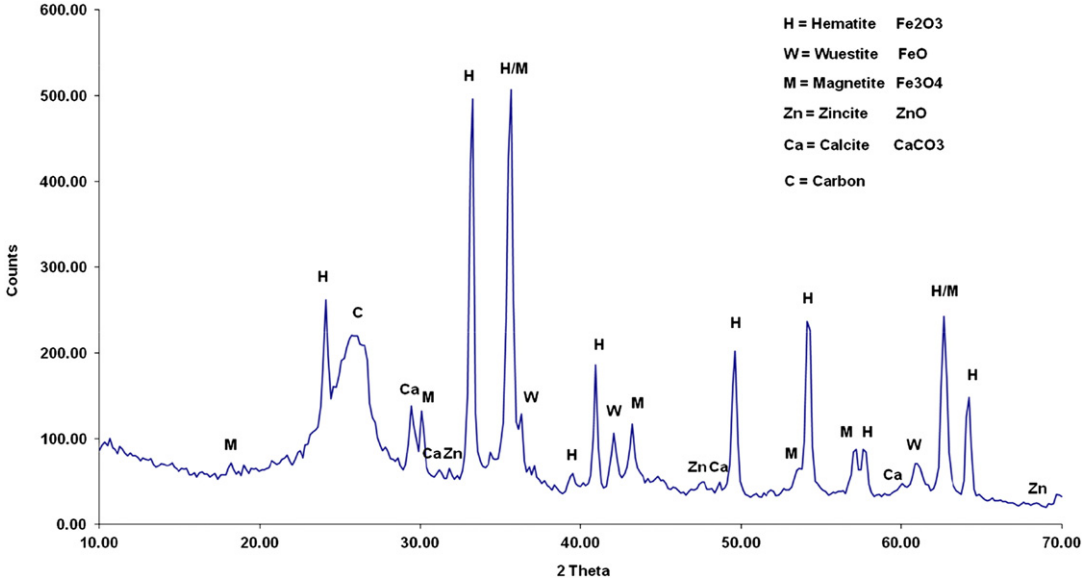

Fig. 2. Qualitative X-ray diffraction analysis of blast furnace dust slurry sample.

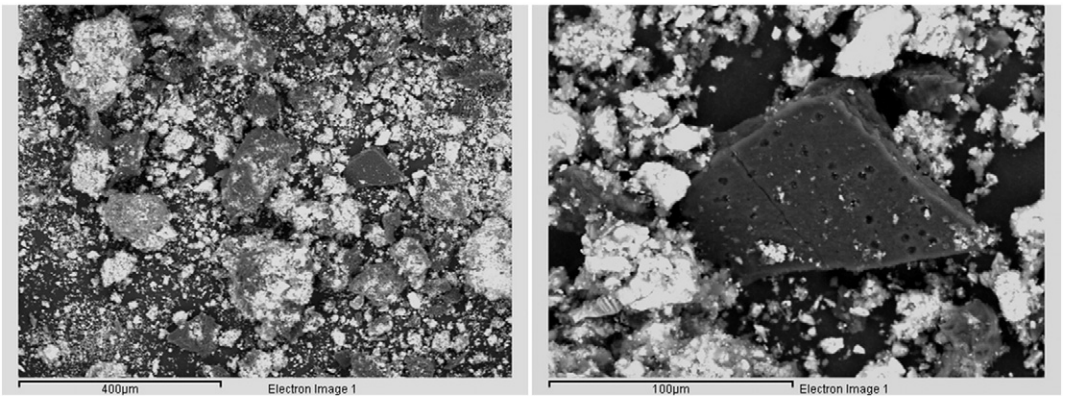

Fig. 3. Scanning electron micrographs of blast furnace slurry dust particles.

(0.1–2 mol/L H_2SO_4) and temperatures (Guśpiel and Riesenkampf, 1993).

In aqueous sulphuric acid, Jandova et al. found that the overall rate of ZnO dissolution appeared to be controlled by mass transport of species between the bulk solution and the particle surface, whereas zinc ferrite dissolves at a chemically controlled rate that is dependent on the acidity. At elevated temperatures they found ZnO reaction to be diffusion controlled in a process that run relatively fast and which was not significantly influenced by the conditions used for the preparation of the samples investigated. However, they also observed that the dissolution kinetics were significantly influenced by the properties of the oxide surface dependent on the oxide sample preparation and purity (Jandova et al., 1999).

It has also been noted in previous work that products of the surface reactions can affect the rate and extent of zinc extraction. Han et al. noted that in oxalate and acetate solutions zinc complexes reached a dissolution equilibrium after a small amount of zinc–ligand complex formation and dissolution, indicating the possibility of a zinc–ligand film layer preventing further reaction and dissolution because of its lower solubility in water (Han et al., 2010).

Guśpiel and Riesenkampf also deduced that considerable adsorption of anions on the oxide surface could form surface complexes. These complexes could contain groups that markedly reduce the effect of hydrogen ion concentration from the acid on the dissolution rate (Guśpiel and Riesenkampf, 1993).

García Rodenas et al. noted that the anions of the acid play an important role through surface complexation of metal ions, enhancement of proton co-adsorption, and labilisation of vicinal metal–oxygen bonds, highlighting the example of Fe(III) oxides' dissolution rates which are enhanced by the presence of reductants, whereas all of the M(II) oxides they studied dissolved faster in the presence of oxidants (García Rodenas et al., 2008).

Table 3
Parameters and experimental conditions used to investigate leaching from blast furnace dust slurry.

Parameter for investigation	Experimental conditions
Acid type	Various acids at 1 mol/L; 24 h; ambient temperature; S:L 1:10
Acid concentration	0–3 mol/L prop-2-enoic; 24 h; ambient temperature; S:L 1:10
Leaching time	2–72 h; 1 mol/L; ambient temperature; S:L 1:10
Leaching temperature	Ambient, 50 °C & 100 °C; 2 h; 1 mol/L; S:L 1:10
Solid:liquid ratio	1:10, 1:1 & 1:2; 24 h; 1 mol/L; ambient temperature
pH effect	1 mol/L; 24 h; ambient temperature; S:L 1:10
Lixiviant re-use	1 mol/L; 24 h; ambient temperature; S:L 1:10
Solvent effects	1 mol/L; 24 h; ambient temperature; S:L 1:10
Salt effects	1 mol/L; 24 h; ambient temperature; S:L 1:10

4.1. Zinc and iron extractions using carboxylic acids

A selection of carboxylic acids with different structures, functionality and acid strength were used to investigate if these partially dissociated organic acids were capable of extracting high levels of zinc.

Although carboxylic acids are only partially dissociated 'weak acids', stabilisation of the carboxylate anion ($RCOO^-$) shown in Eq. (6) could potentially alter the extraction capability. By the consumption of the carboxylate anion in Eq. (7) the concentration of the anion in Eq. (6) decreases and shifts the equilibrium balance to the right, facilitating further dissociation.

$$RCOOH + H_2O \rightleftharpoons RCOO^- + H_3O^+ \quad (6)$$

$$RCOO^- + MO \xrightleftharpoons{(H_3O^+)} RCOOM + H_2O \quad (7)$$

M = metal R = organic substituent group

Table 4 shows the extractions obtained using six different carboxylic acids to compare their acid dissociation constants in water (pK_a); the final post extraction pH; and chemical structure. In addition to the solution pH value, it is well understood that organic compounds such as these can act as Lewis acids and that the substituent groups attached to the carboxylic acid functionality can play an important role. These can affect not only the pK_a but also the stabilisation of reactants and products through processes such as electron rearrangement via the induction, resonance and mesomeric effects.

When comparing the structural analogues prop-2-enoic acid and ethanoic acid the former has an acrylol group ($H_2C{=}CH-CO-R$), the

Table 4
Extraction of zinc and iron using a variety of carboxylic acids at 1 mol/L.

Acid	Formula	pK_a	pH	Extraction	
				Zinc (%)	Iron (%)
Propanedioic (malonic)	$HOOC-CH_2-COOH$	2.8[a] 5.7[b]	1.4	93.9	16.9
Prop-2-enoic (acrylic)	$H_2C{=}CH-COOH$	4.3	3.3	83.1	8.5
2-Hydroxypropane-1,2,3 tricarboxylic (citric)	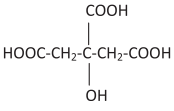	3.1[a] 4.8[b] 5.4[c]	1.0	82.6	32.2
Ethanoic (acetic)	$H_3C-COOH$	4.8	2.9	58.1	2.7
Ethanedioic (oxalic)	$HOOC-COOH$	1.2[a] 4.1[b]	0.8	18.5	31.2
Benzoic acid	C_6H_5-COOH	4.2	3.9	37.0	0.1

[a] First proton dissociation.
[b] Second proton dissociation.
[c] Third proton dissociation.

latter has an acyl group ($H_3C-CO-R$) and both acids have similar pK_a and pH values; however the level of extraction was much better for prop-2-enoic acid (83.1%) compared to ethanoic acid (58.1%). In the case of prop-2-enoic acid, the presence of the π-bonding of the unsaturated group means that the unsaturated α-carbon atom is sp^2 hybridised and the electron density is held closer to the carbon than the σ-bonded saturated CH_3 group in ethanoic acid. The sp^2 carbon atoms of prop-2-enoic acid are less electron donating compared to the CH_3 group of ethanoic acid, which results in less stabilisation of the carboxylate anion and facilitates improved extraction.

The diprotic acids propanedioic and ethanedioic differ structurally by a methylene bridge ($-CH_2-$) only. However, although the pH value for ethanedioic is 0.8 compared to 1.4 for propanedioic, the zinc extraction was only 18.5% compared to 93.9% although its iron extraction was 31.2% compared to 16.9%. It appears that the increased acidity of ethanedioic acid facilitates additional iron extraction, but structural differences result in less zinc extraction.

The results suggest that there are additional mechanisms for the zinc extraction compared to the iron extraction. The zinc extraction might be better explained by substituent group effects from the Lewis acid/base theory. In Eq. (8) the carboxylic acid acts as an electron pair receiver from the non-bonded electrons of the oxygen in zinc oxide. For example, prop-2-enoic acid extracted 83.1% zinc at pH 3.3, compared to ethanedioic which only extracted 18.5% even though the pH was a much lower than 0.8.

$$2\ RCOOH + ZnO \rightleftharpoons (RCOO)_2Zn + H_2O \quad (8)$$

In contrast to this, it would seem that the iron extraction follows the Bronsted–Lowry theory where the carboxylic acid donates protons to the iron oxide, shown in Eq. (9). The results indicate that the iron extraction was more effected by pH with the three highest iron extractions all occurring at low pH values (<1.5).

$$6\ RCOOH + Fe_2O_3 \rightleftharpoons 2\ (RCOO)_3Fe + 3\ H_2O \quad (9)$$

4.2. Zinc and iron extractions using prop-2-enoic acid

Because prop-2-enoic acid was successful at leaching high levels of zinc (83.1%) and low levels of iron (8.5%) it was chosen as the basis of more detailed study. The concentration was varied from 0.15 mol/L to 2.9 mol/L; held for 24 h with constant stirring at ambient temperature; and at a sample and lixiviant (S:L) ratio of 1:10. The results plotted in Fig. 4 indicate that the maximum level of zinc and iron extractions with prop-2-enoic acid occurs at a concentration around 1 mol/L before reaching a plateau, after which the level of extraction remains the same. For this reason, an aqueous solution with a concentration of 1 mol/L would be sufficient for leaching blast furnace dust slurry.

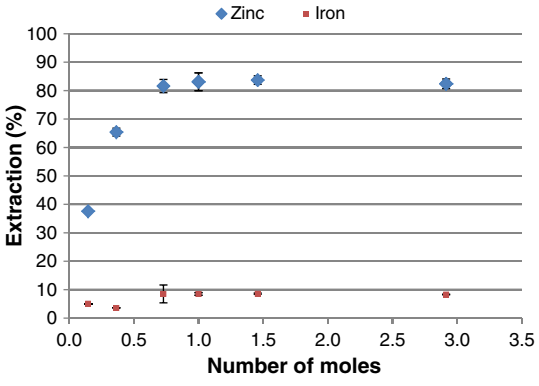

Fig. 4. Extraction of zinc and iron at varying concentrations of prop-2-enoic acid.

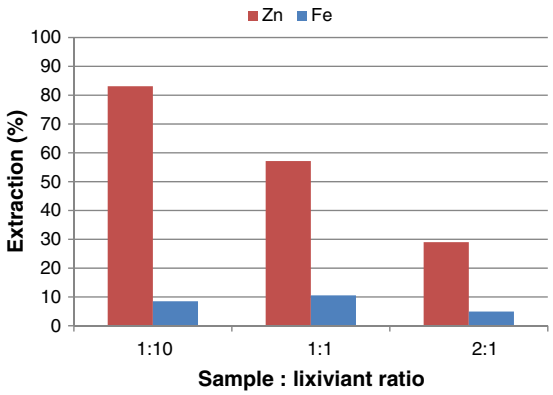

Fig. 5. Extraction of zinc and iron with different samples: lixiviant ratios using 1 mol/L prop-2-enoic acid.

4.3. Sample: lixiviant ratio (S:L)

The leaching of metal cations into solution occurs at the solid/liquid boundary and so it would be expected that the ratio between these would affect the extraction. As the concentration gradient of dissolving cations surrounding the solid sample changes it is expected that the level of extraction also changes.

Three different S:L mass ratios: 1:10; 1:1; and 2:1 were investigated using an aqueous 1 mol/L solution of prop-2-enoic acid lixiviant held at ambient temperature for 24 h with constant stirring. The results shown in Fig. 5 indicate that the best zinc extraction occurred at the 1:10 S:L ratio. At this ratio the concentration gradient at the solid:liquid boundary would be the greatest. At the 1:1 and 2:1 ratios the extraction of zinc was considerably lower, and although the iron extraction was lower at 2:1, the zinc extraction was very poor.

4.4. Lixiviant reuse

Reusing the lixiviant used for leaching zinc would maximise the efficiency of any extraction process for blast furnace dust slurry. To investigate the efficacy of this, the same lixiviant solution was used to repeat the test on fresh dust sample four times. A 1 mol/L aqueous prop-2-enoic acid solution was used to extract zinc from a 1:10 sample:liquid ratio held at ambient temperature with constant stirring. The solid was filtered from the mixture and the lixiviant solution recovered and reused to run another extraction using a fresh sample of blast furnace dust slurry.

The extraction results for reusing the lixiviant, shown in Fig. 6, were lower for reused lixiviant compared to fresh material. Each extraction run showed a reduction in the iron extracted; and although the 1st,

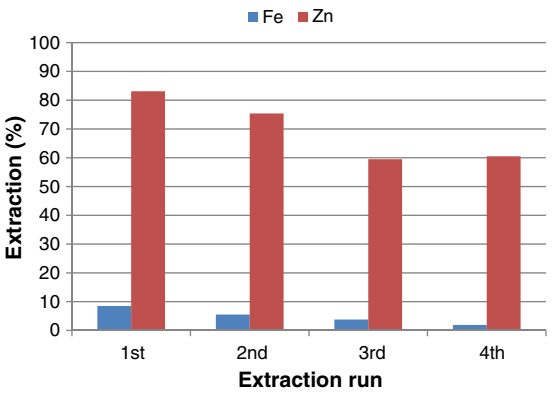

Fig. 6. Extraction of zinc and iron when reusing 1 mol/L prop-2-enoic acid lixiviant.

2nd and 3rd runs had lower zinc extractions the fourth did not show the same reduction. The results suggest that it would be worth investigating a counter current extraction system, where a consistent concentration gradient, is maintained to get the maximum zinc extraction with the minimum quantity of fresh lixiviant.

4.5. Leaching time

A 1 mol/L aqueous solution of prop-2-enoic acid, at a 1:10 sample ratio, was held at ambient temperature with constant stirring for 2 to 72 h; to investigate the optimum leach time at these conditions. The results plotted in Fig. 7 indicate that, for these reaction conditions, the maximum zinc extraction took around 24 h before a plateau in the level of extraction was reached. This was also found to be the same for the iron extraction.

4.6. Leach temperature

By increasing the leaching temperature the energy available for atomic and molecular collisions increases. Activation energy; mass transfer co-efficient; reaction constant; and diffusivity are all affected by the available energy which can alter the rate of extraction.

A 1 mol/L concentration of prop-2-enoic acid was used at a 1:10 sample ratio with constant stirring for 2 h, to investigate the effect of temperature on the extraction. The results in Fig. 8 show an increase in the extraction of zinc to yield a maximum after only 2 h of 82.4%, compared to 83.1% after 24 h at ambient temperature.

At ambient temperature the extraction profiles were similar for the zinc and iron. In comparison for a 2 h extraction time, varying in temperature between 22 °C and 95 °C, the iron and zinc profiles exhibit the same relationship reaching a maximum extraction at 50 °C. The results suggest that both the iron and zinc are equally accessible for extraction by the reagents.

4.7. The effect of non-aqueous solvents on zinc and iron extractions

The choice of solvent for a chemical process can have an important effect on the solubility, stability and reaction rate of that process. In acid–base reactions the presence of non-aqueous solvents is known to influence the reaction kinetics and thermodynamics by processes such as stabilisation; ionisation; or solubilisation of the reactants, products or intermediates.

A series of 1 mol/L prop-2-enoic acid solutions were made up with water:non-aqueous solvent blends that were also capable of solubilising prop-2-enoic acid. A 1:10 sample ratio was used with stirring for 24 h at ambient temperature. The three non-aqueous solvents chosen were acetonitrile, propan-2-ol (isopropanol), and methylbenzene (toluene). These solvents were chosen because of their range of polarities.

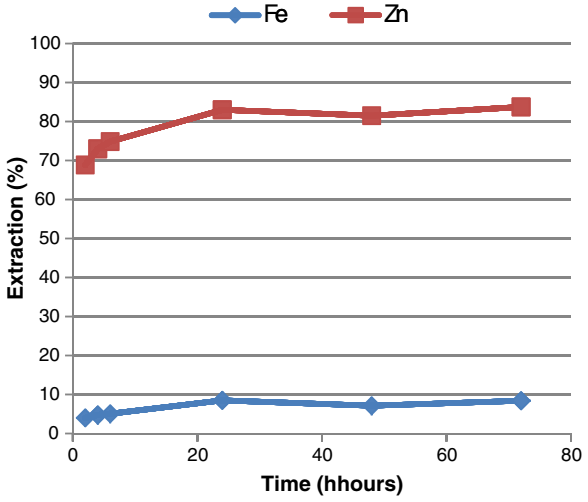

Fig. 7. Extraction of zinc and iron using 1 mol/L prop-2-enoic acid for various leach times.

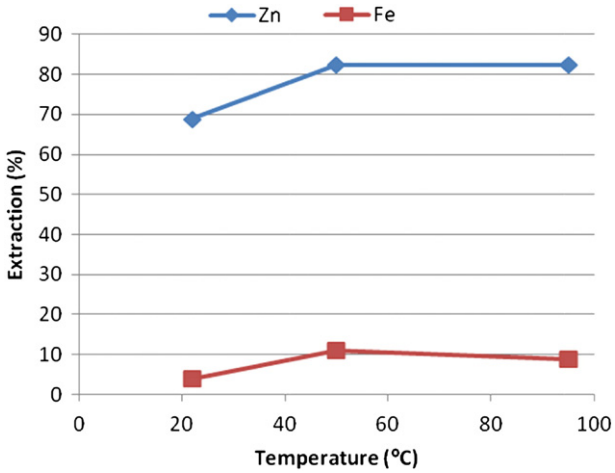

Fig. 8. Extraction of zinc and iron using 1 mol/L prop-2-enoic acid at various temperatures.

Methylbenzene is a non-polar solvent, immiscible in water, with a low dielectric constant of 2.4. Acetonitrile is a polar aprotic solvent, miscible in water, with a larger dielectric constant of 36.6 capable of solvating cations. Propan-2-ol is a polar protic solvent with a dielectric constant of 20.2 capable of solvating anions by hydrogen bonding. Water is a polar protic solvent characterised by a very high dielectric constant of 80.1 and has ion-solvating ability which polarises nearby solvent molecules by hydrogen bonding (David, 2005-2006). This creates a solvation envelope of surrounding solvent molecules which can stabilise both anions and cations to solvate the extracted species by delocalising their charge.

The results plotted in Fig. 9 are compared against the aqueous 1 mol/L prop-2-enoic acid solution which extracted 83.1% zinc and 8.5% iron from the blast furnace dust slurry. Extractions incorporating a portion of methylbenzene showed very good zinc extractions of 85.8% and 85.7%, but importantly the iron extractions were lower in comparison, 3.1% and 0.1%.

As previously discussed with carboxylic acids in Section 4.1, iron extraction was more affected by pH, but zinc extraction was more affected by substituent group effects. The reduced extraction of iron might be explained by a reduced solubility of the iron extracts into the aqueous/non aqueous solvent mixture. However, a mass balance of the distribution of extracted iron and zinc mass between the aqueous and

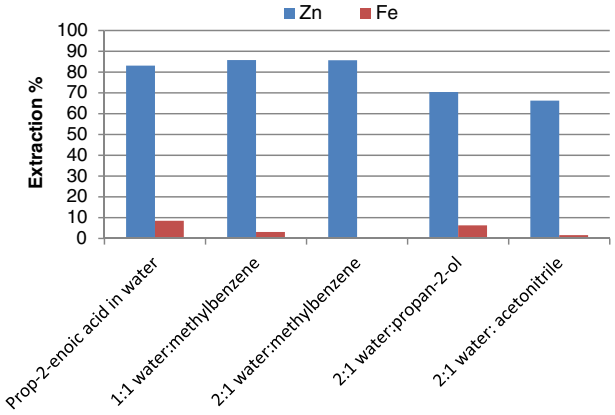

Fig. 9. Extraction of zinc and iron using 1 mol/L prop-2-enoic acid in different non-aqueous solvents.

the non-aqueous phase of the immiscible solvent mixture confirmed that both were extracted into the aqueous phase. Consequently, the aqueous phase should still facilitate extraction of the iron compounds in the solvent mixture.

Alternatively, it is well understood that different solvents affect the ionisation and acidity of an acid and in this case prop-2-enoic acid is soluble in both phases of the immiscible solvent mix used in this extraction (Reichardt, 1990). It is possible that the non-aqueous solvent reduces the acidic proton dissociation associated with its Bronsted Lowry behaviour, therefore reducing the acids' ability to extract iron in particular. However, in comparison, the zinc extraction, explained in terms of the substituent group theory, would not be affected in the same way by reduced proton dissociation.

In comparison, the water:organic solvent blends using propan-2-ol and acetonitrile show both lower iron and zinc extractions. It seems that these solvents have lower ion solvating ability, reducing the iron extraction and also reducing the Lewis acid strength of the prop-2-enoic acid, thus reducing zinc extraction.

4.8. Comparison of various acids against prop-2enoic acid

A range of different types of acids were compared against the carboxylic acids tested at concentrations of 1 mol/L; held for 24 h at ambient temperature with constant stirring; and at a sample and lixiviant (S:L) ratio of 1:10. Both organic carboxylic acids and mineral acids were used to compare the effect of acid strength and structure on the extraction of zinc and iron shown in Fig. 10. Overall the extraction of zinc ranged from 18.5% to 98.3%; whilst the extraction of iron ranged from 0.1% to 47%.

Sulphuric acid, nitric acid, and hydrochloric acid, are defined as 'strong' mineral acids because they completely ionise in water. The other acids, including the other mineral acid phosphoric acid, are known as 'weak' acids that do not completely ionise in water. However, the results show that the 'weak' acids are also capable of high levels of zinc extraction, suggesting that it is not only acid protonation (pH) that plays a role, but also additional mechanisms for zinc.

Sulphuric acid extracted the highest levels of zinc at 98.3%; unfortunately it also extracted 47.0% of the iron, which makes it unsuitable as a candidate for leaching the blast furnace dust slurry. This level of extraction is larger than literature figures quoted for other sulphuric acid extractions which ranged between 80 and 86% zinc extraction and 4 to 7% iron extraction (Asadi Zeydabadi et al., 1997; Havlik et al., 2012b; Vereš et al., 2011). It would seem that the zinc and iron were more leachable in this test sample of blast furnace dust slurry used in this study.

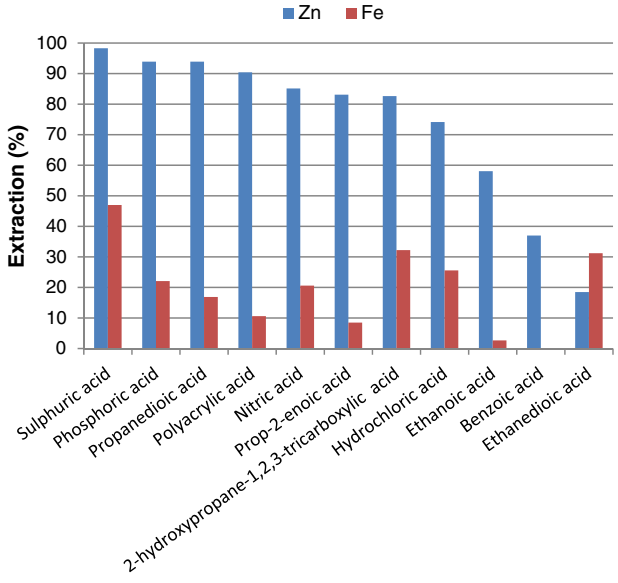

Fig. 10. Zinc and iron extractions for a range of acids at 1 mol/L concentration.

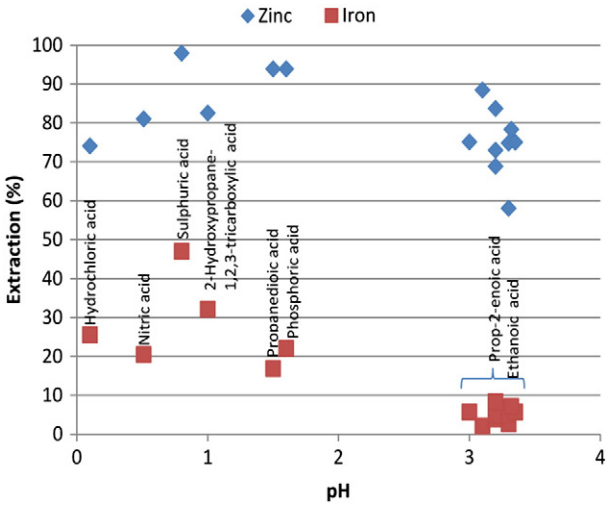

Fig. 11. Extraction of zinc and iron plotted against pH values postextraction.

Two samples with high zinc extractions and low iron extractions are the 10% solution of poly(acrylic acid-co-maleic acid) and the 1 mol/L solution of prop-2-enoic acid, extracting 90.4% and 83.1% zinc; and 10.6% and 8.5% iron respectively. For this reason, these acids are particularly suitable candidates for leaching blast furnace dust slurry.

For pH values between 0 and 3.5, the zinc extractions, shown in Fig. 11, show a low dependency on the pH, ranging from 58.1% to 98.0%; although the highest extraction occurs at a pH < 1 and the lowest extraction occurs at a pH > 3. This agrees with results comparing the carboxylic acids in Section 4.1, and comparing the non-aqueous solvents in Section 4.6, which suggest that substituent group effects also influence zinc extraction.

Comparison of the iron extraction and pH also agrees with the results discussed previously where the extraction is more dependent on the pH. The iron extractions ranged between 2.1% and 47.0%; but importantly, only pH values >3 gave low iron extractions less than 10%, whilst iron extraction greater than 10% occurs at pH values <3.

5. Conclusion

The extraction of zinc and iron, from a composite sample of dried blast furnace dust slurry, was investigated using different organic carboxylic acids, and non-aqueous solvents, to establish if they were capable of extracting high levels of zinc and low levels of iron. The following conclusions were drawn from this investigation.

- For extractions using partially dissociated carboxylic acids, not only does the pH play an important role, but also the organic substituent groups. The results indicate that the iron extraction was most affected by the pH, which could be explained by the Bronsted–Lowry theory. However, when comparing the extractions against the chemical structure differences and acidity of prop-2-enoic acid, ethanoic acid, propanedioic acid and ethanedioic acid, the zinc extraction was less dependent on the pH and could be better explained by substituent group effects from the Lewis acid/base theory.

When comparing the carboxylic acids and mineral acids, the extraction results against the pH also show that, over the range tested, the iron extraction was more dependent on the pH. However, the less dissociated carboxylic acids were still capable of high zinc extractions.

This paper seeks to highlight that, in terms of carboxylic acids, additional mechanisms, where the chemical structure contributes due to electron transfer, must be also considered to play a role in extraction.

- When using prop-2-enoic acid, a 2:1 blend of water and the non aqueous solvent methylbenzene was found to be a novel way to reduce the level of iron extraction further from 8.5% to 0.1%, whilst still achieving 85.8% zinc extraction. The results suggest that the non-aqueous solvent methylbenzene altered the acid proton dissociation associated with Bronsted Lowry behaviour, therefore reducing the acid's ability to extract iron, but not affecting the zinc extraction explained in terms of the Lewis acid theory.

Acknowledgements

The authors would like to kindly thank the Tata Steel Strip Products UK for supplying samples for this experimentation. In particular, we would like to thank Claire Grainger and Fiona Abbot for their help and co-operation.

References

Asadi Zeydabadi, B., Mowla, D., Shariat, M.H., Fathi Kalajahi, J., 1997. Zinc recovery from blast furnace flue dust. Hydrometallurgy 47 (1), 113–125.
Besta, P., Samolejová, A., Janovská, K., Lenort, R., Haverland, J., 2012. The effect of harmful elements in production of iron in relation to input and output material balance. Utjecaj štetnih elemenata pri proizvodnji sirovog željeza u odnosu na ulaznu i izlaznu materijalnu bilancu 51 (3), 325–328.
British-standards, 2006a. PD CEN/TR15310-2:2006. Characterisation of waste — sampling of waste materials. Part 2: Guidance on Sampling.
British-standards, 2006b. PDCEN/TR15310-3:2006.Characterisation of Waste—Sampling of Waste Materials—Part 3 Guidance on Procedures for Sub-sampling in the Field.
Callenfels, S., Je, V., 2004. Hydrocyclone installation for blast furnace sludge treatment. Kang T'ieh/Iron Steel (Peking) 39 (1), 59–62 (+58).
Das, B., Prakash, S., Reddy, P.S.R., Misra, V.N., 2007. An overview of utilization of slag and sludge from steel industries. Resour. Conserv. Recycl. 50 (1), 40–57.
David, L.R., 2005-2006. CRC Handbook of Chemistry and Physics.
Delhaes, C., Hauck, A., Neuschutz, D., 1993. Mechanisms of dust generation in a stainless steelmaking converter. Steel Res. 64 (1), 22–27.
Doronin, I.E., Svyazhin, A.G., 2012. Properties of steelmaking dust and the mechanism of its formation. Metallurgist 55 (11–12), 879–886.
Duan, D., Han, H., Chen, S., 2012. Efficient and comprehensive utilization of blast furnace dust in metalized pelletizing process. Metal. Int. 17 (4), 74–77.
Environment-agency, 2011. Hazardous Waste, Interpretation of the Definition and Classification of Hazardous Waste — Technical Guidance WM2. Environment Agency.
García Rodenas, L.A., Blesa, M.A., Morando, P.J., 2008. Reactivity of metal oxides: thermal and photochemical dissolution of MO and MFe2O4 (M = Ni, Co, Zn). J. Solid State Chem. 181 (9), 2350–2358.
Guśpiel, J., Riesenkampf, W., 1993. Kinetics of dissolution of ZnO, MgO and their solid solutions in aqueous sulphuric acid solutions. Hydrometallurgy 34 (2), 203–220.
Han, J., Qiu, W., Gao, W., 2010. Potential dissolution and photo-dissolution of ZnO thin films. J. Hazard. Mater. 178 (1–3), 115–122.
Havlik, T., Turzakova, M., Stopic, S., Friedrich, B., 2005. Atmospheric leaching of EAF dust with diluted sulphuric acid. Hydrometallurgy 77 (1–2), 41–50.
Havlik, T., Kukurugya, F., Orac, D., Parilak, L., 2012a. Acidic leaching of EAF steelmaking dust. World Metall.ERZMETALL 65 (1), 48–56.
Havlik, T., et al., 2012b. Leaching of zinc and iron from blast furnace dust in sulphuric acid solutions. Metallurgica 66 (6), 267–270.
Heard, R., Hansmann, T., Roth, J.L., Bolten, D., 2002. Recycling of zinc bearing residues with the PRIMUS® process. Proceedings — Ironmaking Conference, pp. 683–692.
Hilber, T., Marr, R., Siebenhofer, M., Zapfel, W., 2001. Solid/liquid extraction of zinc from EAF-dust. Sep. Sci. Technol. 36 (5–6), 1323–1333.
Huang, Z.H., Wu, X.Q., Peng, G.L., 2007. Removal of zinc from blast furnace dust by chemical leaching. Zhongguo Youse Jinshu Xuebao/Chinese J. Nonferrous Met. 17 (7), 1207–1212.
Jandova, J., Prosek, T., Maixner, J., 1999. Leaching of zinc oxide in aqueous sulfuric acid solution. Acta Metallogr. Slovaca 3 (172).
Kryachko, G.Y., Orel, G.I., Vasyuchenko, P.A., Safina, L.A., 2005. Maintaining the working profile of blast furnaces during service. Metallurgist 49 (11–12), 424–431.
Kurunov, I.F., 2012. Environmental aspects of industrial technologies for recycling sludge and dust that contain iron and zinc. Metallurgist 55 (9–10), 634–639.
Langová, Š., Leško, J., Matýsek, D., 2009. Selective leaching of zinc from zinc ferrite with hydrochloric acid. Hydrometallurgy 95 (3–4), 179–182.
Leclerc, N., Meux, E., Lecuire, J.M., 2002. Hydrometallurgical recovery of zinc and lead from electric arc furnace dust using mononitrilotriacetate anion and hexahydrated ferric chloride. J. Hazard. Mater. 91 (1–3), 257–270.
Ma, N.Y., 2008. On the separation of zinc from dust in ironmaking and steelmaking off-gas cleaning systems. TMS Annual Meeting. 547–552.
Makkonen, H.T., et al., 2002. Optimisation of steel plant recycling in Finland: dusts, scales and sludge. Resour. Conserv. Recycl. 35 (1–2), 77–84.
Nyirenda, R.L., 1991. The processing of steelmaking flue-dust: a review. Miner. Eng. 4 (7–11), 1003–1025.
Oda, H., Ibaraki, T., Abe, Y., 2006. Dust recycling system by the rotary hearth furnace. Nippon Steel Technical Report (94). 147–152.
Offenthaler, D., Antrekowitsch, J., Edlinger, A., 2005. Zinc containing steel mill dusts — between recycling and landfilling. REWAS'04 — Global Symposium on Recycling. Waste Treatment and Clean Technology. 2133–2141.
Oustadakis, P., Tsakiridis, P.E., Katsiapi, A., Agatzini-Leonardou, S., 2010. Hydrometallurgical process for zinc recovery from electric arc furnace dust (EAFD). Part I: Characterization and leaching by diluted sulphuric acid. J. Hazard. Mater. 179 (1–3), 1–7.
Rainer Remus, M.A.A.M., Roudier, Serge, Delgado Sancho, Luis, 2013. Best available techniques (BAT) reference document for iron and steel production-industrial emissions directive 2010/75/EU. In: J.R.C.o.t.E. Commission (Ed.), Publications Office of the European Union.
Reichardt, C., 1990. Solvents and Solvent Effects in Organic Chemistry. VCH.
Soria-Aguilar, M.J., Carrillo-Pedroza, F.R., Preciado-Nuñez, S., 2008. Treatment of BF and BOF dusts by oxidative leaching. Proceedings of the 2008 Global Symposium on Recycling. Waste Treatment and Clean Technology, REWAS 2008, pp. 589–596.
Trung, Z.H., et al., 2011. Acidic leaching both of zinc and iron from basic oxygen furnace sludge. J. Hazard. Mater. 192 (3), 1100–1107.
Van Herck, P., Vandecasteele, C., Swennen, R., Mortier, R., 2000. Zinc and lead removal from blast furnace sludge with a hydrometallurgical process. Environ. Sci. Technol. 34 (17), 3802–3808.
Vereš, J., Jakabský, S., Lovás, M., 2011. Zinc recovery from iron and steel making wastes by conventional and microwave assisted leaching. Acta Montanist. Slovaca 16 (3), 185–191.
Yang, X., Chu, M., Shen, F., Zhang, Z., 2009. Mechanism of zinc damaging to blast furnace tuyere refractory. Acta Metall. Sin.(English Letters) 22 (6), 454–460.

Energy Conversion and Management 66 (2013) 285–294

Contents lists available at SciVerse ScienceDirect

Energy Conversion and Management

journal homepage: www.elsevier.com/locate/enconman

Biomass co-firing trials on a down-fired utility boiler

Julian Steer [a,*], Richard Marsh [a], Anthony Griffiths [a], Alf Malmgren [b,1], Gerry Riley [c,2]

[a] Cardiff School of Engineering, Cardiff University, Queen's Buildings, The Parade, Cardiff CF24 3AA, United Kingdom
[b] BioC Ltd., Cirencester, Gloucestershire, United Kingdom
[c] RWE npower, Windmill Hill Business park, Whitehill way, Swindon, SN5 6PB, United Kingdom

ARTICLE INFO

Article history:
Received 4 September 2012
Received in revised form 20 October 2012
Accepted 20 October 2012
Available online 7 December 2012

Keywords:
Biomass
Co-firing
Renewables
Utility boilers
Fuel characterisation

ABSTRACT

This paper describes the practical combustion issues encountered with biomass co-firing on a large scale trial in a 500 MW down fired utility boiler at Aberthaw power station. It also investigates and discusses the effect of biomass particle size and physical properties on devolatilisation; flame stability; and slagging by using the biomass energy crop miscanthus.

During large scale biomass co-firing, the air flow around the injectors plays an important part in the fuel combustion and stable boiler operation. Secondary air flow at the point of biomass injection was adjusted during the experiments to provide higher airflows around the biomass injectors, hence the mixing, and air available for biomass combustion, was improved producing less unburnt material in the ash and reducing potential filter blockages. However, higher biomass air flows disrupt the temperature distribution in the boiler causing a wider variation of superheater temperatures compared to the baseline condition firing coal only. This reduces the combustion efficiency and can lead to localised hot spots, in the superheaters, with the potential to cause equipment damage. The trials indicated during the experiments that a secondary biomass air flow of 50% of its maximum, gave an optimum balance between air/biomass mixing and variations in the superheater temperatures.

1. Introduction

This paper describes research undertaken on the behaviour of biomass co-firing in a large scale utility boiler. The aim of the trials was to co-fire biomass with coal in one of the 500 MW down-fired units at Aberthaw power station, in order to characterise the impact of the biomass particle size and biomass secondary air flow (degree of mixing) on combustion and emissions performance, to optimise of biomass firing. Additionally, the properties of biomass (miscanthus) were evaluated with a drop tube furnace to determine and understand the relationship between the loss of volatiles in biomass, as a function of temperature and particle size. This investigative work was complemented by a visual investigation of the effect of miscanthus co-firing on flame stability, slagging and a discussion on the operational safety of using high volatile content biomass compared to coal.

The apparatus used for this research was Aberthaw power station, a coal fired power station, owned and operated by npower, part of the RWE group. It began full operation in 1971 and can generate 1560 MW of electricity for the UK national grid system [1]. It has three turbine generating units consisting of a boiler, supplying steam to a turbine that powers an associated generator. The station is designed to burn local, low volatile semi-anthracitic coal. Because of this the fuel is required to have a longer residence time for complete burnout, so consequently the boiler design is a 'down-fired' type where the pulverised coal fuel is injected downwards into the furnace combustion zone [2,3]. The heat produced in the boiler converts water in the heat exchangers into high pressure and temperature steam, generating steam at 16,500 kPa and 565 °C.

1.1. Biomass co-firing

The UK government introduced legislation to meet targets for renewable electricity in 2002 which took the form of the Renewables Obligation, setting out a requirement for generators to produce up to 15% of the electricity they generate from renewable sources by 2015. Now, as part of broader EU-wide action to increase the use of renewables energy, the UK has committed to generating 15% of its energy from renewable sources by 2020 [4]. For conventional coal fired power stations one method is to co-fire a certain percentage of renewable biomass with the coal [5–9]. In a study by Ayhan Demirbas (2003), results of extensive applications showed that co-firing biomass with coal accomplished (a) increased boiler efficiency, (b) reduced fuel costs and (c) reduced emissions of NO_x and fossil CO_2 [10]. Similar findings were also

* Corresponding author. Tel.: +44 29 20870599; fax: +44 29 20874939.
E-mail address: SteerJ1@cardiff.ac.uk (J. Steer).
[1] www.BioC-ltd.com.
[2] www.rwenpower.com.

0196-8904/$ - see front matter © 2012 Elsevier Ltd. All rights reserved.
http://dx.doi.org/10.1016/j.enconman.2012.10.010

published by Bennetto et al. whose results showed that biomass co-combustion is environmentally better than the sole CO_2 capture and/or biomass combustion [11] and also by Chaouki et al. who describe the reduction of NO_x and CO_2 emissions when using co-combustion [12].

In order to avoid issues associated with co-feeding biomass and coal such as feeder blockages [13], RWE chose to co-fire by direct injection as a means to comply with the Renewables Obligation. They have been co-firing biomass into one of the boiler units at Aberthaw since 2003, using a dedicated screening and feeding system for a sawdust feedstock into that unit. This material is a co-product from sawmilling activities, and is supplied as a particle less than 5 mm in length which requires no milling on site.

In 2007, a new biomass handling facility was built to feed Aberthaw's two other boiler units by taking biomass in the form of woodchips (around 5 cm long, less than 9 cm^3) and process them into smaller particles. The system starts with an unloading hopper where woodchips are delivered and screened before being transferred into a large woodchip silo. Material is fed into three hammer mills which break down the woodchips through screens to a target particle size specification of more than 90% <5 mm before being fired through dedicated nozzles into the boiler.

Previous literature has discussed the importance of biomass particle size and shape on combustion; both experimental and theoretical investigations indicate particle shape and size influence drying, devolatilisation, heating rate, and reaction rate [14–19]. Asadullah et al. describe how the size of the biomass particles is one of the determining parameters for the structure of char which in turn affects the reactivity by increasing the opportunity for recombination reactions with larger particles [20]. Holtmeyer et al. showed that large biomass particles that are not entrained in the near-burner region breakthrough the flame envelope, which can be detrimental to controlling NO formation [21].

Austin et al. illustrated that both the volatile burning times and the ignition delay times are shown to be functions of the product of the initial particle density with the square of the initial particle diameter, indicating that convective heat transfer to the particle is the rate controlling mechanism for both processes.

Another potential issue using biomass is associated with the composition of the ash produced after its combustion. Biomass ash has a composition which can lead to deposition onto the surfaces of the boiler. There are two types of deposit formation: *Slagging* refers to deposition in the high temperature refractory sections of boilers where radiative heat transfer is dominant and is due to the presence of molten ashes. *Fouling* refers to deposition in the convective heat transfer zones of the boiler where the gases cool and deposit material [22–24].

2. Methods and materials tested

2.1. Materials tested

Table 1 shows the proximate analysis for the coal, coal ash, sitka spruce and miscanthus biomass. In comparison, the coal and biomass are very different types of fuel [25]. Coal is characterised by a comparatively high higher heating value (HHV), ash and fixed carbon, but low moisture content and volatiles. Biomass on the other hand has a lower HHV, ash and fixed carbon content, but much higher moisture and volatiles content [26]. The biomass used in the boiler trials contained significantly more moisture than the miscanthus used in the drop tube trials, since this material had been seasoned (hence partially dried) prior to testing.

Samples of the biomass were taken corresponding to the British standard BS EN14778:2011, using a systematic increment extraction method from a conveyor over the course of the trial [35]. This sample was then subdivided in the laboratory to reduce the sample volume for further testing using a riffle box, as defined by BS EN14780:2011 [36]. Because of the high moisture content of the biomass, the sample was dried at 40 °C as defined in this standard, then classified by a dry sieving method that met the specification defined by BS EN 15149-1:2010 using four sieves of wire mesh size 1.18 mm; 3.35 mm; 5.00 mm; and 6.70 mm [37]. The cumulative particle size distribution curve in Fig. 1 shows the actual mass percentage of sample, <5 mm in size, was 93.3% and that the [d50] median value of the particle size distribution was 3.30 mm.

Table 2 shows the constituents of the ash identified by a Perkin–Elmer Optima 2100DV inductively coupled plasma spectrometer and presented as their oxides. The ash constituents play an important role in operational issues such as slagging and fouling. Alkaline salts, such as alkaline silicates present in biomass ash, have lower melting and softening points which are particularly problematic to boiler combustion processes [38–41]. The biomass samples in Table 2 have much higher potassium oxide (K_2O) levels compared to the coal and Nielsen et al. reported that potassium salts, formed by reactions during combustion, play a significant role in ash deposition by bonding the individual fly ash particles together [42,43].

2.2. Drop tube furnace

A drop tube furnace was used to characterise the devolatilisation behaviour of *miscanthus goliath.* It was not possible to use the same biomass used in the boiler trial because the particle size was too large to fit in the drop tube furnace apparatus. It should be noted this analysis was conducted on dried samples, not at the moisture content used during the power station trial, due to the difficulty of feeding 'wet' biomass into the tube without 'bridging' leading to blockages.

A drop tube furnace measures the rate of volatiles loss (in an inert atmosphere) or the rate of burn out of a fuel (in an oxidising atmosphere). This facility was located at RWE's Combustion Test Facility in Didcot, UK. It is a vertical tube furnace, shown in Fig. 1, which is heated by four 4.2 kW silicon carbide main heaters; two 2 kW trim heaters; and a 1.7 kW pre heater. Particles are fed into the top at feed rates between 3 and 50 g/h, carried down into the main hot gas stream at around 20 l/min via a water cooled probe, then collected at the bottom by means of a cyclone collector, a schematic of which is shown in Fig. 2.

Table 1
Proximate analyses of coal and biomass (as received).

	Moisture content (wt.%) [27]	Volatiles content (wt.%) [28]	Fixed carbon (wt.%) [29,30]	Ash content (wt.%) [31,32]	HHV (GJ/t) [33,34]
Coal	4.1	15.8	68.9	11.2	31.4
Coal ash	0.0	1.5	2.4	96.1	n/a
Sitka spruce biomass	45.3	47.3	7.2	0.2	10.6
Miscanthus biomass	7.4	74.8	15.1	2.7	17.6

Moisture content BS 14774-3:2004; volatiles content BS 15148:2005; carbon content BS EN15104:2011/BS ISO29541:2010; ash content BS 14775:2004/BS ISO1171:2010; calorific value BS EN14918:2009/BS ISO1928:2009.

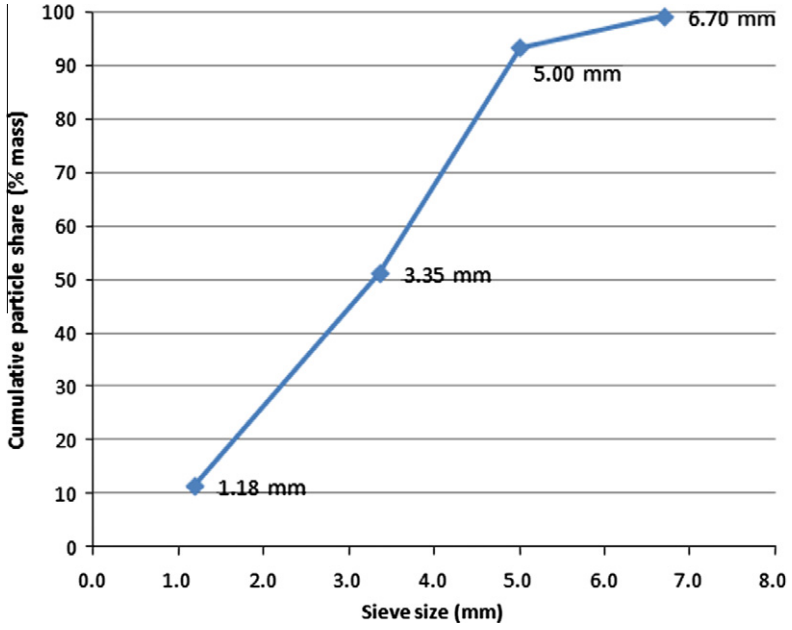

Fig. 1. Particle size classification obtained by sieving.

Table 2
Ash constituent analysis presented as oxides (wt.%, dried).

	Al_2O_3	CaO	Fe_2O_3	K_2O	MgO	Mn_3O_4	Na_2O	TiO_2	P_2O_5	SiO_2	RCO_3	Rest
Sitka spruce biomass	7.1	12.6	6.7	13.1	3.3	2.0	0.9	0.4	2.5	26.0	11.4	14.0
Miscanthus biomass	1.1	6.9	1.6	21.1	4.5	0.2	2.2	0.1	3.0	42.3	1.3	15.7
Coal	31.6	3.3	6.5	2.2	0.6	<0.1	0.9	0.9	<0.1	51.0	0.5	2.5

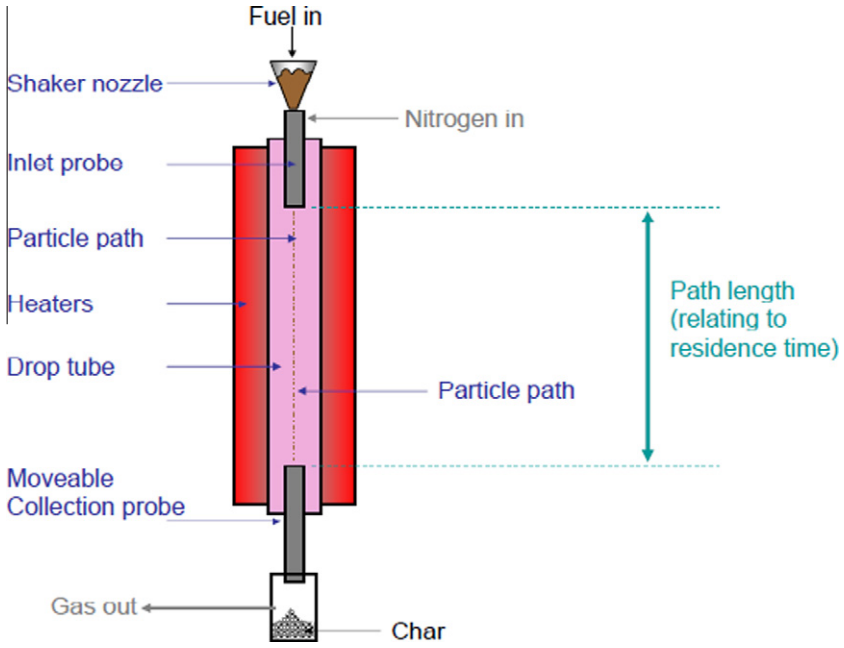

Fig. 2. Diagram of the drop tube furnace apparatus.

The sealed alumina work tube allows an entrained laminar gas flow to carry individual particles for a chosen residence time (from 30 ms to 500 ms) and chosen temperature (up to 1400 °C) to characterise the fuel, temperature and time relationships. The residence time in this tube is controlled by raising and lowering the water cooled inlet feeder and collection probe, as indicated in Fig. 2. The temperature is controlled by two 818S Eurotherm microprocessor controllers plus an 818P controller/programmer for the main elements and measured by five R-type thermocouples along the length of the furnace tube.

Two sample particle size ranges were prepared for testing by sieving according to the British standard BS EN15149-1:2010 as, 1.18–2.0 mm, and 0.18–0.85 mm [37]. These were tested at two temperatures, 1200 °C and 1400 °C, for different residence times measuring the volatiles content of the residue collected from the experiments using British standard BS15148:2009 [28]. The results of these tests were then used in conjunction with the subsequent boiler trials at the power station in order to estimate residence times for the devolatilisation and hence total combustion times of the biomass, in comparison to coal.

2.3. Down-fired boiler units

The utility boilers used in this study were single reheat boilers with water wall tubes with an evaporation rate of 422 kg/s. The water wall tubes form two box-like compartments, the furnace and the heat recovery area, above these is a steam drum together with a complex of tubes and headers which supply the water wall tubes. In the upper part of the furnace are the platen, secondary, and radiant superheaters. In the heat recovery area are the primary superheater, primary reheater and secondary reheater.

The boiler design investigated differs from many wall shot or corner shot boiler designs by charging the pulverised fuel and primary air into the furnace from down-fired burners. The secondary and tertiary air supplies are fed into the furnace separately and by using plenum dampers the flow can be directed to alter the depth of the flame and change the fuel residence time. Pulverised fuel for the boiler is supplied by six tube ball mills; each mill supplies the fuel to six burners which have individual on and off control and individual air control per burner. The wide, shallow depth layout of the boiler, with a total of 36 burners, results in larger variations from side to side but small variations front to back.

Biomass in the form of woodchips is milled through hammer mills fitted with screens with a nominal hole size between 10 mm and 14 mm, the target top size of the milled product is 5 mm in length. This is conveyed and then fed into the boiler pneumatically with unheated primary air through four nozzles at a rate of 5 t/h per nozzle.

Each biomass nozzle consists of a central tube carrying biomass at a constant flow rate by the primary air and a wider diameter outer tube that supplies the biomass secondary sir (SA). In difference to the down-fired coal, the biomass is fed horizontally into the furnace at a point just above the coal burners on each of the side walls, as shown in Fig. 3.

The burner configuration for co-firing coal and biomass is known to affect the formation of nitrogen oxides (NO_x) [44]. Hein et al. discussed how fuel added to the sub-stoichiometric inner recirculation zone results in low NO_x emissions but fuel added by the annular clearance devolatilises in high oxygen conditions leading to an increased conversion to NO_x [7].

The biomass secondary air is tapped off from the main boiler through the secondary air duct and can be regulated by manually adjustable dampers in the supply lines to the biomass nozzles. The secondary air is essential for combustion and influences the flow of the particles and the depth that they are carried into the boiler.

The boiler system has a computer controlled logic system, and is designed to maintain steam pressure in the steam drum of the heat exchangers as required to meet the generator load demand. Primary air flow supplying the pulverised fuel mills controls this drum pressure. As a result, when the boiler conditions are altered, such as adding the biomass, the system automatically adjusts to compensate. This means in a dynamic system that is constantly changing it is sometimes difficult to quantify the effect of such changes.

Combustion performance can be optimised by the process operators who have manual control of the quantity and balance of the air distributed between the burners; which of the pulverised coal burners are in service; and adjustment of the total air quantity by means of a 'trim' control.

The pulverised coal is input with the primary air into the boiler, and under normal operating conditions, with a maximum feed rate at full load of around 180–200 t/h. The coal mills are fitted with volumetric feeders and the feed rate of the coal is adjusted by the logic control system in order to meet the required load output from the unit (load sensitive). During the trial the boiler system was run in "frequency insensitive" mode so the unit output was constant.

3. Biomass trial objectives

The process of co-firing biomass not only changes the balance of fuel input into the boiler, but it also alters the distribution of com-

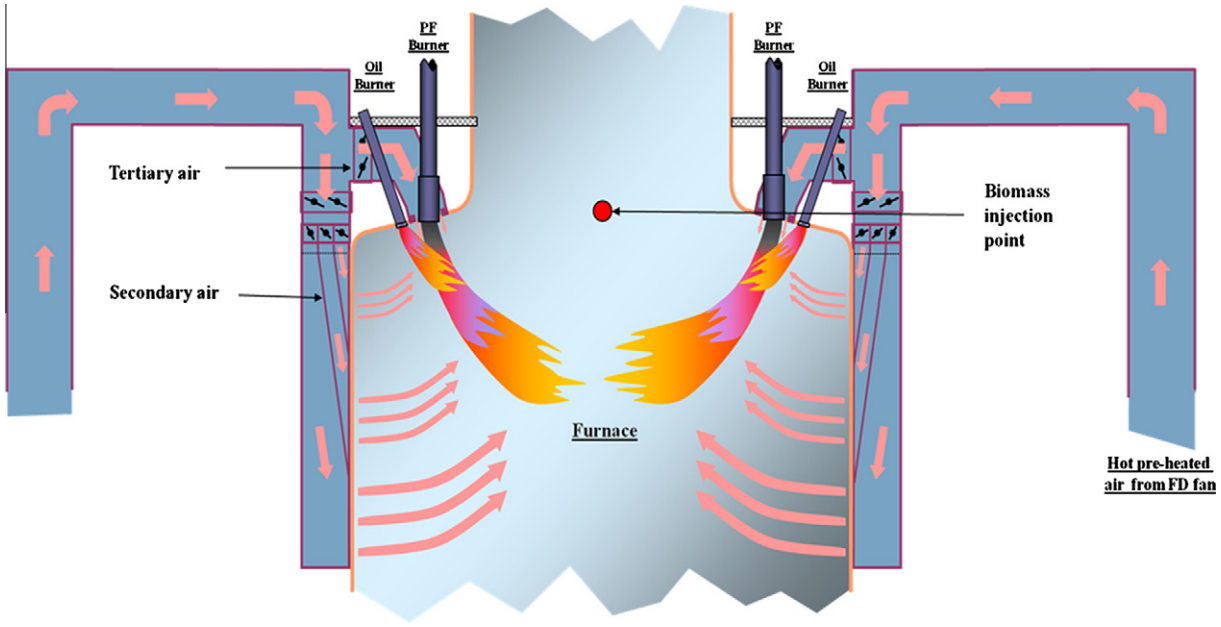

Fig. 3. Schematic cross section of the Aberthaw boiler.

bustion air in the furnace [7]. Previous trials at Aberthaw determined that the quantity of primary air used to feed the biomass into the boiler has a negligible impact on its running, but further work was required to investigate the effect of the biomass secondary air.

By changing the quantity of air fed around the nozzle the amount available for biomass combustion, and the mixing of biomass with air is affected, altering the ignition and burnout characteristics. The main coal combustion is also affected because air is being supplied above the primary combustion zone; also because half of the biomass mass is its moisture content (see Table 1); and also because the biomass combustion can reduce the amount of oxygen available for coal combustion.

Following the installation of the new biomass handling and feed system at Aberthaw power station a trial was necessary to characterise combustion in terms of two process variables:

The impact of biomass secondary air flow rate, and hence degree of mixing, on combustion performance.
The impact of biomass particle size on flue gas emissions and the carbon remaining in ash (burnout).

To obtain the most comparable and meaningful results from the biomass co-firing trial a number of conditions were necessary. The first of these was a steady state generator load (frequency insensitive mode), where the coal input into the boiler was maintained at a constant rate of 200 t/h to achieve a constant measured maximum load output from the unit of 481 MW, with an observed variation ±1%. Also, the same single source of coal was used to maintain a constant thermal output. The biomass system however is independent of the logic control for the unit and is measured gravimetrically. For the trial, biomass was fed into the boiler at a constant rate of 20 t/h and negligible variation was observed. The following trial test conditions were run over a period of 3–4 h to obtain a steady operational state, and the results were averaged over this period to account for any variation.

Two biomass milling screen sizes (12 mm and 14 mm).
Three different biomass secondary air damper settings (30%; 50%; and 80% of the maximum flow).
Three baseline conditions (coal firing only, no biomass).

4. Results

4.1. Miscanthus devolatilisation in a drop-tube furnace and its application in co-firing

In the case of large-scale co-firing, practical issues usually mean that biomass is not ground to the same particle size as coal. Therefore, the particle size of biomass is much larger and the particle size distribution much greater, which reduces the rate of volatiles loss from the biomass.

Table 3 shows the drop tube results for the larger Miscanthus particles (1.18–2.00 mm) at 1200 °C and 1400 °C. For a particle residence time of 500 ms a drop in mass was measured of 16.3% at 1200 °C and 35.1% for the same residence time at 1400 °C. As expected the higher temperature the more complete the devolatilisation, but even at 1400 °C for 500 ms, 45.7% of the volatile content remains.

Table 3
Devolatilisation of miscanthus particles (1.18–2.00 mm).

Particle residence time (ms)	Volatiles (%)	
	1200 °C	1400 °C
0	80.8	80.8
65	80.3	77.7
125	80.1	75.2
350	72.5	57.0
500	64.5	45.7

Table 4
Devolatilisation of miscanthus particle size (0.18–0.85 mm) at 1200 °C and at 1400 °C.

Particle residence time (ms)	Volatiles (%)	
	1200 °C	1400 °C
0	80.8	80.8
35	71.9	71.2
65	72.7	68.1
100	65.3	59.2
125	64.7	n/a
200	n/a	38.7
350	29.3	17.4

Table 4 highlights the results for the smaller particle size (0.18–0.85 mm). These show a faster devolatilisation compared to the larger particle size. The lower rate of devolatilisation for the larger particle sizes could be an issue when co-firing in a utility boiler, particularly as some particle sizes will be up to 5 mm.

Fig. 4 shows the plots of biomass devolatilisation, which is expressed as the relationship between volatile content of the fuel versus residence time in the drop tube furnace. The smaller particle size (0.18–0.85 mm) shows complete devolatilisation after 0.4 s at 1400 °C and 0.6 s at 1200 °C respectively (via extrapolation). The larger particle size (1.18–2 mm) takes significantly longer to devolatilise completely; extrapolated as 1.2 s at 1400 °C and 2.9 s at 1200 °C.

With a 500 ms residence time at 1450 °C a sample of Colombian coal with low volatiles content (31% by mass) lost 53% of its volatiles content, which works out as a 16.4% loss of its mass. In comparison, for the miscanthus biomass, an equivalent loss of 53% of its volatiles content gives a mass loss of 42.8% because of its higher initial volatiles content. Table 5 compares the residence times required to lose equivalent volatiles content for coal and miscanthus.

Despite much larger particle sizes the biomass samples devolatilise quickly compared to coal even at a lower temperature. Williams et al. discuss how volatile combustion dominates biomass combustion and claim that the volatile content of biomass usually contributes about 70% of the heat of biomass combustion compared with about 36% for coal volatile combustion [18]. In the down-fired boiler, indicative particle residence times of 2.0–2.5 s from inlet to furnace outlet (superheaters) would give sufficient time for biomass particles less than 2 mm to be completely devolatilised [45]. In comparison during the power station trials, biomass particle sizes up to 5 mm were encountered which would require longer residence times to devolatilise and burn out.

Because of the high volatile yields associated with biomass, tests were carried out at the RWE combustion test facility (CTF) at Didcot, to investigate flame stability associated with co-firing. The results show that it is possible to burn Miscanthus at 25% blended with coal in an unmodified low NO_x coal burner and get a stable flame, see Fig. 5.

A very important consideration with high volatile content biomass is storing the material safely. The devolatilisation process in miscanthus starts at a significantly lower temperature (ca. 200 °C) than a typical coal (ca. 400 °C), as can be seen in Fig. 6. This means that a complete safety review has to be carried out before this type of fuel can be introduced at a coal fired power station. The risks for ignition and dust explosions are completely different compared to coal.

It has been shown at RWE's combustion test facility at Didcot, that the tendency to form slag increases with increasing fraction of miscanthus in the fuel blend. Fig. 7 shows how the amount of slag increases with the fraction of miscanthus. This correlates with

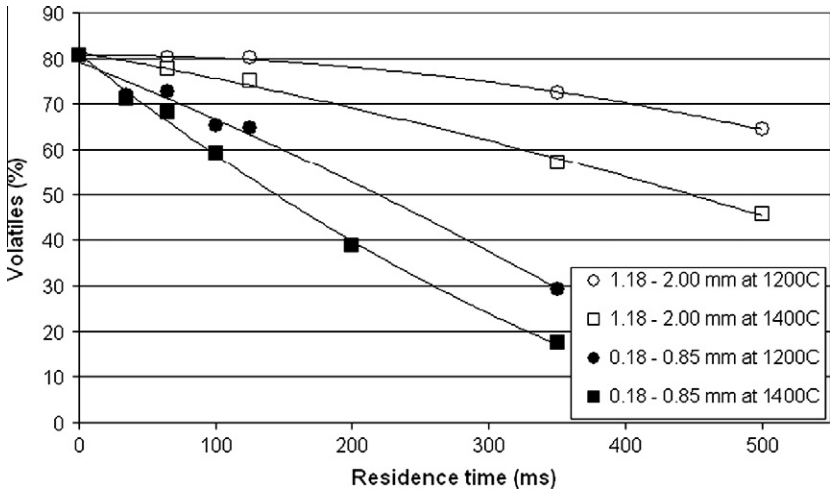

Fig. 4. The loss of volatiles as a function of temperature and particle size.

Table 5
Comparison of the loss of volatiles of coal and biomass.

	Particle size range (mm)	Temp. (°C)	Extrapolated residence time required for complete devolatilisation (ms)
Coal	0.05–0.07	1450	945
Miscanthus	0.18–0.85	1200	565
Miscanthus	0.18–0.85	1400	430
Miscanthus	1.18–2.00	1400	1200

the high potassium levels recorded in the ash analysis which are understood to cause difficulties due to its slagging behaviour when it reacts with silicon to form salts having low melting temperatures which deposit themselves on the boiler surfaces [41–43,46].

4.2. Power station trials – process data during co-firing trials

The data for the boiler unit was taken from the process information (PI) system which records data points approximately every 10 s depending on the particular set-up for any process variable. Due to the scale and complexity of the unit, data recorded by this system tends to be noisy. In addition, the unit is slow to settle to a new steady state following alterations in operating conditions, so it is left for 30 min after any changes then the data recorded is averaged over a 15 min period to give a single figure for each parameter measured.

Among the most important parameters for operation efficiency are the steam temperatures in the superheater (S/H) heat exchangers. These are measured at four different positions to establish the distribution of temperature across them. Ideally these temperatures will be around 565 °C and when optimal combustion is achieved the variation between these temperatures should be as small as possible. A wide variation in these temperatures indicates uneven combustion distribution across the chamber, reducing the system efficiency and leading to damaging hot spots in the boiler. The maximum tolerable temperature differential is 16 °C.

Table 6 compares the superheater temperature ranges after adjusting for the baseline variation. The screen size used to process the biomass during shredding is shown, along with the quantity of biomass secondary air fired into the combustion chamber. The data shows that the higher secondary airflow results in a wider variation across these tubes. In all these cases the rate of biomass addition remained constant, but as the additional mass flow of secondary air supplied with the biomass was increased, the temperature distribution through the boiler was disrupted.

4.3. Power station trials – plant emissions during co-firing trials

Co-firing biomass affects the levels of unwanted combustion products which exit the boiler in the flue gas such as nitrogen oxides (NO_x), sulphur oxides (SO_x), dust and carbon monoxide (CO)

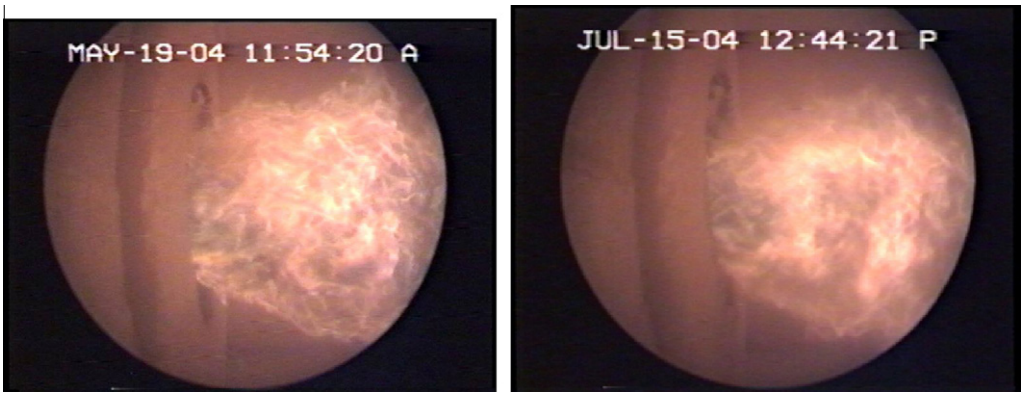

Fig. 5. Neat coal flame (left) and 25/75 miscanthus/coal flame (right).

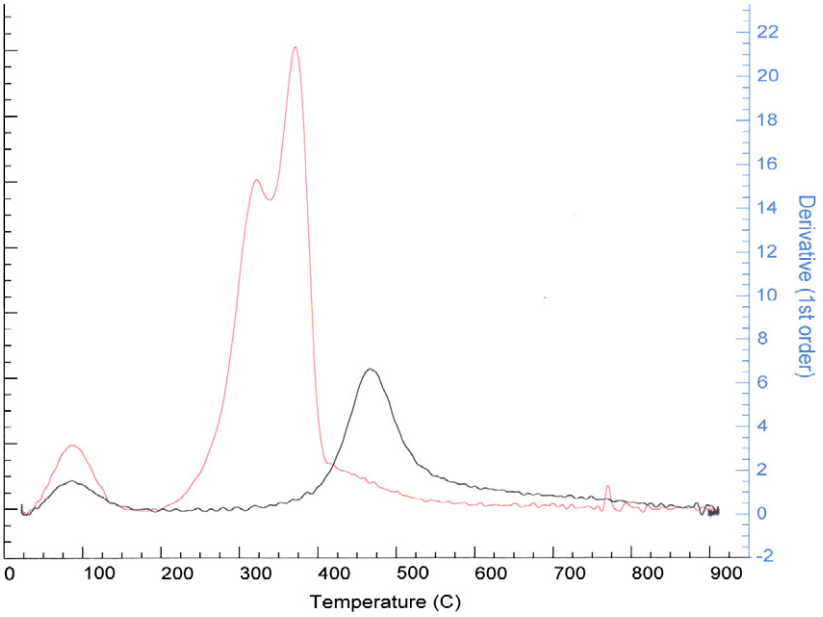

Fig. 6. TGA analysis of miscanthus (red) and a typical coal (black). (For interpretation of the references to colour in this figure legend, the reader is referred to the web version of this article.)

Fig. 7. Impact of the blend composition on the slagging tendency (5% miscanthus in the foreground rising to 25% in the background).

Table 6
Comparison of superheater temperature ranges.

	Average temperature across superheater zones (°C)	Temperature range relative to the baseline (°C)
12 mm mill screen, 80% secondary air flow	553	23
12 mm mill screen, 50% secondary air flow	554	5
12 mm mill screen, 30% secondary air flow	556	5
14 mm mill screen, 80% secondary air flow	565	20
14 mm mill screen, 30% secondary air flow	565	3

[47,48]. Dust is defined as particulate carry over (fly ash) from the combustor. Table 7 shows the amount which these values deviate from the baseline (100% coal only, no co-firing) for each run. Baseline data is not supplied due to plant confidentiality.

As the data shows, the dust levels increased by a small amount during co-firing and were attributed to unburnt or incomplete combustion of fuel due to the redirection of airflow from the primary coal combustion zone to the biomass combustion.

Co-firing had a variable effect on the NO_x levels observed during the trials because of a number of the competing effects: combustion air being diverted to the biomass nozzles; lower combustion temperatures of the biomass resulting in less thermal NO_x formation; lower nitrogen content in the biomass compared to typical coals; and the re-burn effect caused by the addition of higher volatile content fuel (biomass) after the main combustion zone above the main burners. This alters the combustion conditions in the furnace to create fuel rich and fuel lean zones, which promotes or limits the formation of reactive nitrogen radical species respectively, and which are precursors to the formation of NO_x [49].

Carbon monoxide levels increase on co-firing due to the fast release of volatiles from biomass which is not completely combusted, resulting in the partial oxidation to carbon monoxide rather than carbon dioxide. This can also be due to the comparatively high moisture content of the biomass fuel, resulting in lower flame temperatures, hence incomplete combustion and CO production. The SO_x levels are consistently low because of the flue gas desulphurisation system installed on the units at Aberthaw in compliance with the Large Combustion Plant Directive [50].

4.4. Fly ash analysis

At the test power station in Aberthaw, each boiler unit has three electrostatic precipitators which remove fly ash from the flue gas exiting the boiler. Under normal operating conditions at this power station 90% of the ash produced is recovered as precipitator ash and 10% as bottom ash.

The carbon content and particle size of the fly ash give important information about the completeness of the biomass combustion in the boiler. The presence of carbon in the fly ash indicates incomplete 'burn out' of the fuel, and it is important to maintain combustion process conditions that keep this to a minimum [51]. Fig. 8 compares the variation in carbon content in the fly ash samples relative to the baseline condition burning coal only with no

Table 7
Comparison of flue gas emissions relative to baseline emissions.

	Dust (mg/m^3)	NO_x (ppm)	CO (ppm)	SO_x (ppm)
12 mm mill screen, 80% secondary air flow	+26	−15	+77	0
12 mm mill screen, 50% secondary air flow	+2	−67	+14	−2
12 mm mill screen, 30% secondary air flow	+4	−56	+20	−2
14 mm mill screen, 80% secondary air flow	+30	+10	+128	+2
14 mm mill screen, 30% secondary air flow	+35	+49	+155	+2

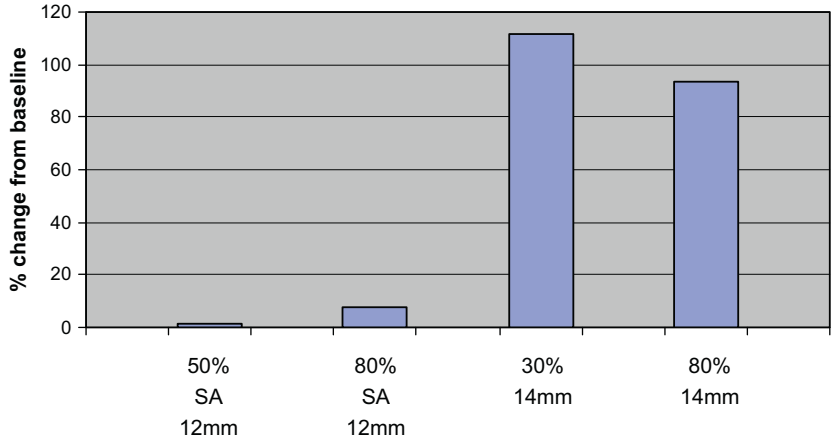

Fig. 8. Carbon remaining in ash for different biomass fuel particle sizes and quantities of biomass secondary air, relative to baseline (burning coal only, no co-firing).

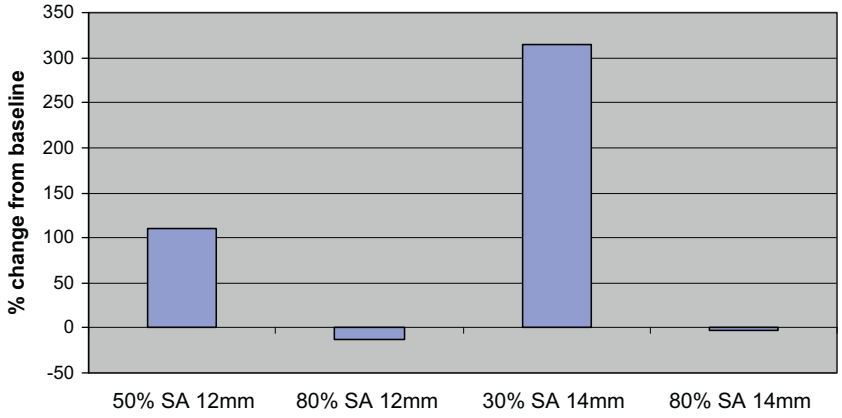

Fig. 9. Fly ash particle size for different biomass fuel particle sizes and quantities of biomass secondary air, relative to baseline (100% coal and no biomass co-firing).

co-firing. The samples were taken from three points in the electrostatic precipitators and the results were averaged.

The results indicate that the biomass secondary airflow rate does not appear to affect the amount of carbon in the ash. The dominating factor appears to be the biomass particle size (i.e. screen size after milling). The fly ash from the 12 mm screened fuel is almost identical in carbon content to that of the baseline fuel at 50% and 80% secondary air. However the 14 mm screened fuel has a carbon content in its fly ash of almost twice the baseline case at both 30% and 80% biomass secondary air settings.

The fly ash samples were tested on a Malvern Mastersizer laser particle size analyser. To ensure consistency, each sample was selected from the same precipitator and from the same sample position. This technique does have limitations because it requires spherical particles to give an accurate measurement.

Fig. 9 compares the percentage of larger ash particles (>200 μm in size) from the different trial conditions relative to the baseline condition firing with coal only, i.e. no co-firing.

The data shows that the presence of these larger particles indicates incomplete combustion of the biomass. Some of the co-firing trials have a higher proportion of large particles compared to the baseline conditions indicating unburnt material in the ash. Fig. 8 suggests that at higher biomass secondary airflows there is more air and fuel mixing which results in less unburnt material, since good mixing of air and biomass is vital to a balanced and efficient combustion setup. It seems that it is possible to achieve reduced emissions of incompletely burned particles during co-firing if the biomass secondary air flow is optimised and the biomass particle size is sufficiently fine.

5. Conclusions

Co-firing of biomass with coal has important implications on the operation of a large scale utility boiler as shown in the power station trial. The experimental work also highlighted some

important issues regarding the use of biomass and discussed the potential implications on large scale co-firing.

The drop tube furnace illustrated how miscanthus biomass devolatilised more quickly than coal even with larger particle sizes at temperatures of 1200 °C. When compared by TGA analysis, the initial devolatilisation temperature of miscanthus (ca. 200 °C) was significantly lower than a typical coal (ca. 400 °C), highlighting the implication on the safe storage and handling of biomass. In addition, the combustion test facility experiments showed how stable flames could be obtained co-firing up to 25% miscanthus but it illustrated how much slagging is an issue at these levels.

With regard to boiler trails, increasing the biomass secondary combustion air flow reduces the unburnt material in the ash; this is attributed to an improvement in the air and fuel mixing which leads to more complete combustion. However, on the Aberthaw boiler unit higher biomass secondary air flows increase the variation across the superheater temperatures; this reduces the combustion efficiency which could lead to localised damaging hot spots.

There is an optimum biomass secondary air flow rate of 50% of the maximum which gives the best balance available using the current biomass nozzle setup. It gives sufficient flow for good mixing of the biomass with air for combustion and burnout, while the flow is not too great to disrupt the distribution of temperature in the superheaters.

Co-firing can increase the dust levels in the flue gas by redirecting some airflow to the biomass combustion, which in turn reduces the air available for the coal combustion and increases the levels of unburnt dusts. It was shown that it is possible to avoid this if the fuel is ground to a sufficient fine size and the mixing with combustion air is efficient. Carbon monoxide levels also increase when co-firing; this is expected because the fast release of the biomass volatiles which are not completely combusted. It is often observed that co-firing biomass reduces emissions of NO_x, this was observed for the 12 mm mill screened particles, but not with the 14 mm mill screened particles where NO_x levels increased.

The ash analysis showed evidence of some larger and unburnt particles of biomass carrying through to the precipitators. It is not clear if the differences between these particle sizes have a significant effect on the amount of unburnt particles, however, higher biomass secondary air volumes produce better burnout due to the improved mixing of air and fuel.

Acknowledgments

The authors are grateful to David Fong, Jason Powis, Richard Kadim and all those at RWEnpower Aberthaw who helped with the trials for their technical assistance, access to plant, and for providing data.

References

[1] Malmgren A., Goh B. Guidance document on biomass co-firing on coal fired power stations DTI project 324-2. Dti reference number TECH/JJB/858/07, Issue 2; 2007.
[2] Li Z, Ren F, Chen Z, Liu G, Xu Z. Experimental investigations into gas/particle flows in a down-fired boiler: influence of down-draft secondary air. Energy Fuels 2009;23(12):5846–54.
[3] Zhang L, Huang J, Fang Y, Wang Y. Gasification reactivity and kinetics of typical Chinese anthracite chars with steam and CO_2. Energy Fuels 2006;20(3):1201–10.
[4] Department of energy and climate change. <http://www.decc.gov.uk/en/content/cms/meeting_energy/renewable_ener/renew_obs/renew_obs.aspx> [accessed September 2012].
[5] Baxter L, Koppejan. Biomass-coal co-combustion: opportunity for affordable renewable energy. Fuel 2005;84(10):1295–302.
[6] Woods J, Tipper R, Brown G, Diaz-Chavez R, Lovell J, de Groot P. Evaluating the sustainability of co-firing in the UK. Themba Technology Ltd., 139 Lavenham road, London, SW18 5EP. Dti report URN 06/1960; September 2006.
[7] Hein KRG, Bemtgen JM. EU clean coal technology co-combustion of coal and biomass. Fuel Process Technol 1998;54(1–3):159–69.
[8] Sami M, Annamalai K, Wooldridge M. Co-firing of coal and biomass fuel blends. Prog Energy Combust Sci 2001;27(2):171–214.
[9] Baxter L. Biomass-coal co-combustion: opportunity for affordable renewable energy. Fuel 2005;84(10):1295–302.
[10] Demirbas A. Sustainable co-firing of biomass with coal. Energy Convers Manage 2003;44:1465–79.
[11] Benettoa E, Popovicia E-C, Rousseaux P, Blondin J. Life cycle assessment of fossil CO_2 emissions reduction scenarios in coal-biomass based electricity production. Energy Convers Manage 2004;45(18–19):3053–74.
[12] Ghenaia C, Janajrehb I. CFD analysis of the effects of co-firing biomass with coal. Energy Convers Manage 2010;51(8):1694–701.
[13] Hunt EF, Prinzing DE, Battista JJ, Hughes E. The Shawville coal/biomass co-firing test: a coal/power industry cooperative test of direct fossil-fuel CO_2 mitigation. Energy Convers Manage 1997;38:S551–6.
[14] Lu H, Ip E, Scott J, Foster P, Vickers M, Baxter LL. Effects of particle shape and size on devolatilization of biomass particle. Fuel 2010;89(5):1156–68.
[15] Peters B, Bruch C. Drying and pyrolysis of wood particles: experiments and simulation. J Anal Appl Pyrol 2003;70(2):233–50.
[16] Austin PJ, Kauffman CW, Sichel M. Ignition and volatile combustion of cellulosic dust particles. Combust Sci Technol 1996;112:187–98.
[17] Guo Q, Chen X, Liu H. Experimental research on shape and size distribution of biomass particle. Fuel 2012;94:551–5.
[18] Williams A, Jones JM, Ma L, Pourkashanian M. Pollutants from the combustion of solid biomass fuels. Prog Energy Combust Sci 2012;38(2):113–37.
[19] Backreedy RI, Fletcher LM, Jones JM, Ma L, Pourkashanian M, Williams A. Co-firing pulverised coal and biomass: a modelling approach. Proc Combust Inst 2005;30:2955–64.
[20] Asadullah M, Zhang S, Li C-Z. Evaluation of structural features of chars from pyrolysis of biomass of different particle sizes. Fuel Process Technol 2010;91(8):877–81.
[21] Holtmeyer ML, Kumfer BM, Axelbaum RL. Effects of biomass particle size during co-firing under air-fired and oxyfuel conditions. Appl Energy 2012;93:606–13.
[22] Teixeiraa P, Lopesa H, Gulyurtlua I, Lapab N, Abelhaa P. Evaluation of slagging and fouling tendency during biomass co-firing with coal in a fluidized bed. Biomass Bioenergy 2012;39:192–203.
[23] Pronobis M. The influence of biomass co-combustion on boiler fouling and efficiency. Fuel 2006;85(4):474–80.
[24] Dai J, Sokhansanj S, Grace JR, Bi X, Lim CJ, Melin S. Overview and some issues related to co-firing biomass and coal. Can J Chem Eng 2008;86(3):367–86.
[25] Demirbas A. Combustion characteristics of different biomass fuels. Prog Energy Combust Sci 2004;30(2):219–30.
[26] Werther J, Saenger M, Hartage E-U, Ogada T, Siagi Z. Combustion of agricultural residues. Prog Energy Combust Sci 2000;26(1):1–27.
[27] BSI Standards Publication. Solid biofuels. Determination of moisture content. Oven dry method. Moisture in general analysis sample. BS 14774-3; 2009.
[28] BSI Standards Publication. Solid biofuels. Determination of the content of volatile matter. BS 15148; 2009.
[29] BSI Standards Publication. Solid biofuels. Determination of total content of carbon, hydrogen and nitrogen. Instrumental methods. BS EN15104; 2011.
[30] BSI Standards Publication. Solid mineral fuels. Determination of total carbon, hydrogen and nitrogen content — Instrumental method. BS ISO29541; 2010.
[31] BSI Standards Publication. Solid biofuels. Determination of ash content. BS 14775; 2009.
[32] BSI Standards Publication. Solid mineral fuels. Determination of ash. BS ISO1171; 2010.
[33] BSI Standards Publication. Solid biofuels. Determination of calorific value. BS EN14918; 2009.
[34] BSI Standards Publication. Solid mineral fuels. Determination of gross calorific value by the bomb calorimetric method and calculation of net calorific value. BS ISO1928; 2009.
[35] BSI Standards Publication. Solid biofuels.sampling. BS EN14778; 2011.
[36] BSI Standards Publication. Solid biofuels, Sample preparation. BS EN14780; 2011.
[37] BSI Standards Publication. Solid biofuels. Determination of particle size distribution. Part1: oscillating screen method using sieve apertures of 1 mm and above. BS EN15149-1; 2010.
[38] Dti, 2007. Effects of high levels of biomass co-firing – reducing slagging and fouling constraints. Project number 418.
[39] Brown RC. Thermochemical processing of biomass: conversion into fuels. Chem Power 2011:330.
[40] Peter M. Energy production from biomass (Part 1): overview of biomass. Biores Technol 2002;83(1):37–46.
[41] Zbogar A, Frandsen F, Jensen PA, Glarborg P. Shedding of ash deposits. Prog Energy Combust Sci 2009;35(1):31–56.
[42] Baxter LL, Miles TR, Miles Jr TR, Jenkins BM, Milne T, Dayton D, et al. The behavior of inorganic material in biomass-fired power boilers: field and laboratory experiences. Fuel Process Technol 1998;54(1–3):47–78.
[43] Nielsen HP, Baxter LL, Sclippab G, Morey C, Frandsen FJ, Dam-Johansen K. Deposition of potassium salts on heat transfer surfaces in straw-fired boilers: a pilot-scale study. Fuel 2000;79(2):131–9.

[44] Dti 2005. Low-NO_x combustion systems. Capability brochure, cleaner fossil fuels programme CB008. DTI/Pub URN 05/903.
[45] Wagenaar BM, Van den Heuvel EJMT. Co-combustion of Miscanthus in a pulverised coal combustor: experiments in a drop tube furnace. Biomass Bioenergy 1997;12(3):185–97.
[46] Jenkins BM, Baxter LL, Miles Jr TR, Miles TR. Combustion properties of biomass. Fuel Process Technology 1998;54(1–3):17–46.
[47] Tilman D, Harding NS. Fuels of opportunity: characteristics and uses in combustion systems. Elsevier Science; 2004.
[48] Turn SQ, Jenkins BM, Jakeway LA, Blevins LG, Williams RB, Rubenstein G, et al. Test results from sugar cane bagasse and high fiber cane co-fired with fossil fuels. Biomass Bioenergy 2006;30(6):565–74.
[49] Fernando R. Fuels for biomass co-firing. IEA clean coal centre CCC/102. ISBN 92-9029-418-3; October 2005. 37pp
[50] European Union, 2001. Large Combustion Plants Directive – LCPD, 2001/80/EC.
[51] Spliethoff H, Hein KRG. Effect of co-combustion of biomass on emissions in pulverised fuel furnaces. Fuel Process Technol 1998;54(1–3):189–205.

Fuel 151 (2015) 40–49

Contents lists available at ScienceDirect

Fuel

journal homepage: www.elsevier.com/locate/fuel

Opportunities to improve the utilisation of granulated coals for blast furnace injection

Julian M. Steer [a,*], Richard Marsh [a], Mark Greenslade [b], Andrew Robinson [c]

[a] Cardiff School of Engineering, Cardiff University, Queen's Buildings, The Parade, Cardiff CF24 3AA, United Kingdom
[b] Tata Steel UK, Port Talbot, United Kingdom
[c] Specific, Baglan Bay Innovation & Knowledge Centre, Central Avenue, Baglan, Port Talbot SA12 7AX, United Kingdom

HIGHLIGHTS

- Blending coals improved the burnout of low volatile content semi anthracitic coals.
- Granulated samples showed a fragmentation effect in a drop tube furnace.
- Granulated particle fragmentation improved blend burnouts at lower residence time.
- Higher volatile content mass loss improved burnout at lower residence times.
- Included minerals with higher K/Al ratios gave non-additive burnout improvements.

ARTICLE INFO

Article history:
Received 2 October 2014
Received in revised form 5 November 2014
Accepted 16 December 2014
Available online 29 December 2014

Keywords:
Blast furnace
Granulated coal injection
Combustion
Devolatilisation
Blends

ABSTRACT

Coal injection plays an important role to the economic success of ironmaking by substituting a portion of the coke input and improving the blast furnace productivity. Manufacturers are looking at opportunities to increase their coal selection options by using higher proportions of technically challenging lower volatile matter content coals; this paper investigates the kinetics, devolatilisation and burnout of these in granulated coal blends using thermogravimetric analysis (TGA) and a drop tube furnace (DTF).

The char residue from the semi-anthracitic low volatile coal selected for this blending investigation had a much reduced reactivity at higher conversions which affected the blends in different ways. Burnout of the blends with the low volatile bituminous coals was improved by fragmentation of the granulated particles, but at longer residence times the lower reactivity of the more structurally ordered carbon in the semi anthracitic coal dominated. In contrast, the higher volatile coals showed improvements at low residence times corresponding to rapid volatile loss, but also showed non-additive blend improvement at longer residence times which may be explained by the more obvious presence of included minerals and the higher K/Al ratios associated with illite mineral phases known to improve burnout.

1. Introduction

Coal injection in the blast furnace is understood to reduce the consumption of expensive coking coals, increase productivity, increase flexibility in operation, improve the consistency of hot metal quality, and reduce the overall emissions from steel plants [1]. Typically, coal is injected into the blast line at temperatures around 1100 °C, and the particle residence time in the 'raceway' void formed by this hot blast is typically around 30–50 ms [2]; however, Guo et al. described work showing how raceway residence times could range from 25 to 1000 ms depending on the particle size due to turbulent conditions experienced in this region [3].

In most cases, coal is injected in a pulverised form where the particle size is typically below 75 μm; but this paper looks at granulated coal injection, which involves less energy to mill into specification, with a nominal sieve specification of 100% <1000 μm and 50% <250 μm [4,5]. However, the wider range and larger particle sizes are known to affect the devolatilisation and combustion of coals to a lesser or greater extent due to reasons such as heat transfer, mass diffusion, reactive surface area available, and maceral or mineral segregation affects [6–9].

Variability in coal properties can influence the quality of the hot metal, furnace stability, productivity and the off gas composition. Because of the short residence time in the raceway the devolatilisation and combustion of coal particles are vitally important, because unburnt particulates indicate un-utilised coal which increases the carbon input per tonne of hot metal and can interfere

* Corresponding author. Tel.: +44 2920876765.
E-mail address: SteerJ1@cardiff.ac.uk (J.M. Steer).

http://dx.doi.org/10.1016/j.fuel.2014.12.060
0016-2361/

with the permeability of the furnace [10–12]. For this reason the volatile content, or fuel ratio (fixed carbon/volatile matter), is often used by manufacturers as a measure of the suitability of a coal for injection and consists of combustible gases, incombustible gases, and condensable tars [13,14].

Higher volatiles generally have better combustion efficiency and produce more reactive chars and hence better burnout [15]. In comparison, low volatile coals with higher calorific values give better coke replacement ratios with less raceway cooling, but usually have lower combustion efficiency leading to unburnt chars [16,17]. However, higher volatile matter content coal can produce more soot which has lower reactivity than unburnt chars [18].

In order to utilise the optimum properties of both volatile scenarios, coals are often blended, but mixing has been found to alter the combustion properties depending on the coals chosen [16,19]. Kunitomo et al., found that high volatile matter coal formed a higher temperature combustion field that promoted the combustion of low volatile coals [20] whereas when Artos et al. blended high and low-rank coals they found it did not affect the combustion behaviour of the component coals when investigated in a thermogravimetric analyser or drop tube furnace [21]. However, there is also potential for individual coals to cause specific issues with grindability, combust at different rates and temperatures, and burnout at varying rates [18]. Recently Moon et al., showed non-additive behaviour between parent coals and their blends as the volatile matter content of the low rank coal (higher VM) influences the ignition temperature in the blend, whereas the char of the high rank coal (lower VM) in the blend influences the burnout temperature in the high temperature region [17].

Particularly important for the combustion of lower volatile content coals is the char reactivity and this has been studied in great depth [22–24]. The combustion of char is predominately controlled by chemical reactivity and pore diffusion of reactive and non-reactive gases in and out of the char [25–28]. The mineral content of coals, and the association of this in the coal, has also been shown to have an influencing effect on the devolatilisation and combustion giving effects that range from synergistic, catalytic or inhibitory depending on their levels and composition [29–34].

Although high volatile coals are often chosen for coal injection because of the concerns mentioned previously, more recently there has been a trend to utilise higher proportions of low volatile coals. However, increasing the proportion of these has the potential to reduce the furnace operation stability and increase top gas particulate emissions [1,18,35,36].

This paper measures the reactivity and burnout of coal blends with the more challenging high rank low volatile coals, aiming to establish the reasons how and why they affect the performance. In comparison to the state of the art, this work looks more closely at the use of granulated coals for blast furnace injection, instead of the pulverised coals more extensively covered by the literature for this application; it focuses on the novel way these coals and their blends fragment, swell and act synergistically on the burnout in a drop tube furnace.

2. Materials and methods

2.1. Materials

Five coals, ranging from the high rank semi-anthracitic LV1 to the lower rank high volatile bituminous HV, were chosen based on their variation in volatile matter shown in Table 1. The low volatile samples LV1, LV2 & LV3 ranged from 8.2% to 14.7% while the medium volatile MV was 24.6% and the high volatile HV up to 32.5%. For the investigation into coal blending, a 'reference' particle size specification was chosen, typical of a granulated coal specification for blast furnace injection, 100% $\leqslant$1000 μm with 50% $\leqslant$250 μm. The samples were milled to this specification using a TEMA™ disc mill and classified by dry sieving using the standard BS1016-109:1995. Because high rank semi-anthracitic coals can lead to unburnt particulates when injected into a blast furnace manufacturers are limited to how much they can incorporate, so for this research blends with 40 wt% LV1 were used.

The coal ash from each of the samples was analysed to identify the constituent elements and their variation, shown in Table 2, represented as the most stable oxide form.

2.2. Methods

2.2.1. Proximate and petrographic analysis

The classified samples were dried at 105 °C using BS11722:2013 until a constant weight and the volatile matter content was measured using standard BS15148:2005. Ash contents were carried out using the standard method BS 1171:2010.

The petrographic maceral analysis was carried out in accordance with ISO7404 by preparing a polished particulate block and carrying out a point count under reflected light microscopy to identify the different macerals present.

A Perkin Elmer Optima 2100D inductively coupled plasma spectrophotometer (ICP–OES) was used to determine the analysis of metal in the coal ash. Samples were prepared for analysis by microwave digestion using aqua regia (1 part HNO_3, 3 parts HCl), followed by hydrofluoric acid (HF, 48%) and boric acid (H_3BO_3).

TGA was carried out using a Perkin Elmer Pyris 1 TGA with an air flow rate or 30 mL/min at 4 different heating rates 5, 10, 15 & 20 °C/min. Kinetic analysis of the TGA mass loss and derivative data was used to determine the activation energy by standard BS ISO 11358-2:2005. Ozawa, and later, Flynn and Wall derived the relationship in Eq. (1), where E_a is the activation energy (kJ mol^{-1}) and R is the gas constant which for the four different heating rates and temperatures becomes Eq. (2) for a given degree of conversion.

$$\log\beta + 0.4567(E_a/RT) = \text{constant} \tag{1}$$

Eq. (1). Ozawa, Flynn and Wall model free kinetic relationship.

$$\begin{aligned}\log\beta_1 + 0.4567(E_a/RT_1) &= \log\beta_2 + 0.4567(E_a/RT_2)\\ &= \log\beta_3 + 0.4567(E_a/RT_3)\\ &= \log\beta_4 + 0.4567(E_a/RT_4)\end{aligned} \tag{2}$$

Eq. (2). Ozawa, Flynn and Wall iso-conversional relationship.

By plotting the logarithm of the heating rate, $\log\beta$, against the reciprocal of the absolute temperature, T^{-1}, for each degree of conversion, α, a series of straight lines were plotted from which the activation energy, E_a, was calculated from the slope ($-0.4567E_a/R$) [37,38]. The measured activation energy quoted in Table 3 was obtained from the average activation energy for each degree of conversion plot.

Scanning electron microscope (SEM) images were obtained using a FEI SEM-EDX instrument XL30 ESEM FEG at 512 × 384 resolution in back scattered and secondary electron detection modes.

Particle size analysis work was carried out using a Malvern Mastersizer 3000 laser diffraction particle analyser using a wet cell accessory with obscuration levels between 4% and 8%.

2.2.2. Devolatilisation and burnout testing using drop tube furnace

A drop tube furnace (DTF) was used to characterise the devolatilisation and burnout behaviour of the coal samples at 1100 °C in air for residence times between 35 ms and 700 ms. The high heating rate and short residence times in the DTF environment closely resemble those experienced when coal is injected into the blast air of the blast furnace raceway making this a particularly relevant technique [12,18,24,39]. Particles were fed into the top at feed

Table 1
Analyses of coals (dried).

Coal type	Proximate analyses				Petrographic analyses			
	Volatile matter content (wt%)	Ash content (wt%)	Fixed carbon content (wt%)	Gross Calorific value (MJ/kg)	Vitrinite (vol%)	Liptinite (vol%)	Inertinite (vol%)	Mineral matter (vol%)
LV1	8.2	5.1	86.7	34.4	83	1	14	2
LV2	13.3	8.1	78.6	32.3	60	0	39	1
LV3	14.7	4.3	81.0	34.4	78	1	18	3
MV	24.6	8.1	67.3	31.3	52	1	46	1
HV	32.5	7.0	60.5	32.3	71	10	17	2

Table 2
Inductively coupled plasma analysis of coal sample ash (wt%).

	Al_2O_3	Fe_2O_3	CaO	ZnO	TiO_2	MgO	CuO	Na_2O	P_4O_5	SiO_2	K_2O	Total
LV1	25.0	7.6	2.6	0.0	0.9	0.8	0.1	0.7	1.3	40.1	1.9	81.0
LV2	26.1	6.1	2.1	0.0	1.8	0.8	0.0	0.9	0.8	42.5	1.4	82.5
LV3	29.0	8.3	2.1	0.0	0.7	1.4	0.0	1.0	0.8	40.8	1.9	86.1
MV	19.7	6.9	2.1	0.0	0.8	1.0	0.0	0.5	0.3	55.9	2.2	89.4
HV	25.3	4.6	1.6	0.0	1.5	0.6	0.0	0.5	0.1	49.5	1.7	85.5

Table 3
TGA and kinetic parameters.

Samples	LV1	LV2	LV3	MV	HV	LV2:LV1 60:40	LV3:LV1 60:40	MV:LV1 60:40	HV:LV1 60:40
Ignition temperature (°C)	545	492	501	447	400	519	512	472	444
Theoretical value						513	519	486	458
% Change compared to theoretical						1.1	−1.3	−2.9	−3.1
Peak temp (°C)	675	636	637	625	570	631	626	622	621
Theoretical value						652	652	645	612
% Change compared to theoretical						−3.2	−4.0	−3.6	1.5
Burnout temp (°C)	1032	861	916	848	806	978	901	843	841
Theoretical value						929	962	922	896
% Change compared to theoretical						5.2	−6.4	−8.5	−6.2
Activation energy (E_a)[a] (kJ mol^{-1})	86.0	50.3	50.3	38.8	36.3	66.9	42.7	53.7	54.4
Theoretical value						68.1	68.1	62.4	61.1
% Change compared to theoretical						−1.8	−59.5	−16.3	−12.4
Combustibility index ($\times 10^{-8}$)	0.9	1.99	1.25	1.52	2.08	0.90	1.48	1.65	1.94
Theoretical value						1.56	1.12	1.28	1.61
% Change compared to theoretical						−36.7	32.7	29.1	20.0

[a] Average measurement of different degrees of conversion.

rates of 30 g/h, entrained in a laminar air flow at 20 L/min and collected at the bottom by means of a cyclone collector. The particle residence time was controlled by altering the distance of a moveable water cooled collection probe up to a maximum path length of 1.2 m from a water cooled inlet feeder.

The ash tracer method was used to calculate the burnout of the coals, sometimes referred to as the combustion efficiency [40,41]. This method assumes that the coal ash remains conserved in the char residue in the test conditions and that no ash species are volatilised. This was tested for all the coal samples at 1100 °C. It is important to note that because the burnout figures are calculated using the ash tracer method, there is room for error propagation which can lead to repeatability issues [42] and the measured standard deviations ranged from 0.2% to 5.2% with an average of 2.6%.

The burnout (%) is calculated from the ash balance of the initial content of ash in the coal (A_0) and the ash content of the residue collected post DTF (A_1).

$$\text{Burnout } (\%) = \frac{10^4\ (A_1 - A_0)}{A_1(100 - A_0)} \tag{3}$$

Eq. (3). Ash tracer burnout.

The extent of devolatilisation was determined by measuring the volatile matter content of the residues collected post DTF. These results were then adjusted using the ash tracer method to account for any differences in burnout and to obtain absolute figures for comparison.

3. Results and discussion

3.1. Coal blending

To investigate the effects of incorporating lower volatile coals for blast furnace coal injection, four blends were prepared of the HV, MV, LV2 and LV3 coals with 40% of the semi anthracitic low volatile matter content coal LV1. This proportion was chosen as an aspirational target because the injection of these coals in the blast furnace has been shown to be problematic at higher levels [10]. The Thermogravimetric analyser (TGA) was used to compare some of the specific parameters affected by blending because of its suitability to accurately measure thermal mass loss change with controlled heating rates. From this measurement the ignition temperature, peak mass loss temperature and mass loss rates were obtained and the Ozawa- Flynn, iso-conversional, model free, kinetic method used to calculate the activation energy.

In relation to a blast furnace raceway where the heating rates are in the order of 10^4–10^5 °C/s [10], the heating rates of a TGA (10 °C/min) are orders of magnitude lower with small sample masses (~20 mg) and a bulk sample analysis method where there are potential interaction and gas diffusivity effects. However, the technique is fast, reliable and convenient. In contrast to this, the drop tube furnace (DTF) measures burnout and devolatilisation under high particle heating rate conditions (10^4 °C/s) [43], dilute particle phase and high temperatures. Because of its similarity to the raceway conditions, this makes the DTF a very useful comparison technique.

3.2. Thermogravimetric (TGA) and kinetic analysis

Thermal analysis profiles of the mass loss versus temperature are shown in Fig. 1a for the unblended coals and Fig. 1b for the blended coal samples as measured using the TGA at a 10 °C/min ramp rate. The derivative curves plot the rate of mass loss for the coals versus temperature for the unblended coals in Fig. 2a and for the blended coals in Fig. 2b.

Because of the short particle residence time in the raceway ca. 35 ms [2], blast furnace iron manufacturers use the volatile matter loss as an important technical parameter to determine the suitability of coal. With respect to temperature, the mass loss profiles approximately follow the order of volatile matter content from highest to lowest as might be expected HV, MV, LV2, LV3 and LV1. However, it is worth noting that the profile shape of LV2, in Fig. 1a, indicates higher char reactivity at high conversion levels with a lower burnout temperature compared to the other lower volatile coals. Although higher volatiles have been shown by some authors to produce more reactive chars [15], this is not always the case, and Australian low volatile coals with similar volatile matter contents have been shown to display different char reactivities, suggesting differences between coals of similar VM [44]. Conversely, the lowest volatile coal LV1 had the broadest derivative curve with the lowest rate of mass loss change suggesting that in addition to a low volatile content this coal had lower char reactivity.

For the coal blends, shown in Fig. 2b, the profiles were closer with a narrower band of variation reflecting the smaller volatile blend range of 10.6–23.2%, compared to the unblended coals 8.2–32.5%. As expected because of the higher volatile matter content, the HV and MV blends show mass loss at a lower temperature than the lower volatile blends of LV2 and LV3. However, although the unblended LV2 coal had a mass loss profile at a lower temperature relative to the other low volatile coals, the profile for the blended LV2 showed a negative effect with the incorporation of LV1 coal with mass loss occurring at higher temperatures.

The quantitative measured figures for the unblended coals shown in Table 3 show a generally decreasing trend of lower ignition temperature, peak temperatures, burnout temperatures, and activation energy associated with higher volatile contents. To compare the effect of blending, the theoretical values for the different parameters were calculated from the measured figures for the unblended coals assuming simple proportional additive behaviour.

A combustibility index was used to compare the different parameters together and incorporates the mass loss and the derivative mass loss; the higher this figure, the better the overall combustibility. The index is defined in Eq. (4) and is made up of the maximum rate of weight loss $(dw/dt)max$, the average rate of weight loss $(dw/dt)mean$, the ignition temperature (T_i) and burnout temperature (T_b) [45].

$$S = \frac{(dw/dt)mean\ (dw/dt)max}{Ti^2 Tb} \tag{4}$$

Eq. (4). Combustibility index.

The lowest VM LV1 coal had a significantly lower reaction index (0.9) compared to the other unblended coals, but although their VM contents were quite different (Δ = 19.2%), the combustibility index of the LV2 coal and the HV were close (1.99 and 2.08) due to the faster combustion rate of the LV2 char. In addition to the benefit of blending coals with better combustibility properties, the process of blending showed both synergistic and inhibitory non-additive blending results.

Compared to the theoretical values the ignition temperature, peak temperature and to a lesser extent the burnout temperature exhibited additive behaviour on blending. However, there was a marked reduction in the activation energy and a marked increase in the combustibility with the higher volatile coals and particularly with the LV3 coal. Considering the relatively small difference in volatile contents (6.5%) for the LV1 and LV3 this suggests a synergistic effect separate to the VM order. In contrast, the LV1 had an inhibitory effect on the mass loss rates in particular which, when blended with LV2, severely reduced the combustibility index (−36.7%).

Table 4 shows the activation energy and correlation coefficients for the coals and blends at different levels of conversion and describes more specifically what happens when the samples are blended. For the unblended low volatile LV1 the activation energy increases with conversion and indicates the lower reactivity of its char which affects each coal blend differently, this is consistent with increased carbon structure ordering and preferential consumption of less ordered carbon. The crystalline phase of carbon is expected to increase with coal rank which agrees with the order of the unblended samples from the semi anthracitic LV1 to the high

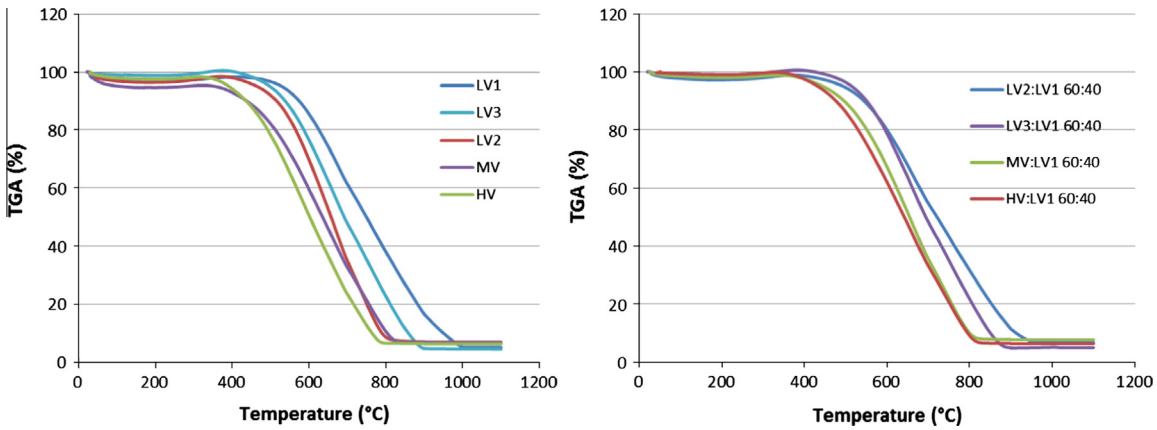

Fig. 1. Thermogravimetric mass loss curves for (a) unblended and (b) blended coals at 10 °C/min heating rate.

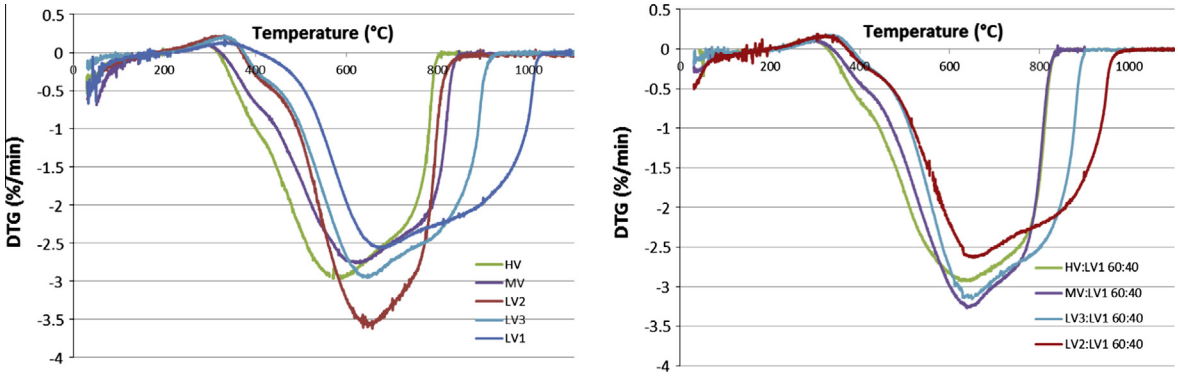

Fig. 2. Derivative thermogravimetric rate of mass loss curves for (a) unblended and (b) blended coals.

Table 4
Activation energy and correlation coefficients at different levels of mass conversion.

Conversion	R^2	E_a (kJ/mol)	R^2	E_a (kJ/mol)	R^2	E_a (kJ/mol)	R^2	E_a (kJ/mol)	R^2	E_a (kJ/mol)
	LV1		LV2		LV3		MV		HV	
0.1	0.9127	64.5	0.8495	48.4	0.8866	55.0	0.9260	35.9	0.9903	43.0
0.3	0.9956	81.0	0.8178	53.3	0.8389	52.8	0.9998	44.0	0.9908	38.3
0.5	0.9864	96.7	0.7410	52.1	0.7906	47.4	0.9854	40.7	0.9972	33.9
0.7	0.8837	101.6	0.6580	47.5	0.7552	46.1	0.9459	34.8	0.9999	30.2
			LV2:LV1		LV3:LV1		MV:LV1		HV:LV1	
0.1			0.9972	58.5	0.8694	54.6	0.9274	60.2	1.0000	71.8
0.3			0.9996	68.2	0.8306	46.1	0.9950	57.5	0.9855	54.5
0.5			0.9887	67.6	0.7966	37.6	0.9912	52.4	0.9753	48.4
0.7			0.9718	73.4	0.7465	32.7	0.9350	44.6	0.9636	42.9

volatile bituminous HV which affects the char reactivity [22–24,28]. However, the TGA blend results showed a non-additive coal specific behaviour for the LV2 blend which measured decreasing char reactivity whereas with the LV3 the char reactivity increased. With the higher volatile coals the LV1 had a negative effect on the devolatilisation but the MV and HV coals improved the char reactivity.

3.3. Drop tube furnace

A drop tube furnace (DTF) was used to investigate and compare the burnout of coals in air at 1100 °C, a similar temperature to that used for the hot air blast used for coal injection. The high heating rates and dilute particle phase make this equipment and technique very useful because of the similarities with the raceway region of the blast furnace.

The burnouts for the unblended coals shown in Fig. 3 closely follow the order of increasing volatile matter content with improving burnouts from LV1 (48.1%) to a much higher HV (86.2%) and similar profile shape. The exception to this pattern was LV3 which exhibited a slightly steeper profile shape at longer residence times. The low volatile coals were all characterised by low burnout (<10%) at low residence times which has particularly important implications for blast furnace injection where residence times in the raceway are low contributing to the challenge of using these coals. However, the higher volatile coals HV and MV both have better burnouts at low residence times because of the volatile matter mass loss.

Each of the sample burnouts for the blends with LV1 has been plotted alongside the unblended constituent coals and against the theoretical blend profile assuming additive behaviour to compare the relative effects. Blends with the lower volatile coals LV2 and LV3 in Fig. 4 had little effect at residence times of 35 ms because the unblended coals perform poorly. However, both showed equivalent or improved burnout relative to theoretical at

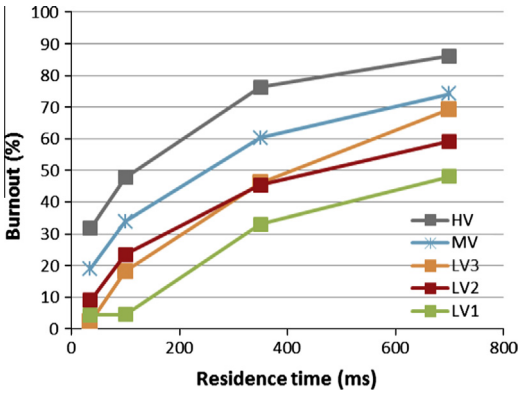

Fig. 3. Sample burnout of unblended coals in drop tube furnace at 1100 °C.

100 ms and 350 ms but LV1 influenced the blend most at longer residence times (700 ms) with reductions of 6.1% and 7.5% compared to the theoretical values. This is consistent with the TGA kinetic data at higher conversions where there was a measured increase in the activation energy for LV1 from 64.5 kJ/mol at 10% conversion to 101.6 kJ/mol at 70% conversion. The decrease in reaction rate and therefore burnout at higher conversions is affected by the higher activation requirement required for LV1 and suggests that the coal with lower activation energy burnt out first. However, it should be noted that the synergistic effect of the LV3 blend and the inhibitory effect of the LV2 blend measured by the TGA was not replicated in the DTF burnouts. This may in part be due to the lower overall conversion levels measured in the DTF and because of the much higher heating rates affecting the reactivity of the char formed.

In comparison, blending the higher volatile coals MV and HV, shown in Fig. 4, had a beneficial effect on the burnouts due to the

volatile matter release which was expected to contribute to a higher particle temperature and burnout [20]. The higher volatile coals appear to have a synergistic effect on the burnouts, particularly at the lower residence times, compared to the theoretical profiles.

Because of the measured burnout variation of the blended coals, the devolatilisation has also been plotted to investigate its behaviour. The blend profiles of the LV2, LV3 and MV in Fig. 5 showed very little variation compared to the theoretical profiles with no measured synergistic benefit on blending. However, blending the higher volatile content HV, in Fig. 5, showed some improvement in the devolatilisation. This effect is believed to be due to an increased particle temperature associated to the rapid burnout of the higher volatile matter content increasing the temperature surrounding the particle, which in turn might be expected to increase the measured volatile yield [20].

3.4. Particle size analysis

The sample residues after passing through the drop tube furnace at different residence times showed obvious visual changes. Residues after shorter residence times <100 ms were characterisatically dark with relatively high levels of unburnt carbon, whereas after longer residence times >350 ms the residues become distinctly lighter with obvious particle swelling. The observations with increasing burnout implied decreasing carbon with reduced density and potentially increased porosity which would affect the reactivity and burnout of the chars formed.

To investigate this more closely, laser diffraction particle size distributions were determined using a Malvern™ Mastersizer 3000. Two distinct effects in the particle size distributions were measured the fragmentation and swelling. The fragmentation occurs where larger particles heat very quickly and break into smaller pieces [46] and would be expected to have a positive effect on the sample burnout as the surface area exposed for reaction increases correspondingly.

Fig. 6 shows the difference in the Dv90 (the maximum particle diameter below which 90% of the sample volume exists) sample particle size before and after 35 ms in the drop tube furnace. The histogram indicates only a small decrease (50 μm) in the Dv90 particle size for the LV1, whereas the other coals all show larger changes particularly with LV2 and LV3 coals with reductions of 554 and 520 μm respectively.

Considering the importance of particle size and surface area with respect to reactivity and burnout, this fragmentation of the particles measured at 35 ms could explain why LV2 and LV3 coals measured improved burnout at longer residence times even though the difference in volatile matter content (5.1% and 6.5%) is low. The MV and HV coals also show reductions in the Dv90 (206 and 241 μm) but lower than LV2 and LV3 which could be due to a swelling effect noted in Fig. 7 associated with the larger volatile matter content release and offsetting the fragmentation.

For the blended coals there was a measured fragmentation effect at 35 ms compared to the LV1, with reductions in Dv90 ranging from 223 to 462 μm compared to the small change of 49 μm with the LV1. For the blends with lower volatile matter, the fragmentation could explain the improved burnouts at 100 and 350 ms relative to theoretical, particularly for the LV3 coal blend.

The second measured change in particle size distribution was a particle swelling effect which occurred at longer residence times (700 ms) in the drop tube furnace, as shown in Fig. 7, measured by the Dv90 particle size increase between 35 and 700 ms. An increase in the size of the particles relative to their mass could potentially decrease the density and increase porosity, unless the effect is due to agglomeration.

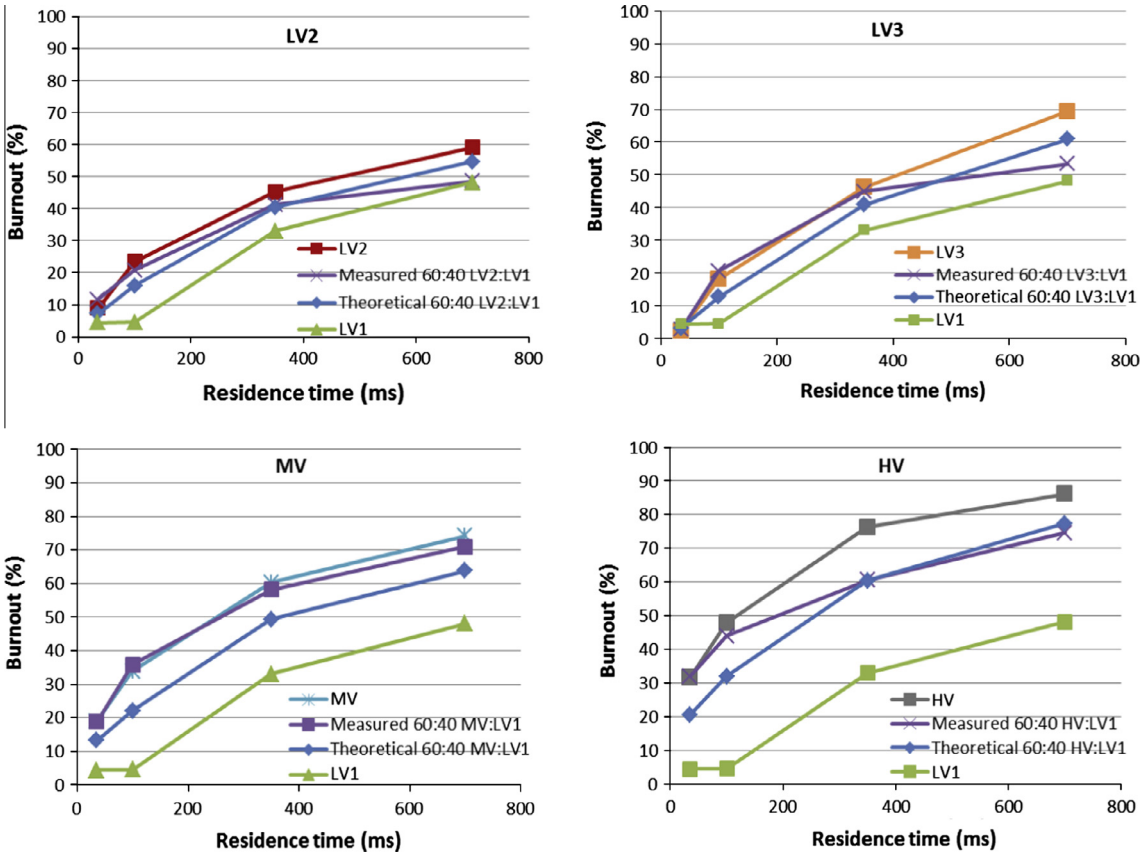

Fig. 4. Sample burnouts of unblended and blended coals in drop tube furnace at 1100 °C.

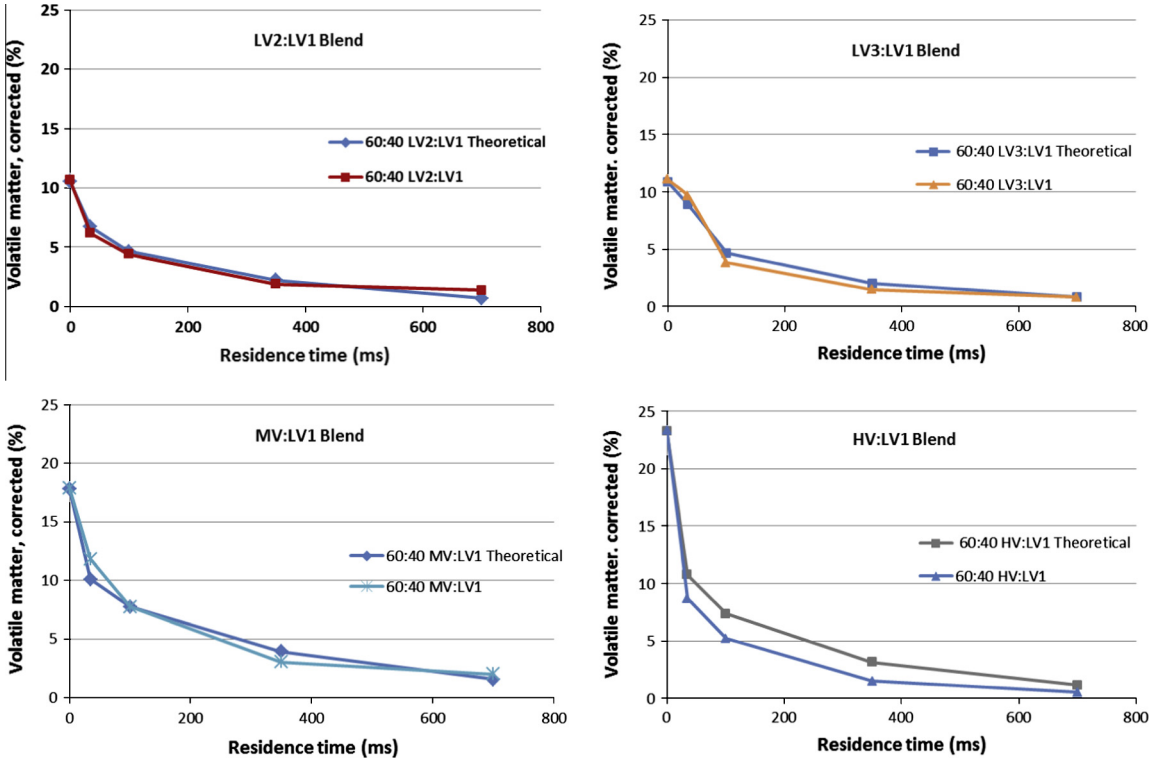

Fig. 5. Devolatilisation curves for blends compared to the theoretical profiles.

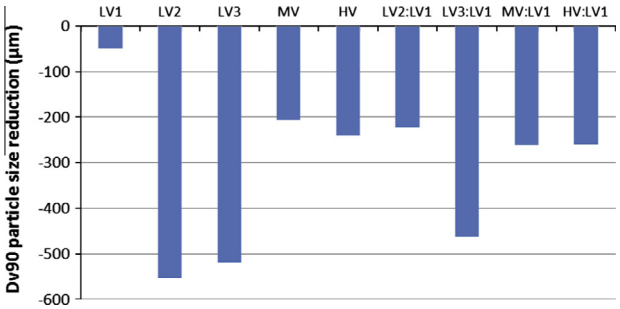

Fig. 6. Dv90 particle size reduction after 35 ms post DTF compared to initial pre DTF values.

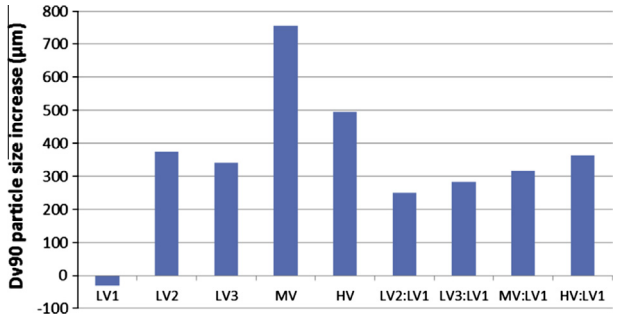

Fig. 7. Dv90 particle size increase after 700 ms post DTF compared to initial pre DTF values.

For the unblended coals, the lowest volatile content LV1 showed little change (−32 µm) in the relative Dv90 particle size of the unburnt DTF residues corresponding to the lowest burnout (48%) and consistent with its semi anthracitic rank. However, the other lower volatile content coals, LV2 and LV3, with higher burnouts (59% and 69%), both show relative increases by 375 and 342 µm even though LV3 has a very similar petrographic composition to LV1. The high volatile, MV and HV, both have better DTF burnouts (74% and 86%) and show large relative increases of 755 and 455 µm, caused by the escaping volatile matter and viscoelastic plastic flow of these samples.

For the coal blends with LV1, all the samples measured an increase in the relative particle sizes ranging from 249 to 364 µm. For the lower volatile coals LV2 and LV3, the swelling effect actually corresponded to a reduction in the burnout at 700 ms relative to the theoretical values which might suggest agglomeration of the particles reducing the surface area and porosity and consequently affecting the reactivity. For the HV coal blend there was no change in burnout relative to theoretical, but the highest swelling coal MV gave the coal blend with the best burnout profile and the only coal to show improvement at all the residence times.

3.5. SEM particle analysis

3.5.1. Particle shape and structure post DTF

To investigate the effect of residence time in the DTF on the coal samples, scanning electron microscope images were used to visualise the char forming behaviour of the unblended coals to correlate with blending behaviour. Backscattered electron detection was used to obtain images to look at the fragmentation and compare with the particle effects measured using the Malvern particle size distributions; but it was also selected to highlight the distribution of higher atomic weight elements contributed by the mineral content, because of their potential effect on the reactivity of the samples.

LV1 particles after 35 ms in the DTF are shown in Fig. 8a and are characterised by sharp edges and brittle fractures from milling, with little evidence of any physical thermal change consistent with the low DTF burnout (4.0%), high TGA activation energy (64.5 kJ/

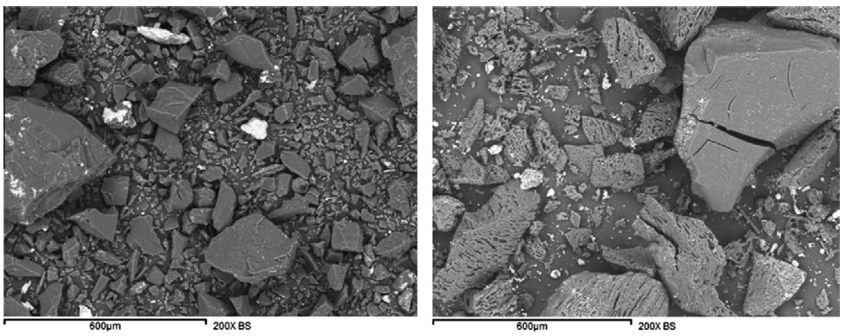

Fig. 8. Backscattered images of the DTF residue of LV1 after (a) 35 ms and (b) 700 ms.

mol @ 10% conversion) and low levels of fragmentation measured by laser diffraction. In comparison, in Fig. 8b, after 700 ms burnout the particles show some surface pores associated with burnout; however, the char formed had the appearance of a solid structure consistent with the semi anthracitic rank with little change in particle shape, suggesting that phases of this coal are very unreactive. This agrees with the much higher char activation energy (101.6 kJ/mol @ 70%) and lower TGA combustibility index at high conversions and lower DTF burnout after 700 ms.

In comparison, the LV2 low volatile coals in Figs. 9a and b produced cenospherical type char with evidence of explosive fracture, hollow structures with thin walls consistent with the fragmentation observed with the particle size measurement and after 700 ms it also showed signs of particle swelling and bubbling. The other low volatile coal LV3 in Fig. 10a and b also showed characteristics of a cenospherical char structure with thin fractured walls but after 700 ms these structures appear to have agglomerated into larger porous chars. These appeared to be bigger than the measured Dv90 figures obtained by laser diffraction which may suggest their hollow nature was more brittle and fracture occurred as the particles were circulated around the diffraction measurement cell.

The images for the MV shown in Fig. 11a and b appear to show a mixture of thin walled fragments and sintered residues at 35 ms and a large swelling effect after 700 ms. The char structure appeared to be less open than the LV2 and LV3 with small surface porous holes which might suggest that the higher burnout measured for this coal is more to do with higher reactivity than porosity. In comparison, the HV images shown in Fig. 12a and b also show the swelling effect, but in difference to the MV, the images after 700 ms indicate a more open hollow structure with exposed thin walls and a higher expected porosity correlating with a high burnout 86.2%.

3.5.2. Particle mineral content post DTF

It is well researched and understood that the mineral content of coals can contribute synergistic, catalytic and inhibitory effects on combustion and devolatilisation [29–34]. With this in mind, backscattered electron SEM images were collected to identify the distribution of the mineral elements. These heavier elements show up as lighter areas on the SEM images due to increased electron scattering.

The lowest burnout LV1 had larger ash particles present as discrete particles not closely associated with the char. The presence of minerals, as inclusions in the residue of the matrix, was less obvious than with the other samples, even after 700 ms in the DTF. In comparison, the other low volatile coals LV2 and LV3, had more obvious mineral inclusions as flecks closely associated in the coal residue which could facilitate improved combustion compared to the LV1 and explain improved burnout compared to theoretical. The higher volatile samples also had very visible mineral inclusions in the coal residue surface at 35 and 700 ms in the DTF.

The other consideration with inert mineral content is that as the sample combusts the mineral concentration relative to the unburnt residue increases. This effect is most noticeable with higher volatile samples whose ash contents after a residence time of 700 ms were HV (35.2 wt%) and MV (24.4 wt%) compared to the lower volatile coals LV1 (9.4 wt%), LV2 (17.7 wt%) and (LV3 14.4 wt%). A synergistic/catalytic effect by the mineral content could be a contributing reason to explain why the chars of the higher volatile coals, containing higher mineral concentrations, show good burnouts across all the residence times tested in the DTF.

In particular, the MV coal had better burnout compared to theoretical across all residence times despite a high inertinite content, which might be expected to reduce its reactivity. Coal ash samples are widely reported to contain different aluminosilicate clay min-

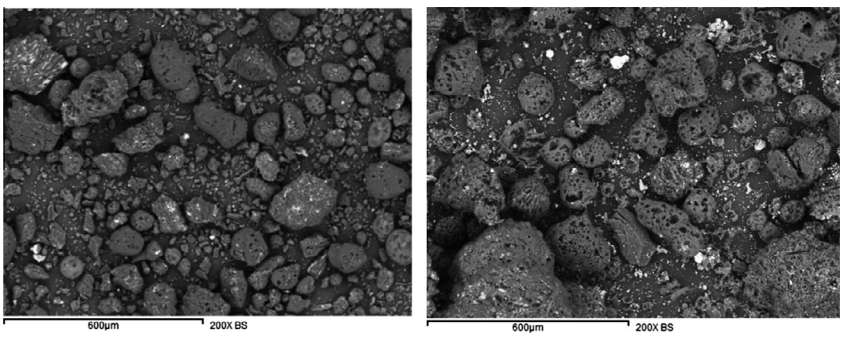

Fig. 9. Backscattered images of the DTF residue of LV2 after (a) 35 ms and (b) 700 ms.

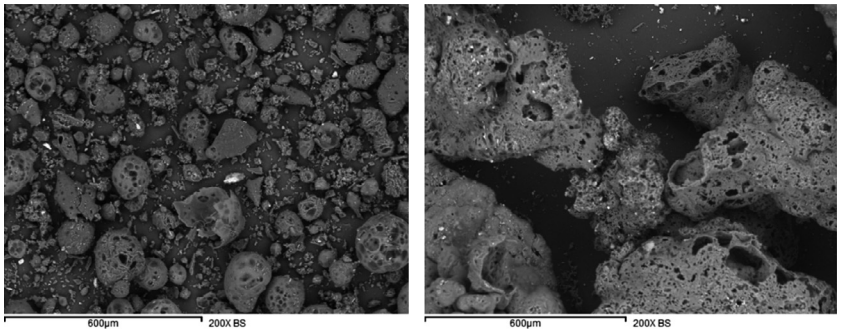

Fig. 10. Backscattered images of the DTF residue of LV3 after (a) 35 ms and (b) 700 ms.

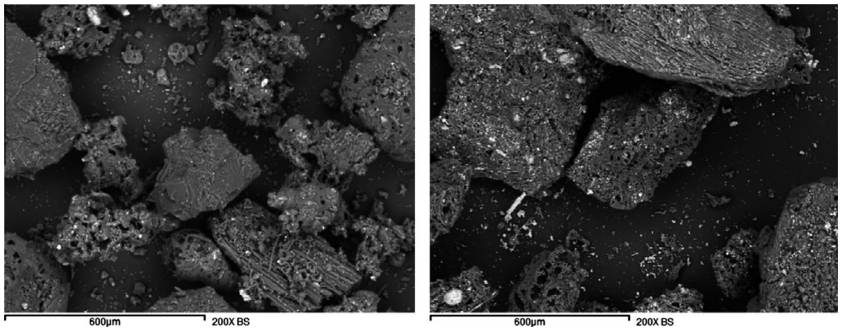

Fig. 11. Backscattered images of the DTF residue of MV after (a) 35 ms and (b) 700 ms.

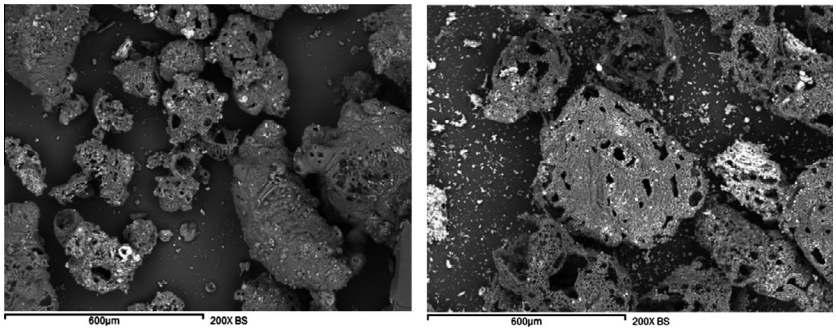

Fig. 12. Backscattered images of the DTF residue of HV after (a) 35 ms and (b) 700 ms.

Table 5
Ash elemental ratio (normalised to LV2 ash content).

	LV1	LV2	LV3	MV	HV
Si/Al ratio	0.89	1.45	0.66	2.5	1.5
K/Al ratio	0.08	0.09	0.06	0.17	0.09
DTF burnout % (700 ms)	48	59	69	74	86

eral phases, which have been reported to produce positive combustion effects such as catalysis and negative effects such as fluxing [29–31,33,34,47]. In Table 5 the elemental ratios of silicon and potassium relative to aluminium, taken from the ICP ash analysis in Table 2, indicate that MV has a higher silicon/aluminium which is likely to contribute to a reduced fluxing and a higher potassium/aluminium ratio which indicates a higher proportion of the illite mineral shown by other authors to have a synergistic/catalytic effect on burnout. There does not appear to be a correlation for all the coals but the higher potassium ratio of the MV coal and its known effect could explain the improved burnout compared to its theoretical profile and particularly on the blend with LV1 coal.

4. Conclusions

The results of this work gave an insight into the blending of a semi anthracitic low volatile content coal (LV1) for granulated coal injection and the way it affects the burnout and devolatilisation with coals of different ranks and volatile content. It was found that not only was it possible to increase the burnout and volatile yield of the LV1 by blending with these other coals, but that they showed non-additive improvements relative to the theoretical values.

Even after 700 ms in the DTF, the unblended higher rank LV1 showed little change in the char form and structure. In comparison, the granulated particles of the other low volatile coals showed strong fragmentation at 35 ms forming cenospherical type, hollow and thin walled char structures with ‘included’ mineral phases which corresponded to burnout improvements. However, blending these low volatile bituminous coals could not offset the effect of increasing activation energy for the LV1 char at higher residence times (700 ms) and burnouts were lower than theoretical.

Blending the highest volatile content coal and LV1 improved the low residence time burnout due to the fast release of volatile mat-

ter with some evidence of an increased particle temperature due to this, as indicated by an increased volatile yield relative to theoretical. Along with a related increase in particle swelling behaviour, and signs of a more porous char, the burnouts were correspondingly higher.

The activation energy and combustibility of the LV1 char was improved on blending with higher volatile coals and the blend with the mid volatile matter bituminous coal showed non-additive burnout improvement above theoretical at all residence times . This coal contained higher K/Al ratios associated with the mineral illite, identified in other work as contributing a synergistic or catalytic effect; along with the presence of other minerals as inclusions through the granulated coal particles, this goes some way to explaining the improved burnout. Further work would benefit from looking at the surface chemistry more closely with XPS to identify reactive or catalytic elemental associations to strengthen this conclusion.

Acknowledgement

The authorship wishes to acknowledge and thank Tata Steel Europe Ltd. for financial assistance with this project and support obtaining samples.

References

[1] Carpenter AM. Use of PCI in blast furnaces. In: IEA Clean Coal Centre; 2006.
[2] Zhang SF, Bai CG, Wen LY, Qiu GB, Lü XW. Gas-particle flow and combustion characteristics of pulverized coal injection in blast furnace raceway. J Iron Steel Res Int 2010;17:8–12.
[3] Guo B, Zulli P, Rogers H, Mathieson JG, Yu A. Three-dimensional simulation of flow and combustion for pulverised coal injection. ISIJ Int 2005;45:1272–81.
[4] Maldonado R, Hanniker G, Pettifor M. Granular coal injection into blast furnaces at the Scunthorpe works of the British steel corporation. In: Proceedings – ironmaking conference; 1985. p. 425–35.
[5] Guo H, Su B, Zhang J, Shao J, Zuo H, Ren S. Energy conservation for granular coal injection into a blast furnace. JOM 2012;64:1002–10.
[6] Barranco R, Colechin M, Cloke M, Gibb W, Lester E. The effects of pf grind quality on coal burnout in a 1 MW combustion test facility. Fuel 2006;85:1111–6.
[7] Li F, Zhang J, Qi C, Pang Q, Rao J, Ma C. Investigation on the dual influence of pansteel pulverized coal combustion process by coal quality and particle size. In: Materials science and technology conference and exhibition 2013, MS and T 2013; 2013. p. 566–73.
[8] Yi B, Zhang L, Mao Z, Huang F, Zheng C. Effect of the particle size on combustion characteristics of pulverized coal in an O_2/CO_2 atmosphere. Fuel Process Technol 2014;128:17–27.
[9] Yu D, Xu M, Sui J, Liu X, Yu Y, Cao Q. Effect of coal particle size on the proximate composition and combustion properties. Thermochim Acta 2005;439:103–9.
[10] Ishii K. Advanced pulverised coal injection technology and blast furnace operation. Elsevier Science Ltd.; 2000.
[11] Chen WH, Du SW, Yang TH. Volatile release and particle formation characteristics of injected pulverized coal in blast furnaces. Energy Convers Manage 2007;48:2025–33.
[12] Li H, Elliott L, Rogers H, Austin P, Jin Y, Wall T. Reactivity study of two coal chars produced in a drop-tube furnace and a pulverized coal injection rig. Energy Fuels 2012;26:4690–5.
[13] Bortz S, Flament G. Experiments on pulverized-coal combustion under conditions simulating blast-furnace environments. Ironmaking Steelmaking 1982;10:222–9.
[14] Suzuki T, Hirose R, Morimoto K, Abe T. Pulverized coal combustion in high temperature furnaces for steel making (First report: evaluation method of combustibility for pulverized coal). Bullet JSME 1984;27:2803–10.
[15] Kalkreuth W, Borrego AG, Alvarez D, Menendez R, Osório E, Ribas M, et al. Exploring the possibilities of using Brazilian subbituminous coals for blast furnace pulverized fuel injection. Fuel 2005;84:763–72.
[16] Raygan S, Abdizadeh H, Rizi AE. Evaluation of four coals for blast furnace pulverized coal injection. J Iron Steel Res Int 2010;17. 8–12, 20.
[17] Moon C, Sung Y, Ahn S, Kim T, Choi G, Kim D. Thermochemical and combustion behaviors of coals of different ranks and their blends for pulverized-coal combustion. Appl Therm Eng 2013;54:111–9.
[18] Du SW, Chen WH, Lucas JA. Pulverized coal burnout in blast furnace simulated by a drop tube furnace. Energy 2010;35:576–81.
[19] Biswas S, Choudhury N, Sarkar P, Mukherjee A, Sahu SG, Boral P, et al. Studies on the combustion behaviour of blends of Indian coals by TGA and drop tube furnace. Fuel Process Technol 2006;87:191–9.
[20] Kunitomo K, Orimoto T, Nishimura T, Naito M, Yagi JI. Effects of volatile matter of pulverized coal on reducing agents rate of blast furnace and combustion behavior of coal mixture. Tetsu-To-Hagane/J Iron Steel Inst Jpn 2004;90:190–7.
[21] Artos V, Scaroni AW. T.g.a. and drop-tube reactor studies of the combustion of coal blends. Fuel 1993;72:927–33.
[22] Davis KA, Hurt RH, Yang NYC, Headley TJ. Evolution of char chemistry, crystallinity, and ultrafine structure during pulverized-coal combustion. Combust Flame 1995;100:31–40.
[23] Russell NV, Beeley TJ, Man CK, Gibbins JR, Williamson J. Development of TG measurements of intrinsic char combustion reactivity for industrial and research purposes. Fuel Process Technol 1998;57:113–30.
[24] Chan ML, Jones JM, Pourkashanian M, Williams A. Oxidative reactivity of coal chars in relation to their structure. Fuel 1999;78:1539–52.
[25] Chagger HK, Jones JM, Pourkashanian M, Williams A, Owen A, Fynes G. Emission of volatile organic compounds from coal combustion. Fuel 1999;78:1527–38.
[26] Jones JM, Pourkashanian M, Rena CD, Williams A. Modelling the relationship of coal structure to char porosity. Fuel 1999;78:1737–44.
[27] Radović LR, Walker Jr PL, Jenkins RG. Importance of carbon active sites in the gasification of coal chars. Fuel 1983;62:849–56.
[28] Lu L, Kong C, Sahajwalla V, Harris D. Char structural ordering during pyrolysis and combustion and its influence on char reactivity. Fuel 2002;81:1215–25.
[29] Zhang H, Pu WX, Ha S, Li Y, Sun M. The influence of included minerals on the intrinsic reactivity of chars prepared at 900 C in a drop tube furnace and a muffle furnace. Fuel 2009;88:2303–10.
[30] Pohl JH. Influence of mineral matter on the rate of coal char combustion. In: ACS symposium series; 1986. p. 430–6.
[31] Shaolong W, Wei-Yin C, Guang S. Roles of mineral matter in the early stages of coal combustion. Energy Fuels 2009;23:710–8.
[32] Gupta S, Al-Omari Y, Sahajwalla V, French D. Influence of carbon structure and mineral association of coals on their combustion characteristics for Pulverized Coal Injection (PCI) application. Metall Mater Trans B 2006;37:457–73.
[33] Wei Z, Michael Moldowan J, Dahl J, Goldstein TP, Jarvie DM. The catalytic effects of minerals on the formation of diamondoids from kerogen macromolecules. Org Geochem 2006;37:1421–36.
[34] Menendez R, Alvarez D, Fuertes AB, Hamburg G, Vleeskens J. Effects of clay minerals on char texture and combustion. Energy Fuels 1994;8:1007–15.
[35] Oka N, Murayama T, Matsuoka H, Yamada S, Yamada T, Shinozaki S, et al. The influence of rank and maceral composition on ignition and char burnout of pulverized coal. Fuel Process Technol 1987;15:213–24.
[36] Su S, Pohl JH, Holcombe D, Hart JA. Slagging propensities of blended coals. Fuel 2001;80:1351–60.
[37] Flynn JHW, Wall LA. General treatment of the thermogravimetry of polymers. J Res Nat Bur Stand A Phys Chem 1966;70A.
[38] B.I. 11358-2:2014. Plastics-Thermogravimetry (TG) of polymers part 2: Determination of activation energy; 2014.
[39] Steer J, Marsh R, Griffiths A, Malmgren A, Riley G. Biomass co-firing trials on a down-fired utility boiler. Energy Convers Manage 2013;66:285–94.
[40] Ballantyne TR, Ashman PJ, Mullinger PJ. A new method for determining the conversion of low-ash coals using synthetic ash as a tracer. Fuel 2005;84:1980–5.
[41] Chen W-H, Du S-W, Tsai C-H, Wang Z-Y. Torrefied biomasses in a drop tube furnace to evaluate their utility in blast furnaces. Bioresour Technol 2012;111:433–8.
[42] Biagini E, Marcucci M. Review of methodologies for coal characterisation. In: International Flame Research Foundation; 2010.
[43] Li H, Elliott L, Rogers H, Wall T. Comparative study on the combustion performance of coals on a pilot-scale test rig simulating blast furnace pulverized coal injection and a lab-scale drop-tube furnace. Energy Fuels 2014;28:363–8.
[44] Juniper LAS, Smith GB. Research achievements in defining the combustion characteristics of Australian coals. In: International coal engineering conference, Institution of Engineers, Australia, Sydney; 1990. p. 129–34.
[45] Wang CA, Liu Y, Zhang X, Che D. A study on coal properties and combustion characteristics of blended coals in northwestern China. Energy Fuels 2011;25:3634–45.
[46] Liu G, Wu H, Gupta RP, Lucas JA, Tate AG, Wall TF. Modeling the fragmentation of non-uniform porous char particles during pulverized coal combustion. Fuel 2000;79:627–33.
[47] Spears DA. Role of clay minerals in UK coal combustion. Appl Clay Sci 2000;16:87–95.

Fuel 160 (2015) 413–423

Contents lists available at ScienceDirect

Fuel

journal homepage: www.elsevier.com/locate/fuel

The effects of particle grinding on the burnout and surface chemistry of coals in a drop tube furnace

Julian M. Steer [a,*], Richard Marsh [a], David Morgan [b], Mark Greenslade [c]

[a] Cardiff School of Engineering, Cardiff University, Queen's Buildings, The Parade, Cardiff CF24 3AA, United Kingdom
[b] Cardiff Catalysis Institute, School of Chemistry, Cardiff University, Park Place, Cardiff CF10 3AT, United Kingdom
[c] Tata steel UK, Port Talbot SA13 2NG, United Kingdom

HIGHLIGHTS

- Some larger coal particle sizes had better burnouts than smaller sizes.
- More surface oxygen bonding on the chars of larger particles compared to smaller ones.
- Grinding reduced sp^2 carbon bonding correlating with better burnout at low conversion.
- Smaller particle size coals tend to swell while larger size coals tend to fragment.
- More mineral phase changes occurred in the larger size coals.

ARTICLE INFO

Article history:
Received 25 March 2015
Received in revised form 24 June 2015
Accepted 29 July 2015
Available online 4 August 2015

Keywords:
Coal injection
XPS
Grinding
Surface properties
Drop tube furnace

ABSTRACT

Grinding coals to a pulverised coal specification for blast furnace injection can be costly, which is why some iron manufacturers choose a larger granulated coal size specification. However, there is a concern that these coals may have lower burnout in the raceway region so there is a technical and economic balance with coal grinding. This paper investigates how the process of grinding alters the physical properties, plus the surface chemistry, of coals and their chars formed in a drop tube furnace; it was found that in many cases the larger particle size coals gave improved combustion burnout compared to smaller sizes.

The physical properties of the chars, formed from grinding coals to different sizes, resulted in char swelling in the smaller particle sizes, compared to char fragmentation for the larger size classifications. Minerals phases associated with better coal reactivity were found to undergo higher conversion to other chemical forms with the larger size coals, suggesting a potential catalytic or synergistic contribution to their burnout. A closer look at the surface chemistry suggests that the action of grinding coals has an important effect on the surface chemistry. The XPS spectra of the chars, formed in a drop tube furnace, indicated that grinding the coals to a smaller particle size reduced the carbon–oxygen and carbon–mineral interactions compared to the larger sizes and correlated with the higher burnouts. An increasing trend was identified for the carbon sp^2 bonding with larger size and higher rank coals which correlated with their burnout at low carbon conversions; however, this did not hold at higher conversions, suggesting other factors were more dominant.

1. Introduction

Coal injection is a widely established technique used in blast furnace ironmaking, but grinding the coal into a pulverised coal specification costs energy, time, and money [1]; in a study using a Western bituminous coal (Oxbow), the U.S. department for energy found there was a 60% increase in the power required to grind it to a pulverised specification [2]. For this reason some manufacturers choose a larger granulated size specification typically in the region of 100% < 2000 μm and 20% < 75 μm to save grinding costs compared to general pulverised specification of 80% < 75 μm [3–6]. However, manufacturers using granulated coal injection risk unburnt materials carrying through the furnace into the top gas and reducing the amount of coal utilised, particularly with coals that combust less well in a blast furnace raceway, such as those with lower volatile matter content [7,8]. This paper seeks

* Corresponding author. Tel.: +44 2920870599; fax: +44 29 20874939.
E-mail address: SteerJ1@cardiff.ac.uk (J.M. Steer).

http://dx.doi.org/10.1016/j.fuel.2015.07.094
0016-2361/

to investigate the effect of particle size on the coal burnout in the context for blast furnace coal injection.

Grinding coal particles to a small particle size has been found to improve their combustion by increasing the surface area, pore volume and devolatilisation [6,9,10], but can also lead to maceral and mineral segregation effects. The maceral content of a coal affects the combustibility (temperature of combustion) and the ordering is considered to be liptinite < vitrinite < inertinite [11]. Work by Morgan et al. and Yu et al. found that burnout temperatures were reduced for smaller coal particle sizes [12,13], but the reactivity of the corresponding chars was intrinsically different due to maceral segregation effects although they were from the same coal [14]. In comparison Cloke et al. discussed this effect, noting that inertinite and fusinite concentrate in the smaller size fractions because they are brittle compared with other macerals, but they also noted that there were exceptions to this due to maceral associations with the mineral matter [15].

Segregation of the mineral constituents by grinding coal also plays an important role as these represent the non-combustible portion of the coal; and due to their inherent hardness, increasing amounts can affect the grinding which in turn increases abrasion and wear to the milling equipment [11,16]. Studies have shown that although the highest ash levels tended to occur in the smallest size fraction this was not the same for all coals as their organic affinity varies [15,17].

Thermal fragmentation of coals is a significant effect related to particle size and composition, but limited work has been carried out relating to surface chemistry and drop tube furnace burnout [18]. Particles have been found to fragment extensively depending on the coal type, particle size, furnace temperature and volatile matter content. Dacombe et al. found that fragmentation increased with particle size and correlated with a decreasing compressive strength, while Senneca et al. and Zhang et al. identified the role of internal overpressure and higher inner pressure due to the volatile content of the larger particles and the contribution to fragmentation [9,19,20].

Some coal particles exhibit a swelling effect which has also been found to be related to particle size. It has been found that small particle sizes have high swelling [21] and that in high vitrinite bituminous coals a greater swelling effect occurred due to the higher content of this maceral, producing more char cenospheres [22]. However, although more porous chars are associated with the swollen chars, agglomeration has also been observed in some coals and may also influence burnout [10].

This paper aims to investigate reasons for differences in the burnout of coal samples, ground and classified to three different sieved particle sizes, <106 μm, <500 μm and <1000 μm, using a drop tube furnace. The different sizes had different physical properties and laser diffraction was used to measure the particle size distributions to investigate fragmentation and swelling effects related to burnout. In comparison to the state of the art, this work relates the coal burnout with the effect of grinding on the surface chemistry and physical properties using X-ray photoelectron spectroscopy (XPS) to identify bonding interactions that contribute to improvements in combustion.

2. Materials and methods

Five coal samples were milled using a TEMA™ disc mill and classified by dry sieving using the standard BS1016 109:1995 into the following three different ranges.

1. 100% < 106 μm
2. 100% < 500 μm
3. 100% < 1000 μm 50% < 250 μm

The classified samples were dried at 105 °C using BS11722:2013 until a constant weight and the volatile matter content was measured using standard BS15148:2009. Ash contents were carried out using the standard method BS 1171:2010. The petrographic maceral analysis was carried out in accordance with ISO7404 by preparing a polished particulate block and carrying out a point count under reflected light microscopy to identify the different macerals present. The samples ranged from high rank semi-anthracitic LV1 to the lower rank high volatile bituminous HV and were chosen based on their variation in proximate analyses shown in Table 1.

A drop tube furnace (DTF) was used to characterise the devolatilisation and burnout behaviour of the coal samples at 1100 °C in air for residence times between 35 ms and 700 ms. The high heating rate and short residence times in the DTF environment closely resemble those experienced when coal is injected into the blast air of the blast furnace raceway making this a particularly relevant technique [23–26]. Particles were fed into the top at feed rates of 30 g/h, entrained in a laminar air flow at 20 L/min and collected at the bottom by means of a cyclone collector. The particle residence time was controlled by altering the distance of a moveable water cooled collection probe up to a maximum path length of 1.2 m from a water cooled inlet feeder.

The ash tracer method was used to calculate the burnout of the coals, sometimes referred to as the combustion efficiency [27,28]. This method assumes that the coal ash remains conserved in the char residue in the test conditions and that no ash species are volatilised. This was tested for all the coal samples at 1100 °C. It is important to note that because the burnout figures are calculated using the ash tracer method, there is room for error propagation which can lead to repeatability issues [29]. The average standard deviation for all the drop tube furnace burnouts was 2.4%, with a range from 0.1% to 4.1%.

The burnout (%) is calculated from the ash balance of the initial content of ash in the coal (A_0) and the ash content of the residue collected post DTF (A_1).

$$\text{Burnout } (\%) = \frac{10^4(A_1 - A_0)}{A_1(100 - A_0)}$$

Scanning electron microscope (SEM) images were obtained using a FEI SEM–EDX instrument XL30 ESEM FEG at 512 × 384 resolution in back scattered and secondary electron detection modes. Particle size analysis work was carried out using a Malvern Mastersizer 3000 laser diffraction particle analyser, capable of measuring between 0.01 and 3500 μm, using a wet cell accessory with obscuration levels between 4% and 8%.

Table 1
Average analyses of different particle size coals (dried).

Coal type	Proximate analyses				Petrographic analyses			
	Volatile matter content (wt%)	Ash content (wt%)	Fixed carbon content (wt%)	Gross calorific value (MJ/kg)	Vitrinite (vol%)	Liptinite (vol%)	Inertinite (vol%)	Mineral matter (vol%)
LV1	8.2	5.8	86.0	34.6	83	1	14	2
LV2	12.5	8.6	78.9	31.9	60	0	39	1
LV3	14.4	4.7	80.9	34.2	78	1	18	3
MV	24.4	7.8	67.8	30.8	52	1	46	1
HV	33.0	6.9	60.1	31.9	71	10	17	2

A Kratos Axis Ultra DLD system was used to collect XPS spectra using monochromatic Al X-ray source operating at 144 W. Data was collected with pass energies of 160 eV for survey spectra, and 40 eV for the high resolution scans. The system was operated in the hybrid mode, which utilises a combination of magnetic immersion and electrostatic lenses and acquired over an area approximately 300×700 μm. A magnetically confined charge compensation system was used to minimise charging of the sample surface, and all spectra were taken with a 90° take off angle. A base pressure of $\sim 1 \times 10^{-9}$ Torr (0.133 μPa) was maintained during collection of the spectra. In all cases a binding energy of 284.5 eV was used for the C 1s peak to account for peak shifts due to differences in sample charging.

3. Results and discussion

3.1. Drop tube furnace combustion

This study was based on coal samples ground to three different particle size classifications to cover a range up to a typical granulated coal specification used by some iron manufacturers for blast furnace injection. The aim of this approach was to measure both the effect of the different particle size, and also the impact of grinding on the sample burnout.

Many studies investigating the effect of particle size are based on a ground coal that is classified by sieving to obtain a portion of a specific size fraction [15]. However, with this approach, mineral and maceral segregation can occur between the different particle sizes obtained, which can affect the combustion properties. Rather than use a selected portion of a ground sample, each sample was classified, separated, ground and reclassified. The process was repeated to meet the required particle specification and to be more representative of an industrial grinding situation, where the entire sample is used rather than a sieved portion.

The graphs shown in Fig. 1 show the relationship between the burnout and residence time through the DTF, for the five different types of coal at the three different size classifications. As expected, the wide variation in the properties of the coals was reflected in the burnouts and the order of the absolute maximum burnout correlates predictably with the order of increasing volatile matter content for the coals. Interestingly, many of the larger particle size classifications had higher burnouts than the smaller ones suggesting that either the larger sizes were more reactive or that additional grinding was detrimental to the burnout of the smaller sizes.

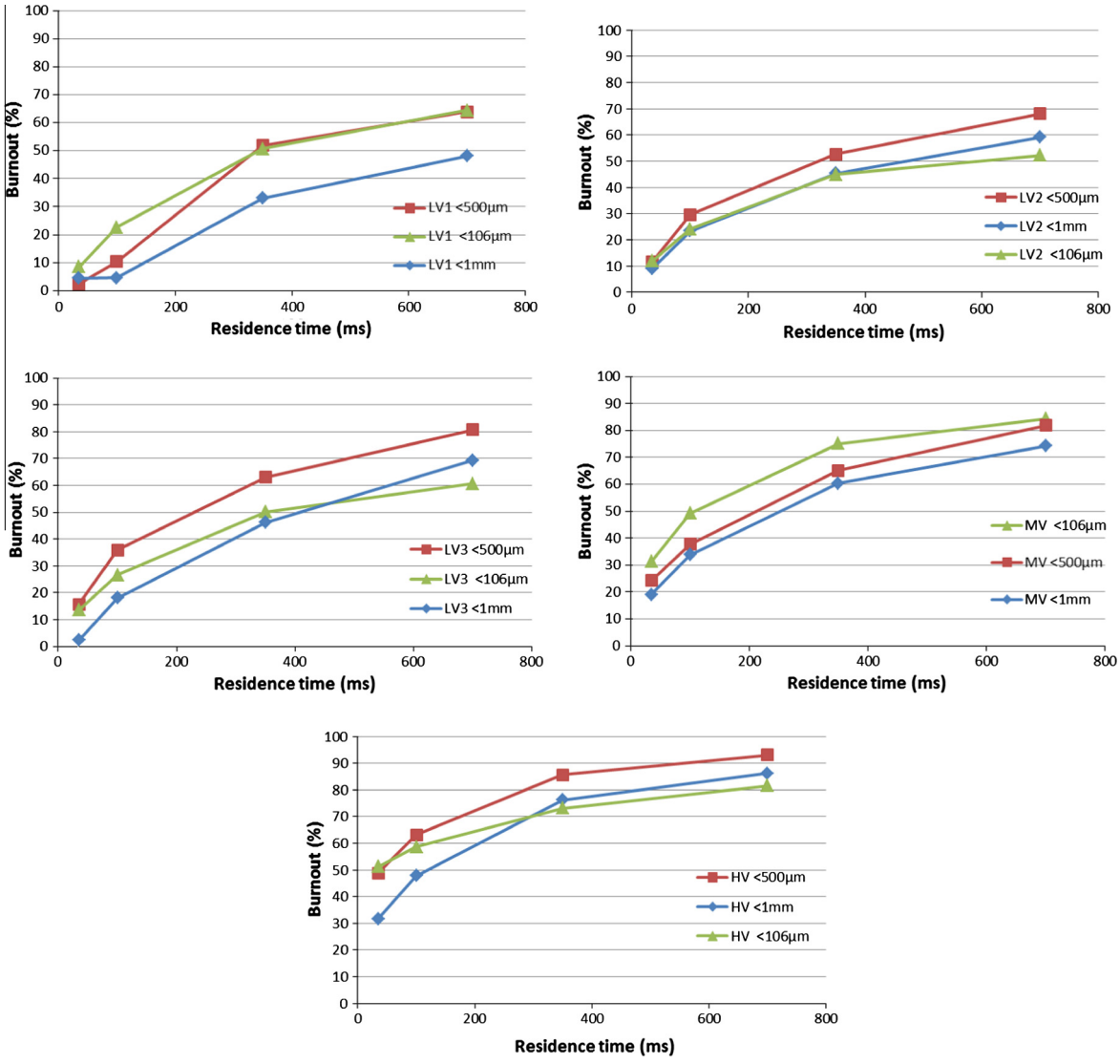

Fig. 1. Burnout of coals classified to particle sizes of 106 μm, 500 μm and 1000 μm in a DTF.

At the low DTF residence time (35 ms) the additional grinding required to meet the smaller particle size classification (<106 μm) gave negligible absolute difference in the burnout for the LV1 and LV2 low volatile content coals. For the LV3 and the HV coals, grinding to the mid-size classification of <500 μm was sufficient to give the same results as grinding and classifying to the smaller <106 μm. Only the medium volatile matter MV coal gave higher burnouts at 35 ms by grinding to the <106 μm classification at such a short residence time.

In comparison, at the higher residence time (700 ms), the <500 μm coal classification gave better burnouts for the LV2, LV3 and HV compared to the <106 μm classification. For the LV1 and MV coals the burnouts were similar for the <500 μm and <106 μm classifications. Therefore at longer residence times the results indicated that grinding to <106 μm gave little benefit to the burnouts, and with the LV2, LV3 and HV coals it had a detrimental effect.

Because of the energy requirement and cost associated with additional grinding, the results have important implications on the preparation requirements and processing of coals for blast furnace coal injection. The performance of some of the larger classifications suggests that for certain coal types, a granulated coal specification could give similar burnout performance to smaller particle size pulverised classification without the need for additional grinding.

To explain these differences in the burnout performance, the physical and chemical effects have been investigated to identify how grinding affects the coals by investigating particle swelling, fragmentation, mineral composition and surface chemistry.

3.2. Particle swelling and fragmentation effects

An important observation for the chars produced in the DTF was the variation in physical size and shape, depending on the particle size classifications of the coals from which they were derived. These changes were quantified by comparing the measured particle size distributions of the coals and the coal chars after different residence times through a drop tube furnace. It appears that the trend is for larger coal size classifications (<1000 μm) to fragment and for smaller coal size classifications (<106 μm) to swell; the coals classified to <500 μm fall somewhere in between the other classifications.

Fig. 2 compares the swelling/fragmentation of the chars produced from the different coal size classifications after 35 ms in the DTF, measured by the absolute change of the Dv90 (particle size below which 90% of the volume of sample exists). For the larger coal size classification of coal particles (<1000 μm), the LV3 and HV fragmented the most followed by the LV1 and LV2 coals. The MV coal char showed little change in the particle size at 35 ms, but for the <106 μm classification the MV and HV samples exhibited the largest swelling effect of the measured samples.

Fig. 3 compares the swelling/fragmentation effects after 700 ms in the DTF and the largest change in the chars was measured for the coals classified to <106 μm. The most significant swelling was measured for the LV3, MV and HV chars. This swelling and fragmentation effect has important implications for burnout. A swollen char is expected to have a more porous and open network allowing increased gas diffusion, while a fragmented char might be expected to have increased particle surface area with a fractured internal surface that could potentially have different surface chemistry.

Scanning electron microscope (SEM) images, shown in Figs. 4–8, were used to visualise the effect of swelling and fragmentation on cross sections of the coal char particles after 35 ms in the DTF. The char types formed from the <106 μm coal, shown in Figs. 4a, 5a, 6a, 7a, and 8a, ranged from cenospheres and network/honeycomb structures to the LV1 which had a mix of thick walled cenospherical and solid char particles as shown in Fig. 4a. In comparison, the char types shown in Figs. 4b, 5b, 6b, 7b, and 8b formed from the larger coal classification (<1000 μm) were all made up of solid particles.

Considering the magnitude of the swelling and fragmenting effect, there was no consistent correlation between the observed effects and the burnout. The overall trend after 35 ms was fragmentation of the <1000 μm classified coals, but this did not improve the burnout relative to the smaller particle size classifications. However, it might go some way to explaining why the burnout of the larger particle classifications do not differ as significantly from the small particle classification as might be expected considering the width of the particle distributions. At a residence time of 700 ms the largest effect was the char swelling, but the chars with the highest swelling showed little advantage from this effect on the burnout. The results suggest that other factors, such as the mineral composition or the surface chemistry, also play an important role on the burnout.

3.3. Mineral composition and interactions

Minerals in coal can have a catalytic, inhibitory and synergistic role on combustion and gasification and is an area that has been thoroughly researched [30–35]. Zhang et al. showed how the minerals affected the macerals and char porosity; for chars prepared in the DTF 'included minerals' facilitated the formation of pores in anthracites, but inhibited the formation of a more porous structure in bituminous coal chars [30]. Feng et al. found evidence of

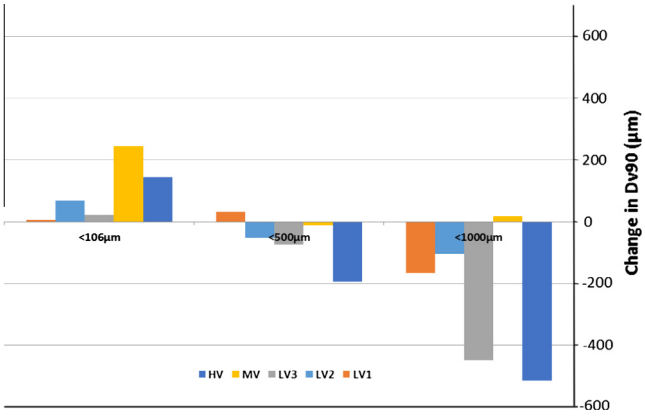

Fig. 2. Change in Dv90 of char relative to the initial coal for 35 ms residence time.

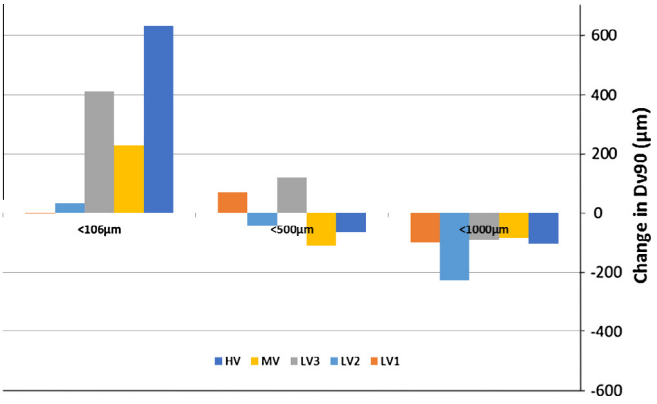

Fig. 3. Change in Dv90 for char relative to initial coal after 700 ms residence time.

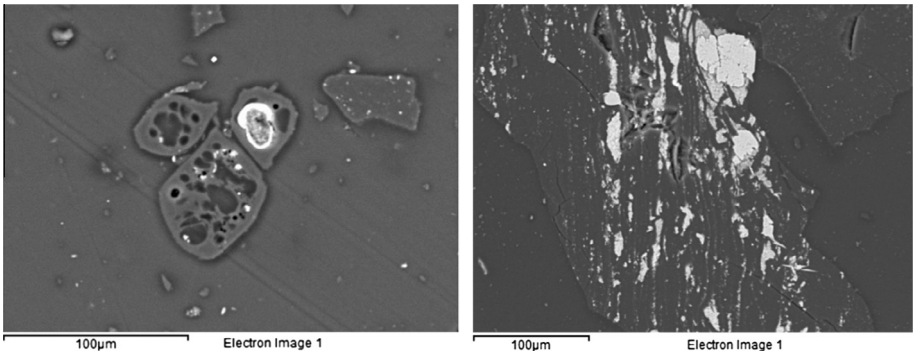

Fig. 4. Backscattered images of the LV1 char after 35 ms residence time (a) <106 µm and (b) <1000 µm.

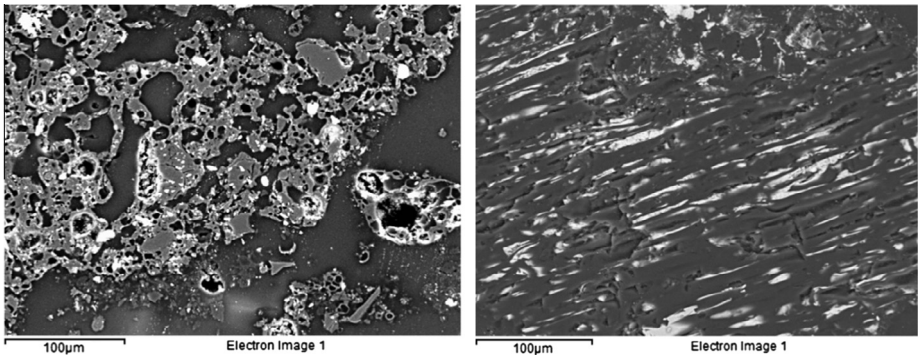

Fig. 5. Backscattered images of the LV2 char after 35 ms residence time (a) <106 µm and (b) <1000 µm.

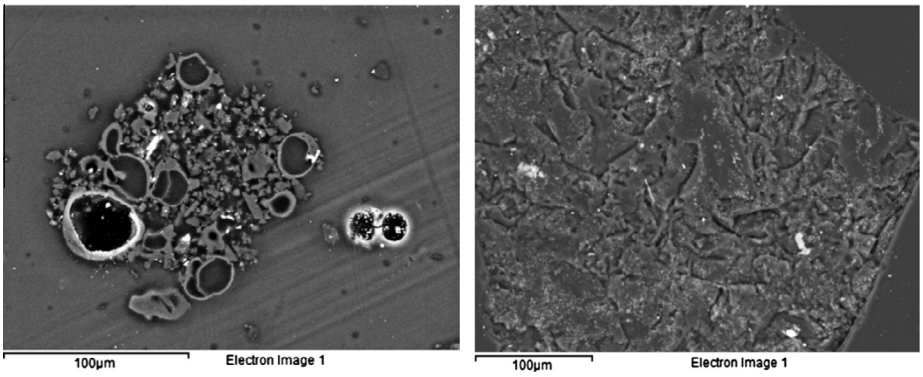

Fig. 6. Backscattered images of the LV3 char after 35 ms residence time (a) <106 µm and (b) <1000 µm.

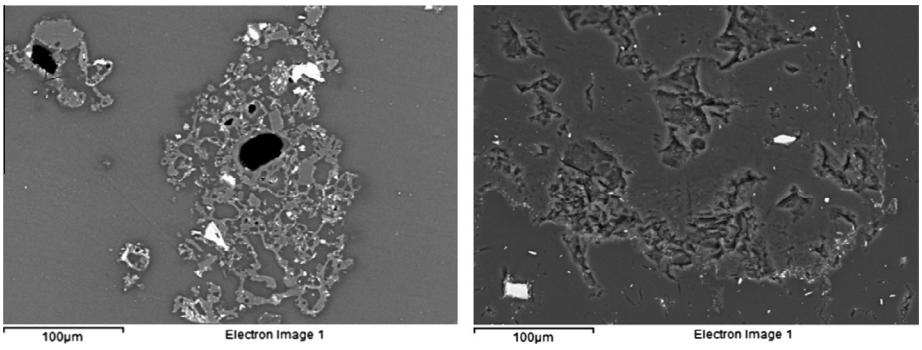

Fig. 7. Backscattered images of the MV char after 35 ms residence time (a) <106 µm and (b) <1000 µm.

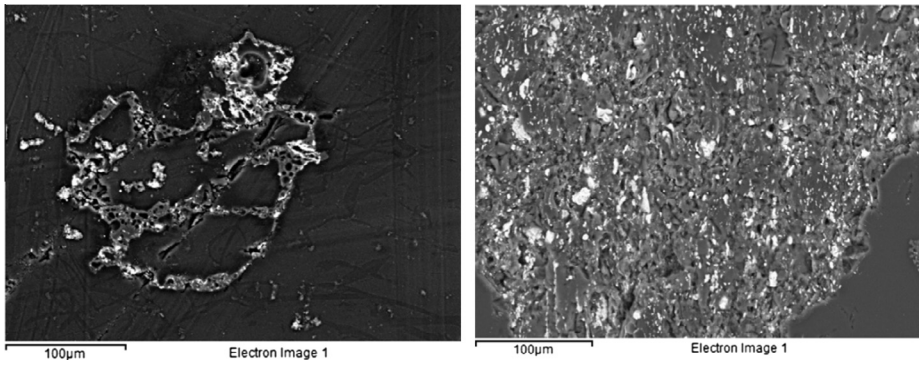

Fig. 8. Backscattered images of the HV char after 35 ms residence time (a) <106 µm and (b) <1000 µm.

catalytic ordering during heat treatment depending on the mineral content. By the relation of electrical resistivity to reactivity of chars in a TGA, they suggested thermal deactivation occurred due to carbon structural ordering catalysed by the inorganic mineral matter in the coal char whereas ash-free coal chars did not vary significantly. It has also been pointed out that there is often a lack of clear and conclusive correlation about the catalytic influence of minerals, particularly combustion of high rank coals and that contradictions and uncertainties associated with the influence of mineral content could be due to inhomogeneity [33].

Coal ash samples are widely reported to contain different aluminosilicate clay mineral phases, which have been reported to produce positive combustion effects such as catalysis and negative effects such as fluxing [30–32,34–36]. In a previous paper, the authors noted differences with the surface association of minerals as inclusions, identifying them as a potential contributory factor to improvements in the burnout of some coals [37] in particular the aluminosilicate mineral illite has been identified for the formation of parallel wide pores, increasing porosity and combustibility [30,35,36].

These aluminosilicates can be present in many different phases and kaolinite is known to lose hydroxyl functionality at around 500 °C, forming metakaolin which can then undergo phase changes to form species such as mullite and cristobalite which persist as solid phases up to 1600 °C [38,39]. The changes in the mineral phases could either contribute to better burnout or conversely might be present as the result of better burnout.

Because the minerals have been shown to affect the rate of combustion, this could contribute to the increased burnout in the larger particle size coal compared to the smaller particle sizes for LV2, LV3 and HV. Table 2 shows the percentage mass of different mineral phases in the post DTF char residue calculated from their concentrations measured by XRD in the ash. The results are grouped according to the classified coal particle size used to obtain each char, and indicate changes in the mineral compositions for the char residues.

In particular, the illite mineral phase present in the <106 µm and <500 µm chars at low 35 ms residence time decreases when held at the 700 ms residence time. For the <106 µm coals it was absent from the LV2 and MV char, but for the <500 µm particle classification it was completely absent for all the coal chars. The results suggest that the illite either converts to another phase or combines to form a non-crystalline amorphous phase and that this occurs more readily for the larger <500 µm particle size coals. Considering the role that the potassium (contained in the illite) has been shown to improve combustion in coal, this

Table 2
Mineral composition (mass %) of char obtained from XRD analysis of the ash.

	Amorphous	Quartz	Illite	Mullite	Anhydrite	Corundum	Hematite	Rutile
106 µm 35 ms								
LV1	3.3	1.2	0.9	0.0	0.0	0.0	0.2	0.0
LV2	5.2	1.7	1.3	0.0	0.0	0.4	0.3	0.0
LV3	2.5	0.0	1.7	0.0	0.4	0.0	0.2	0.0
MV	7.0	2.6	0.9	0.3	0.0	0.0	0.5	0.0
HV	8.6	2.5	0.9	2.7	0.0	0.0	0.0	0.0
500 µm 35 ms								
LV1	2.5	1.2	1.3	0.0	0.0	0.0	0.2	0.0
LV2	5.3	1.7	1.2	0.0	0.0	0.3	0.2	0.0
LV3	3.8	0.0	1.3	0.0	0.5	0.0	0.2	0.0
MV	6.6	2.3	0.7	0.1	0.0	0.0	0.2	0.0
HV	7.4	2.8	1.1	0.6	0.0	0.0	0.2	0.0
106 µm 700 ms								
LV1	7.5	2.9	1.3	1.7	0.0	0.0	0.6	0.0
LV2	11.1	2.0	0.0	1.2	0.0	0.5	0.3	0.3
LV3	6.8	0.0	1.1	2.2	0.0	0.0	0.0	0.0
MV	25.6	6.5	0.0	2.5	0.0	0.0	1.4	0.0
HV	18.9	5.5	1.2	3.5	0.0	0.0	0.0	0.0
500 µm 700 ms								
LV1	9.5	2.2	0.0	2.1	0.0	0.0	0.0	0.0
LV2	14.6	2.6	0.0	2.4	0.0	1.3	0.4	0.4
LV3	15.8	0.0	0.0	4.2	0.0	0.0	1.1	0.0
MV	21.9	4.4	0.0	4.1	0.0	0.0	0.9	0.0
HV	32.4	11.6	0.0	6.6	0.0	0.0	0.0	0.0

conversion/consumption could be a contributing factor to the better burnouts for some of the coals at <500 μm.

Apart from the low levels in MV and HV, the mullite mineral phase absent in the <106 μm chars and the <500 μm chars at 35 ms was present at higher levels after 700 ms, and particularly for the larger <500 μm coal particle size. Fig. 9 plots the change in the mullite as the absolute percentage in the char (calculated using the char ash content and the mullite concentration measured by XRD in the ash) against burnout. An increasing trend in the mullite contained in the char correlates with increasing burnout and suggests that it may either play a role in catalysing burnout or that is indicates the conversion of other mineral phases which might have a role increasing the burnout.

3.4. Surface chemistry analysis using X-ray photoelectron spectroscopy (XPS)

The previous section used bulk analysis techniques to investigate sample changes, but the interfacial gas–solid reaction is fundamental in coal combustion, herein we investigate the surface chemistry using XPS, which looks specifically at the coal surface to a depth of circa 10 nm [40]. A valuable aspect of this technique is the information that it gives regarding the surface chemistry and this has been used previously for coal research to compare the effect of rank, ash mineral associations, and the effect of weathering on the surface of coals [32,41–44].

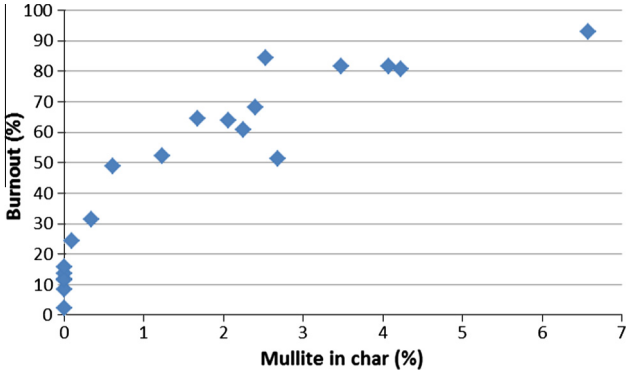

Fig. 9. Sample burnout plotted against the concentration of mullite in the char residue.

The carbon spectral peaks are made up of chemical information which can be deconvoluted by peak fitting to determine carbon–oxygen bonding and carbon hybridisation. This involves the separation of overlapping peak intensities by constructing a peak model from known line-shapes and fitting these synthetic component peaks to the peak data envelope. However, it is well recognised that there is some difficulty in this technique due to C 1s peak asymmetry which affects peak fitting [45–48] and this should be considered in the findings. Coal is a highly heterogeneous material and the high resolution spectra of the C 1s region indicate a range of different carbon–oxygen bonding present on the sample surface which shift the electron binding energies (BE) depending on the chemical environments surrounding the carbons [48]. These shifts can be problematic to accurately determining the split between carbon sp^2 and sp^3 bonding areas by the peak deconvolution method which is why we have also used the C KLL Auger spectra to determine the carbon hybridisation more accurately [49].

Table 3 details the peak fitting figures for the carbon spectra which were deconvoluted into five component peaks corresponding to graphitic sp^2 type carbon bonding (peak I BE = 284.3–284.5 eV); sp^3 type carbon bonding (peak II BE = 285.1–285.5 eV); carbon present in alcohol or ether groups (peak III BE = 285.6–286.5 eV); carbonyl groups (peak IV BE = 287.0–287.8 eV); and carboxyl or ester functions (peak V BE = 288.1–288.8 eV) [42,43,50–53]. Other peaks were also recorded and those at binding energies greater than 290 eV are usually attributed to π–π^* aromatic shake up effects, while those below 284 eV are attributed to plasmon loss features in this region. However, it should be noted that the peaks in the 289.4–290.9 eV range have been associated with multiple

Table 3
Absolute atomic % of deconvoluted high resolution XPS C 1s spectra.

Peak	I	II	III	IV	V	Satellite π–π^* peaks			C 1s
Binding energy range (eV)	284.3–284.5	285.1–285.5	285.6–286.5	287.0–287.8	288.1–288.8	289.4–290.9	291.2–292.1	293.4–293.9	Total %
LV1 coal									
106 μm	49.7	11.0	4.3	–	–	2.2	–	0.6	67.8
500 μm	56.3	13.0	3.3	–	1.4	2.2	–	0.5	76.8
1000 μm	58.9	5.7	3.7	–	1.6	2.7	–	0.7	73.5
LV1 char									
106 μm 700 ms	43.8	16.3	4.7	–	2.4	1.6	–	–	68.8
500 μm 700 ms	41.3	15.2	12.3	–	5.2	1.9	1.5	–	77.4
1000 μm 700 ms	42.4	21.4	6.2	–	6.6	1.8	1.5	–	79.9
LV2 coal									
106 μm	72.7	9.4	1.9	–	1.5	0.3	–	–	85.8
500 μm	56.0	14.3	4.4	–	2.5	0.7	–	–	78.0
1000 μm	50.2	17.0	4.9	–	1.9	0.7	–	–	74.7
LV2 char									
106 μm 700 ms	54.6	16.9	8.1	–	2.3	0.3	–	–	82.2
500 μm 700 ms	42.1	17.7	19.0	2.6	2.7	1.1	–	–	85.3
1000 μm 700 ms	53.5	12.1	11.2	5.4	–	2.7	–	–	84.9
HV coal									
HV 106 μm	40.2	19.0	4.9	1.8	1.2	1.5	–	–	68.5
HV 500 μm	35.6	11.1	11.2	6.1	1.8	–	–	–	65.9
HV 1000 μm	36.3	13.1	5.9	8.3	1.6	0.8	–	–	66.1
HV char									
106 μm 700 ms	45.7	18.5	10.2	2.0	3.2	1.3	–	–	80.9
500 μm 700 ms	43.7	3.8	1.6	13.7	5.4	3.6	–	2.3	74.1
1000 μm 700 ms	38.6	19.8	–	20.7	3.2	3.7	–	–	86.0

oxygen bonding in carbonate and anhydride structures identified by Beamson and Briggs in polymers [53]; their work also identified carbidic bonding in some samples around 283 eV, attributable to the metal–carbon bonding associated with the mineral content in the LV1, LV2 and HV chars derived from the larger particle coal classifications.

The high resolution scans revealed detailed information on the carbon (C 1s) peaks, looking specifically at the changes caused by grinding and related to the burnout. Work by other authors, has identified the importance of surface oxygen species on the reactivity; Cope et al. noted that below 1200 °C the formation of surface oxides inhibits the structural anisotropy and enhances reactivity [54], and Wan et al. noted that the mineral composition of the coals activates the early stage carbon gasification by acting as an oxygen shuttling agent [32].

3.4.1. High resolution C 1s spectra – coals

The C 1s spectra of the high rank semi-anthracitic LV1 coal in Fig. 10, shows little difference in the absolute quantity of C—O bonding for the different particle size classifications which ranged from 4.3% to 5.3%. However the LV2 in Fig. 11, and particularly the lower rank HV coal in Fig. 12, both had higher measured concentrations in the larger particle size classifications which had undergone less grinding. Both showed asymmetrical peak broadening in the higher binding energy region associated with carbon–oxygen bonding as ether groups (C—O) and ester groups (O=C—O), ranging from 3.4% to 6.9% in the LV2 and from 7.9% to 19.1% for the HV coal, which also included carbonyl (C=O) bonding.

3.4.2. High resolution C 1s spectra – chars

Compared to the coals, the spectra for the chars obtained after a burnout residence time of 700 ms had greater peak asymmetry with significant peak shoulders in the higher binding energy region, associated with more carbon–oxygen bonding. The results suggest that the physical process of grinding the coal changes the surface chemistry; either by reducing the number of reactive functional groups, or due to the physical effects associated with different particle size. The trend observed previously in Figs. 2

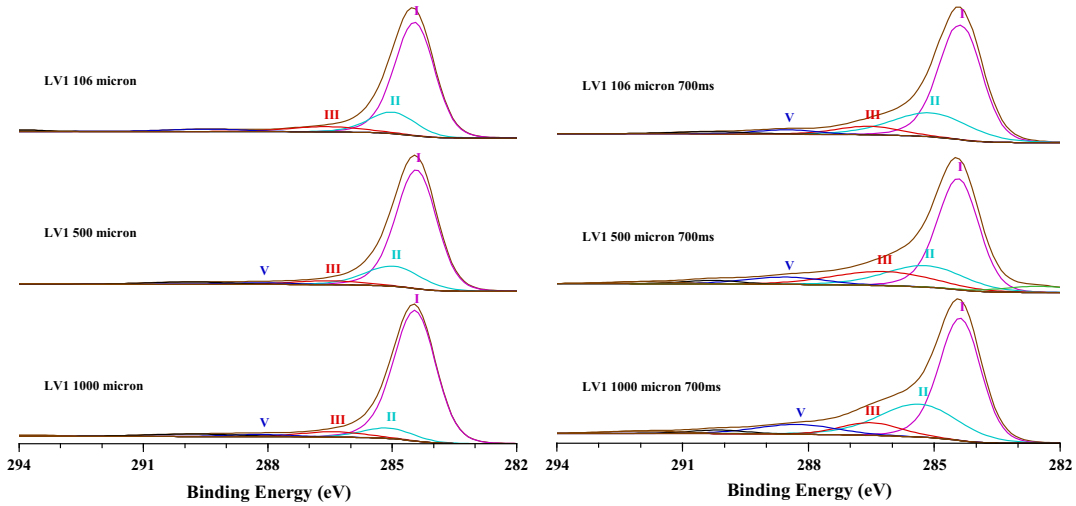

Fig. 10. XPS deconvoluted C 1s spectra for particle size classifications of LV1 (a) coal and (b) char.

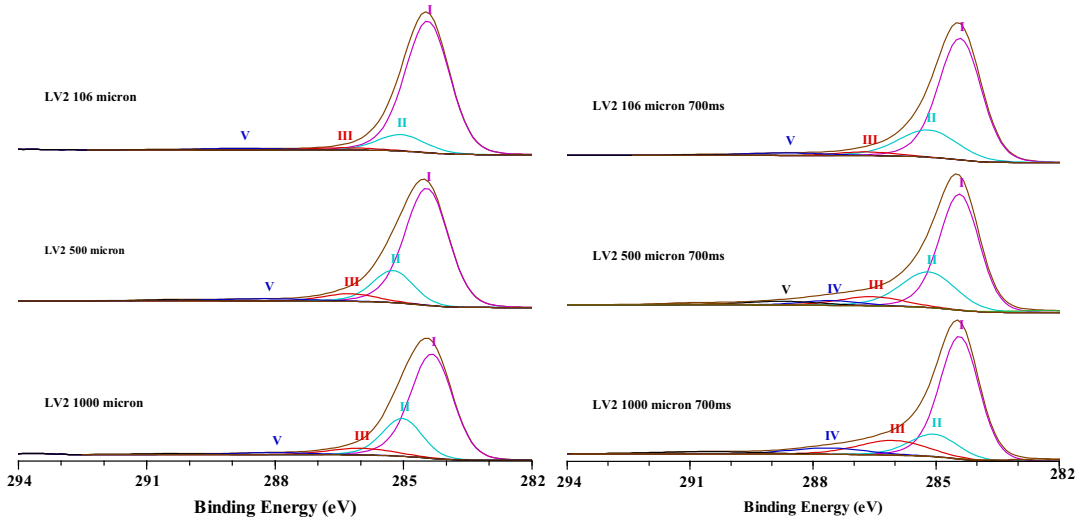

Fig. 11. XPS deconvoluted C 1s spectra for particle size classifications of LV2 (a) coal and (b) char.

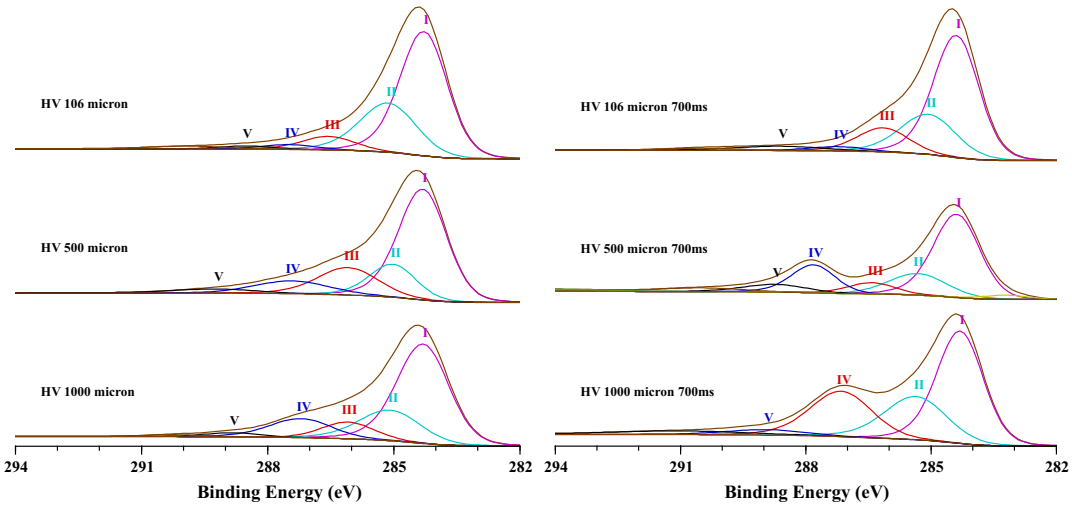

Fig. 12. XPS deconvoluted C 1s spectra for particle size classifications of HV (a) coal and (b) char.

and 3, was for smaller coal particles to swell and the larger particles to fragment, and it is the latter effect which could influence the surface chemistry and reactivity by exposing cleaved surfaces not subjected to the mechano-chemical effects caused by grinding.

Fig. 10 shows the peak fitted spectra for the LV1 chars and indicates higher levels of C—O bonding in the form of ether and ester groups, ranging from 7.1% to 17.5%, compared to the LV1 coals from which they were derived. The LV2 char, shown in Fig. 11, also shows peak broadening for all the particle classifications compared to the coals and it is the larger particle sizes that have the greater concentration ranging from 10.4% to 24.3%.

The most pronounced peak profile changes were observed in the HV char, shown in Fig. 12, which exhibited a bimodal shape for the <500 μm and <1000 μm particle sizes and C—O bonding concentrations ranging from 15.4% in the smallest 106 μm classification to 23.9% in the largest 1000 μm.

3.4.3. Carbon Auger electron spectroscopy

Issues regarding the accuracy of the peak fitting technique for the determination of the carbon hybridisation from the C 1s peak have been widely discussed and other authors have recognised particular difficulties differentiating the subtle differences between sp^2 and sp^3 signals. These are made worse with highly asymmetric peak shapes in hydrogenated samples such as those encountered with heterogeneous coal samples [45–48].

An alternative technique to determine the sp^2/sp^3 carbon hybridisation using the X-ray excited Carbon Auger (C_{KLL}) spectra was originally reported by Lascovich and Scaglione by measuring the distance, *D*, between the positive and negative peaks of the first derivative of the spectrum [55]. A linear approximation was proposed ranging from diamond at $D = 14.2$ eV, in which the carbons are 100% in the sp^3 configuration, to graphite at 22.5 eV where the carbons are 100% in the sp^2 configuration. In this range Lascovich et al. also measured the sp^2/sp^3 ratio of samples of amorphous carbon and hydrogenated amorphous carbon samples and since then other authors have extended this investigation to other forms of carbon such as carbonised wood, which include up to 21% oxygen bound on the surface and still show a linear relationship [47].

It has been previously noted by Leung et al. and Yan et al. that the sp^2/sp^3 values obtained from the *D*-parameter are consistently smaller than those values obtained using the peak fitting method and this is true for these results too. This is thought to be due to the influence of secondary electron emission on the auger peak [48,49,56] and Lascovich et al. found that an increase of the hydrogen content in hydrogenated amorphous carbon films corresponded to an increase in the sp^3 content.

The Carbon Auger data for the coal samples (Table 4) shows a maximum sp^2 percentage of 20.8% in the semi anthracitic LV1 coal, 9.0% in the low volatile bituminous LV2, and 0% in the HV corresponding to different degrees of coalification from the high rank to lower rank.

The sp^2 π-bonding corresponds to resonance stabilised aromatic/double bond character found in graphitic type structurally ordered carbon bonding. The results however, suggest that the predominant bonding in the coal measured using XPS is sp^3, the type of sigma bonding associated with single covalent bonds in aliphatic compounds. Grinding the coals to smaller particle size correlated with a reduction in the sp^2 character corresponding to bond cleavage of the carbon which changes the surface chemistry. This is most relevant to the LV1 coal with 28.3% sp^2 character for the <1000 μm particle size as grinding this to <106 μm gave a much improved burnout profile compared to grinding the other coals.

The results in Table 5 show the measured percentage sp^2 character of the coal chars after 700 ms residence time in the DTF. Compared to the coals from which they were derived, the chars have higher sp^2 aromatic/double bond character. The increase suggests thermal structural ordering of the carbons related to the sp^2 bonding found in highly ordered graphitic carbon, previously observed in the literature and which has been correlated to

Table 4
XPS Carbon Auger (C_{KLL}) *D* parameter and sp^2 bonding character of coal samples.

	D (eV)	% sp^2 (absolute)
Graphite[a]	22.5	–
Diamond[a]	14.3	–
LV1 106 μm	14.2	0.0
LV1 500 μm	15.1	8.2
LV1 1000 μm	16.5	20.8
LV2 106 μm	14.2	0.0
LV2 500 μm	14.6	3.5
LV2 1000 μm	15.2	9.0
HV 106 μm	14.4	1.3
HV 500 μm	14.2	0.0
HV 1000 μm	14.4	1.3

[a] Lascovich et al. [55].

Table 5
XPS Carbon Auger (C_{KLL}) *D* parameter and sp^2 bonding character of coal char samples (700 ms).

	D (eV)	% sp^2(absolute)	% DTF burnout after 35 ms	% DTF burnout after 700 ms
LV1 106 μm	16.4	18.6	8.5	64.5
LV1 500 μm	17.8	34.5	2.4	63.9
LV1 1000 μm	18.4	41.6	4.4	48.1
LV2 106 μm	14.3	0.6	11.9	52.3
LV2 500 μm	15.4	12.4	11.6	68.1
LV2 1000 μm	16.0	18.7	9.0	59.2
HV 106 μm	14.8	5.7	51.3	81.6
HV 500 μm	15.1	7.9	48.8	93.0
HV 1000 μm	15.5	13.5	31.7	86.2

reductions in char reactivity [57–59]. Additionally, the preferential combustion of the more reactive and less ordered sp^3 bonded aliphatic carbons results in higher concentrations of the sp^2 bonded carbons present at the surface of the char.

The smaller particle size classifications of each coal char (Table 5) had lower sp^2 character compared to the larger classifications and correspondingly higher char burnout at low residence time in the DTF. This relative trend was also reflected with an improved burnout with a lower rank of coal (HV > LV2 > LV1). This is consistent with other work such as Lu et al. who showed a relationship with increasing aromaticity and decreasing char reactivity [60]. However the results indicate no direct correlation between the absolute quantity of sp^2 character for each of the coals and burnout.

Also, there is no such correlation between burnout at higher levels of carbon conversion and the sp^2 character. This suggests other variables such as particle swelling, fragmentation, or the type of surface oxygen bonding are likely to play a dominant role in the reactivity compared to the carbon bonding at higher conversion levels.

4. Conclusion

The results suggest that, in addition to the importance of size on coal particle burnout, the process of grinding alters the physical properties and surface chemistry so that in some cases the larger size classifications give improved combustion burnout profiles compared to smaller sizes.

Physical changes to the particle behaviour occurred on grinding where the smallest particle size coals exhibited particle swelling on combustion producing cenospherical and network chars, whereas the larger classifications resulted in fragmented solid chars. The presence of minerals such as illite has been demonstrated by many authors to play an important role in improved combustion of coal, and in most cases in this study, the larger particles resulted in higher conversion of the aluminosilicate minerals mullite and illite. Combined with the trend of increasing burnout with increasing mullite levels there is a suggestion that these changes may indicate a catalytic or synergistic role, although it cannot be discounted that they were the consequence of burnout.

The interaction of oxygen and carbon is fundamental to the surface chemistry of combustion and the larger particle sizes had a wider variety of oxygen–carbon bonding on the char surfaces compared to smaller ones. This positive effect could be related to the particle fragmentation exposing 'cleaved' surfaces which were more reactive.

Other authors have linked sp^2 bonding with structural ordering and reduced reactivity; analysis of the Carbon Auger peak indicated that the coals had up to 20.8% sp^2 bonding which reduced on grinding. However, the sp^2 content increased for the chars, compared to the coals from which they were derived, which was related to the coal particle size and to increasing rank of coal. At lower levels of carbon conversion these higher levels of the sp^2 bonding correlated with reduced burnout, but at higher carbon conversion other variables were more dominant.

Acknowledgement

The authorship wishes to acknowledge and thank Tata Steel Europe Ltd. for financial assistance with this project and support obtaining samples.

References

[1] Guo H, Su B, Zhang J, Shao J, Zuo H, Ren S. Energy conservation for granular coal injection into a blast furnace. JOM 2012;64:1002–10.
[2] U.S.D.o. Energy. Blast furnace granulated coal injection system demonstration project. P.O. Box 880, 3610 Collins Ferry Road Morgantown, WV 26507-0880: National Energy Technology Laboratory; 2000.
[3] Osborne D. The coal handbook: towards cleaner production. Woodhead Publishing; 2013.
[4] Maldonado R, Hanniker G, Pettifor M. Granular coal injection into blast furnaces at the scunthorpe works of the british steel corporation. In: Proceedings – ironmaking conference; 1985. p. 425–35.
[5] Hill DG, Makovsky LE, Sarkus TA, McIlvried HG. Blast furnace granular coal injection at Bethlehem Steel's Burns Harbor Plant. Miner Process Extract Metall Rev 2004;25:49–65.
[6] Barranco R, Colechin M, Cloke M, Gibb W, Lester E. The effects of pf grind quality on coal burnout in a 1 MW combustion test facility. Fuel 2006;85:1111–6.
[7] Moon C, Sung Y, Ahn S, Kim T, Choi G, Kim D. Thermochemical and combustion behaviors of coals of different ranks and their blends for pulverized-coal combustion. Appl Therm Eng 2013;54:111–9.
[8] Raygan S, Abdizadeh H, Rizi AE. Evaluation of four coals for blast furnace pulverized coal injection. J Iron Steel Res Int 2010;17. 8–12, 20.
[9] Zhang H, Cen K, Yan J, Ni M. The fragmentation of coal particles during the coal combustion in a fluidized bed. Fuel 2002;81:1835–40.
[10] Chen WH, Du SW, Yang TH. Volatile release and particle formation characteristics of injected pulverized coal in blast furnaces. Energy Convers Manage 2007;48:2025–33.
[11] Suarez I-R, Crelling JC. Applied coal petrology: the role of petrology in coal utilisation. Academic Press; 2008.
[12] Morgan PA, Robertson SD, Unsworth JF. Combustion studies by thermogravimetric analysis. 1. Coal oxidation. Fuel 1986;65:1546–51.
[13] Yu D, Xu M, Sui J, Liu X, Yu Y, Cao Q. Effect of coal particle size on the proximate composition and combustion properties. Thermochim Acta 2005;439:103–9.
[14] Morgan PA, Robertson SD, Unsworth JF. Combustion studies by thermogravimetric analysis. 2. Char oxidation. Fuel 1987;66:210–5.
[15] Cloke M, Lester E, Belghazi A. Characterisation of the properties of size fractions from ten world coals and their chars produced in a drop-tube furnace. Fuel 2002;81:699–708.
[16] Ural S, Akiylidz M. Studies of the relationship between mineral matter and grinding properties for low-rank coals. Int J Coal Geol 2004;60:81–4.
[17] Huggins FE. Overview of analytical methods for inorganic constituents in coal. Int J Coal Geol 2002;50:169–214.
[18] Liu G, Wu H, Gupta RP, Lucas JA, Tate AG, Wall TF. Modeling the fragmentation of non-uniform porous char particles during pulverized coal combustion. Fuel 2000;79:627–33.
[19] Senneca O, Urciuolo M, Chirone R, Cumbo D. An experimental study of fragmentation of coals during fast pyrolysis at high temperature and pressure. Fuel 2011;90:2931–8.
[20] Dacombe P, Pourkashanian M, Williams A, Yap L. Combustion-induced fragmentation behavior of isolated coal particles. Fuel 1999;78:1847–57.

[21] Yu J, Lucas J, Strezov V, Wall T. Swelling and char structures from density fractions of pulverized coal. Energy Fuels 2003;17:1160–74.
[22] Yu D, Xu M, Liu X, Cao Q. Swelling characteristics of coal chars and formation of residual ash particles. Huazhong Keji Daxue Xuebao (Ziran Kexue Ban)/J Huazhong Univ Sci Technol (Nat Sci Ed) 2006;34:101–4.
[23] Chan ML, Jones JM, Pourkashanian M, Williams A. Oxidative reactivity of coal chars in relation to their structure. Fuel 1999;78:1539–52.
[24] Du SW, Chen WH, Lucas JA. Pulverized coal burnout in blast furnace simulated by a drop tube furnace. Energy 2010;35:576–81.
[25] Li H, Elliott L, Rogers H, Austin P, Jin Y, Wall T. Reactivity study of two coal chars produced in a drop-tube furnace and a pulverized coal injection rig. Energy Fuels 2012;26:4690–5.
[26] Steer J, Marsh R, Griffiths A, Malmgren A, Riley G. Biomass co-firing trials on a down-fired utility boiler. Energy Convers Manage 2013;66:285–94.
[27] Ballantyne TR, Ashman PJ, Mullinger PJ. A new method for determining the conversion of low-ash coals using synthetic ash as a tracer. Fuel 2005;84:1980–5.
[28] Chen W-H, Du S-W, Tsai C-H, Wang Z-Y. Torrefied biomasses in a drop tube furnace to evaluate their utility in blast furnaces. Bioresour Technol 2012;111:433–8.
[29] Biagini E, Marcucci M. Review of methodologies for coal characterisation. International Flame Research Foundation; 2000.
[30] Zhang H, Pu WX, Ha S, Li Y, Sun M. The influence of included minerals on the intrinsic reactivity of chars prepared at 900 °C in a drop tube furnace and a muffle furnace. Fuel 2009;88:2303–10.
[31] Pohl JH. Influence of mineral matter on the rate of coal char combustion. In: ACS symposium series; 1986. p. 430–6.
[32] Wan Shaolong, Chen Wei-Yin, Shi Guang. Roles of mineral matter in the early stages of coal combustion. Energy Fuels 2009;23:710–8.
[33] Gupta S, Al-Omari Y, Sahajwalla V, French D. Influence of carbon structure and mineral association of coals on their combustion characteristics for Pulverized Coal Injection (PCI) application. Metall Mater Trans B: Process Metall Mater Process Sci 2006;37:457–73.
[34] Wei Z, Michael Moldowan J, Dahl J, Goldstein TP, Jarvie DM. The catalytic effects of minerals on the formation of diamondoids from kerogen macromolecules. Org Geochem 2006;37:1421–36.
[35] Menendez R, Alvarez D, Fuertes AB, Hamburg G, Vleeskens J. Effects of clay minerals on char texture and combustion. Energy Fuels 1994;8:1007–15.
[36] Spears DA. Role of clay minerals in UK coal combustion. Appl Clay Sci 2000;16:87–95.
[37] Steer JM, Marsh R, Greenslade M, Robinson A. Opportunities to improve the utilisation of granulated coals for blast furnace injection. Fuel 2014.
[38] Reifenstein AP, Kahraman H, Coin CDA, Calos NJ, Miller G, Uwins P. Behaviour of selected minerals in an improved ash fusion test: quartz, potassium feldspar, sodium feldspar, kaolinite, illite, calcite, dolomite, siderite, pyrite and apatite. Fuel 1999;78:1449–61.
[39] Suárez-Ruiz I, Crelling JC. Applied coal petrology: the role of petrology in coal utilization. Academic Press; 2008.
[40] C. XPS. CASA XPS Manual; 2013.
[41] Gong B, Pigram PJ, Lamb RN. Surface studies of low-temperature oxidation of bituminous coal vitrain bands using XPS and SIMS. Fuel 1998;77:1081–7.
[42] Geng W, Kumabe Y, Nakajima T, Takanashi H, Ohki A. Analysis of hydrothermally-treated and weathered coals by X-ray photoelectron spectroscopy (XPS). Fuel 2009;88:644–9.
[43] Pietrzak R, Grzybek T, Wachowska H. XPS study of pyrite-free coals subjected to different oxidizing agents. Fuel 2007;86:2616–24.
[44] Xia W, Yang J, Liang C. Investigation of changes in surface properties of bituminous coal during natural weathering processes by XPS and SEM. Appl Surf Sci 2014;293:293–8.
[45] Smith RAP, Armstrong CW, Smith GC, Weightman P. Observation of a surface chemical shift in carbon 1s core-level photoemission from highly oriented pyrolytic graphite. Phys Rev B – Condens Matter Mater Phys 2002;66:2454091–96.
[46] Prince KC, Ulrych I, Peloi M, Ressel B, Cháb V, Crotti C, et al. Core-level photoemission from graphite. Phys Rev B – Condens Matter Mater Phys 2000;62:6866–8.
[47] Mezzi A, Kaciulis S. Surface investigation of carbon films: from diamond to graphite. Surf Interface Anal 2010;42:1082–4.
[48] Leung TY, Man WF, Lim PK, Chan WC, Gaspari F, Zukotynski S. Determination of the sp3/sp2 ratio of a-C: H by XPS and XAES. J Non-Cryst Solids 1999;254:156–60.
[49] Jones BJ, Ojeda JJ. Substrate and material transfer effects on the surface chemistry and texture of diamond-like carbon deposited by plasma-enhanced chemical vapour deposition. Surf Interface Anal 2012;44:1187–92.
[50] Biniak S, Szymański G, Siedlewski J, Światkoski A. The characterization of activated carbons with oxygen and nitrogen surface groups. Carbon 1997;35:1799–810.
[51] Gardner SD, Singamsetty CSK, Booth GL, He GR, Pittman Jr CU. Surface characterization of carbon fibers using angle-resolved XPS and ISS. Carbon 1995;33:587–95.
[52] Gong B, Pigram PJ, Lamb RN, Ward CR. Surface characterisation of mineral matter in an Australian bituminous coal (Whybrow seam, NSW) using X-ray photoelectron spectroscopy and laser ionisation mass analysis. Fuel Process Technol 1997;50:69–86.
[53] Beamson G, Briggs D. High resolution XPS of organic polymers – the scienta ESCA300 database. John Wiley & Sons; 1992.
[54] Cope RF, Arrington CB, Hecker WC. Effect of CaO surface area on intrinsic char oxidation rates for Beulah Zap chars. Energy Fuels 1994;8:1095–9.
[55] Lascovich JC, Scaglione S. Comparison among XAES, PELS and XPS techniques for evaluation of Sp2 percentage in a-C:H. Appl Surf Sci 1994;78:17–23.
[56] Yan XB, Xu T, Yang SR, Liu HW, Xue QJ. Characterization of hydrogenated diamond-like carbon films electrochemically deposited on a silicon substrate. J Phys D: Appl Phys 2004;37:2416–24.
[57] Lu L, Sahajwalla V, Harris D. Coal char reactivity and structural evolution during combustion-factors influencing blast furnace pulverized coal injection operation. Metall Mater Trans B: Process Metall Mater Process Sci 2001;32:811–20.
[58] Feng B, Bhatia SK, Barry JC. Structural ordering of coal char during heat treatment and its impact on reactivity. Carbon 2002;40:481–96.
[59] Russell NV, Gibbins JR, Williamson J. Structural ordering in high temperature coal chars and the effect on reactivity. Fuel 1999;78:803–7.
[60] Lu L, Kong C, Sahajwalla V, Harris D. Char structural ordering during pyrolysis and combustion and its influence on char reactivity. Fuel 2002;81:1215–25.

Appendix 2 Supplementary published works and conference papers

Minor contribution	Moderate contribution	Majority contribution

Contribution to supplementary published works and conference papers					
Paper	Concept	Structure & design	Experimental	Data Analysis	Paper writing presentation
Steer, J., Marsh, R., Griffiths, T., Williams, K. Biogas potential and digestion rates of food wastes in anaerobic digestion systems. International Conference on Solid Waste Technology and Management, Philadelphia, USA, March 30- April 2, 2008.					
Steer, J., Greenslade, M., Griffiths, T., The effect of blending coals on their suitability for blast furnace coal injection. 5th International Conference of Applied Energy, Pretoria, South Africa, July 1st-4th 2013.					
Raghuyal, S., **Steer, J.**, Griffiths, A., Hopkins, A. Characterisation of Chromium-Copper- Arsenic (CCA) treated wood waste from a steel-making environment. WIT Transactions on Ecology and the Environment (2012) 163, pp. 271-282					
Jaafar, I., Griffiths, A.J., Hopkins, A.C., **Steer, J.M.**, Griffiths, M.H., Sapsford, D.J. An evaluation of chlorination for the removal of zinc from steelmaking dusts. Minerals Engineering (2011) 24 (9), pp. 1028-1030					

Heinrich, T., Griffiths, A.J., **Steer J.**, Hopkins, A.C., Griffiths, M.H. In-line sampling of basic oxygen steelmaking dust. 5th World conference on sampling and blending, October 25th-28th 2011, Santiago, Chile.					
Marsh, R., **Steer, J.**, Fesenko, E., Griffiths, T., Williams, K. Biomass and waste co-firing in large-scale combustion systems. Proceedings of Institution of Civil Engineers: Energy (161 (3), pp. 115-126					
Marsh, R., **Steer, J.**, Griffiths, T., Williams, K. Quantification of products from thermal decomposition of solid wastes. 23rd International Conference on Solid Waste Technology and Management, Philadelphia, USA, March 30th- April 2nd, 2008.					
Pugh, D., Crayford, A.P., Bowen, P.J., Marsh, R., **Steer, J.** Laminar flame speed and Markstein length characterisation of steelworks gas blends. Applied Energy (2014) 136, pp. 1026-1034					
Marsh R, **Steer J.M.**, Griffiths A.J., Williams K.P., Biomass co-firing: opportunities and considerations, IEA Clean Coal Conference Workshop on Perspectives on Co-combustion, (2008)					

1. **Steer, J**., Marsh, R., Griffiths, T., Williams, K. Biogas potential and digestion rates of food wastes in anaerobic digestion systems. 23rd International Conference on Solid Waste Technology and Management, Philadelphia, PA USA, March 30- April 2, 2008. (PRESENTING AUTHOR)

2. **Steer, J**., Greenslade, M., Griffiths, T., The effect of blending coals on their suitability for blast furnace coal injection. 5th International Conference of Applied Energy, Pretoria, South Africa, July 1st-4th 2013. (PRESENTING AUTHOR)

3. Raghuyal, S., **Steer, J**., Griffiths, A., Hopkins, A. Characterisation of Chromium-Copper-Arsenic (CCA) treated wood waste from a steel-making environment. WIT Transactions on Ecology and the Environment (2012) 163, pp. 271-282 (CO-AUTHOR)

4. Jaafar, I., Griffiths, A.J., Hopkins, A.C., **Steer, J.M**., Griffiths, M.H., Sapsford, D.J. An evaluation of chlorination for the removal of zinc from steelmaking dusts. Minerals Engineering (2011) 24 (9), pp. 1028-1030 (CO-AUTHOR)

5. Heinrich, T., Griffiths, A.J., **Steer J**., Hopkins, A.C., Griffiths, M.H. In-line sampling of basic oxygen steelmaking dust. 5th World conference on sampling and blending, October 25th-28th 2011, Santiago, Chile. (CO-AUTHOR)

6. Marsh, R., **Steer, J**., Fesenko, E., Griffiths, T., Williams, K. Biomass and waste co-firing in large-scale combustion systems. Proceedings of Institution of Civil Engineers: Energy (161 (3), pp. 115-126 (CO-AUTHOR)

7. Marsh, R., **Steer, J**., Griffiths, T., Williams, K. Quantification of products from thermal decomposition of solid wastes. 23rd International Conference on Solid Waste Technology and Management, Philadelphia, USA, March 30th- April 2nd, 2008. (CO-AUTHOR)

8. Pugh, D., Crayford, A.P., Bowen, P.J., Marsh, R., **Steer, J**. Laminar flame speed and markstein length characterisation of steelworks gas blends. Applied Energy (2014) 136, pp. 1026-1034 (CO-AUTHOR)

9. Marsh R, Steer J.M., Griffiths A.J., Williams K.P., Biomass co-firing: opportunities and considerations, IEA Clean Coal Conference Workshop on Perspectives on Co-combustion, (2008) (CO-AUTHOR)